The Pennsylvania State University

The Graduate School

Department of Chemical Engineering

COSOLVENT EFFECTS IN POLYMER-SOLVENT SYSTEMS

A Thesis in

Chemical Engineering

by

Adam Terrell Jones

Submitted in Partial Fulfillment
of the Requirements
for the Degree of

Doctor of Philosophy

August 2007

The thesis of Adam Terrell Jones was reviewed and approved* by the following:

Seong H. Kim
Professor of Chemical Engineering
Co-Chair of Committee

Ronald P. Danner
Professor Emeritus of Chemical Engineering
Co-Chair of Committee
Thesis Advisor

John V. Badding
Professor of Chemistry

Andrew L. Zydney
Professor of Chemical Engineering
Head of the Department of Chemical Engineering

*Signatures are on file in the Graduate School

ABSTRACT

Devolatilization of polymers is important to industrial applications such as film drying, foam production, microelectronics manufacturing, and bulk plastics processing. The mass transport and thermodynamics within such systems often limits production throughput. For example, a common method of foam devolatilization is ambient pressure desorption. In this situation, the diffusion of residual species from the foam to the surrounding air is the limiting step in the manufacturing process. Therefore, the use of a cosolvent to affect the solubility and diffusion favorably is an area of interest to industry. However, little data exist and few models are capable of predicting the influences that occur when a cosolvent is added to a system.

This thesis focuses on measuring and describing cosolvent effects in polymer-solvent systems. Inverse gas chromatography was used to test the influence of CO_2 and ethylene at high pressures on the solubility and diffusion of several solvents in poly(vinyl acetate) and poly(styrene). Through testing at multiple conditions it was possible to determine which gas had the largest effect on the polymer-solvent behavior. In addition, influences due to solvent size were examined.

A ternary experiment was designed to probe the effect of water on the solubility and diffusivity in a poly(ethylene)-ethylene system. The experiment is a simple gravimetric technique for measuring mass uptake of penetrants in polymers.

Lastly, several thermodynamic models are applied to a phase equilibria problem of predicting anomalous solubility behavior in copolymer systems. In certain systems, solvents have been observed to have higher solubility in copolymers compared to the two

respective homopolymers. The goal was to determine which, if any, models could predict such behavior without experimental data for parameterization.

TABLE OF CONTENTS

LIST OF FIGURES

LIST OF TABLES

ACKNOWLEDGEMENTS

This work would not have been possible without the guidance and training provided by my co-advisors, Professors Ronald P. Danner and J. Larry Duda. They not only taught me how to conduct thorough research, they changed the way I thought and molded me into a well-rounded research engineer. I am forever indebted. This thesis is dedicated to Prof. Duda, who passed away during my time at Penn State. He taught me to look for the implicit assumption, always be thinking about interesting problems, and embellish when you have to.

I have benefited tremendously from being a part of the Center for the Study of Polymeric Systems throughout my graduate studies. The Center personnel have provided help on numerous occasions regardless of their own obligations. In particular Roman Galdamez and Ida Balashova have always been willing to discuss problems that were encountered in this work. Also, I thank the undergraduate researchers in the Center for their help on the numerous projects I have been involved with.

The opportunity to interact with Center industrial partners has helped me focus on the big picture in research. I am particularly grateful to John Zielinski and Mike Kimak of Air Products and Chemicals, Inc. for providing the equipment used in the inverse gas chromatography study. Also, interacting with Marty Tusim, Lawrence Hood, and Charlie Berglund of Dow Chemical was a pleasure.

The chief reason for any success I have had in life has been due to my parents' encouragement and their reminding me that I could do anything I set my mind to. I thank God everyday for giving me the chance to be their son. I have also been blessed with a

wonderful sister and brother-in-law that are as much my best friends as they are family. My wife has been my most faithful and loving partner through most of my time here at Penn State. Her support and sacrifices have been an illustration of what it means to be a true companion.

Dedicated to the Memory of

J. Larry Duda

Chapter 1

1.1 Introduction

Cosolvents have an effect on polymer-solvent systems that can be tailored to give desired phase equilibrium and mass transport. The mass transport is influenced when the cosolvent plasticizes the polymer, increasing the mobility of the chains which results in higher diffusion within the polymer matrix. At the same time, the cosolvent can change the equilibrium of the system by hindering or enhancing the interactions of the solvent with the polymer. The change in phase equilibrium of a polymer-solvent system due to addition of a cosolvent can be either positive or negative influence depending on the application. In general, these effects are not known *a priori*. This requires either experimental data on a system or an accurate model of how the cosolvent will affect the system.

A vast amount of work exists in the literature reporting cosolvent effects in polymer-solvent systems. Much of the work focuses on quantifying observed phenomena that was previously treated in a qualitative manner, e.g. [1-14]. In these publications most of the focus has been on dilute polymer systems which exhibit liquid-liquid equilibrium. However, concentrated polymer solutions are often encountered during processing which exhibit a single liquid phase in equilibrium with its vapor phase.

The majority of work on concentrated polymer-mixed solvent systems has been in the area of thermodynamic modeling. Within this realm there are two approaches: prediction and correlation. The first group of models usually employs a group-contribution method for parameterization. These include the activity coefficient models UNIFAC [16], UNIFAC-FV [17],

Entropic-FV [18], and UNIFAC-vdW-FV [19]. In addition, the Group-Contribution Lattice-Fluid equation of state (GCLF-EoS) was recently extended to multicomponent systems by Davis [20]. The second group of models uses experimental data for parameterization. They include the Flory–Huggins [21-22] activity coefficient model as well as the Sanchez-Lacombe [23], Panayiotou-Vera [24], and SAFT equations of state [25].

Modeling of the diffusion behavior in these systems has received less focus, likely owing to the lack of experimental data. Cohen and Turnbull [26] introduced the free-volume theory of diffusion, which Vrentas and Duda [27] extended to polymer solutions. Vrentas et al. [28] extended the theory to ternary systems. Several groups subsequently provided variant forms of the expressions in that theory [29-31]. All of the above diffusion theories require experimental data for parameterization.

Obtaining equilibria and diffusion data on multicomponent polymer-solvent systems remains a challenge. Testing of binary systems proves simple due to the fact that the vapor consists only of a single solvent species. However, when extending such methods to ternary systems it becomes necessary to measure the vapor phase composition during the experiment. Tanbonliong and Prausnitz [32] modified an existing gravimetric sorption technique to study the poly(styrene) (PS)-chloroform-carbon tetrachloride system. They directly measured the amount of solvent introduced to the system. They then performed a mass balance on the system to determine the distribution between the vapor and liquid phases. Liu et al. [33] used a similar apparatus to obtain data on PS-benzene-toluene. Other workers [35-37] have used forced Rayleigh scattering to measure the self diffusion coefficients in ternary polymer-solvent systems. Recently, a magnetic suspension balance apparatus was applied in the study of poly(vinyl acetate) (PVAc)-

toluene-methanol [38]. Surana et al. [34] extended inverse gas chromatography (IGC) to the testing of ternary systems. They studied the behavior of a solvent at infinite dilution in a polymer-solvent mixture in equilibrium at finite concentration. Most recently Zielinski et al. [39] suggested using IGC for probing high pressure gas influences on polymer-solvent behavior. The work in Chapter 3 builds upon the ideas outlined in their paper.

The goal of this work was to characterize the effects an additional component has on a binary polymer-solvent system. It is believed that the effects, once understood, can be tailored to improve many polymer processing steps.

Chapter 2 presents a review of some prevalent thermodynamic models for application to multicomponent systems. Chapter 3 introduces the relatively new technique called high pressure inverse gas chromatography (HPIGC). The technique measures data similar to that obtained by Surana et al. [34]. However, in this work the polymer-solvent system at equilibrium is a polymer and gas. The injected species is a solvent at infinite dilution. This was done to probe the influence of the gas on the diffusion and solubility behavior of the solvent. The particular work is targeted toward devolatilization where it is desirable to increase the diffusion rate and decrease the solubility of the solvent in the polymer. Discussion of the experimental design and application to PS and PVAc systems is presented. Chapter 4 presents results of a study on the influence of water on polyethylene-ethylene. The work has direct application to steam stripping commonly used for devolatilization in industrial processing of polymers. The data were collected using a static sorption technique. Due to a lack of vapor composition sampling, a pseudo-binary approach was taken to treat the data. Chapter 5 is a

comparison of theoretical capabilities for predicting thermodynamic behavior in copolymer-solvent systems. In this situation, the additional copolymer repeat unit was considered the “co-“species. Certain copolymer systems have exhibited solubilities higher or lower than the respective homopolymers. The goal of the work in Chapter 5 was to determine if several of the more capable thermodynamic models could predict such behavior. Concluding remarks are given in the final chapter. Appendices are also provided.

1.2 References

1. Gee, G. Swelling and Solubility in Mixed Liquids. *Trans. Faraday Soc.* **1944**, *40*, 468-480.

2. Moore, W.R. The Swelling of Nitrocellulose in Binary Mixtures. *Trans. Faraday Soc.* **1947**, *43*, 543-552.

3. Scott, R. L. The Thermodynamics of High Polymer Solutions. 4. Phase Equilibria in the Ternary System - Polymer Liquid-1 Liquid-2 *J. Chem. Physics* **1949**, *17*,268-279.

4. Flory, P. J.; Krigbaum, W. R. Thermodynamics of High Polymer Solutions. *Annual Rev. Phys. Chem.* **1951**, *2*, 383-402.

5. Palit, S. R.; Colombo, G.; Mark, H. Osmotic, Viscometric, and Turbidity Studies of Polystyrene in Mixed Solvents. *J. Polym. Sci*., **1951**, *6*, 295-304.

6. Walker, E. E. The Solvent Action of Organic Substances on Polyacrylonitrile. *J. Applied Chem.* **1952**, *2*, 470-481.

7. Kawai, T. Notes on the Polymer-Mixed Solvents System .1. The Refinement of the Free Energy Expression. *Bulletin Chem. Soc. Japan* **1952**, *25*, 336-341.

8. Shultz, A. R.; Flory, P. J. Phase Equilibria in Polymer Solvent Systems .3. 3-Component Systems. *J. Amer. Chem. Soc.* **1953**, *75*, 5681-5685.

9. Krigbaum, W. R.; Carpenter, D. K. Phase Equilibria in Polymer-Liquid 1-Liquid 2 Systems. *J. Polym. Sci.* **1954**, *14*, 241-259.

10. Kawai, T. Note on the Polymer-Mixed Solvent System.4. Deviation from the Single Liquid Approximation in Osmotic, Viscometric and Swelling Measurements. *Bulletin Chem. Soc. Japan* **1955**, *28*, 356-360.

11. Shultz, A. R.; Flory, P. J. Polymer Chain Dimensions in Mixed-Solvent Media *J. Polym. Sci.* **1955**, 15, 231-242.

12. Moore, W. R.; Russell, J. Swelling and Absorption by Cellulose Acetate in Binary Solvent-Hexane Mixtures. *J. Polym. Sci.* **1955**, *18*, 63-86.

13. Scanlan, J. Swelling of Vulcanized Rubbers in Binary Solvent Mixtures. *J. Appl. Polym. Sci.* **1965**, *9*, 241-244.

14. Yamamoto, M.; White, J. L.; Maclean, D. L. Statistical Thermodynamics of Solutions of Polymers in Mixed Solvents *Polymer* **1971**, *12*, 290-308.

15. Cowie, J. M. G.; McEwen I. J. Polymer Cosolvent Systems: 6. Phase Behaviour of Polystyrene in Binary Mixed Solvents of Acetone with n-Alkanes-Examples of "Classic Cosolvency". *Polymer* **1983**, *24*, 1449-1452.

16. Fredenslund, Aa.; Jones, R. L.; Prausnitz, J. M. Group-Contribution Estimation of Activity Coefficients in Nonideal Liquid Mixtures. *AIChE J.* **1975**, *21*, 1086-1099.

17. Oishi, T.; Prausnitz, J. M. Estimation of Solvent Activities in Polymer Solutions Using a Group-Contribution Method. *Ind. Eng. Chem. Process Des. Dev.*, **1978**, *17*, 333-339.

18. Elbro, H. S.; Fredenslund, Aa.; Rasmussen, P. A New Simple Equation for the Prediction of Solvent Activities in Polymer-Solutions. *Macromolecules* **1990**, *23*, 4707-4714.

19. Kannan, D. C.; Duda, J. L.; Danner, R. P. A Free-Volume Term Based on the van der Waals Partition Function for the UNIFAC Model. *Fluid Phase Equilib.*, **2205**, *228-229*, 321-328.

20. Davis, P. K. Experimental and Theoretical Aspects of Studying Thermodynamics and Mass Transport in Polymer-Solvent Systems. Ph.D. Thesis, The Pennsylvania State University, University Park, PA, **2003**.

21. Flory, P. J. Thermodynamics of High Polymer Solutions. *J. Chem. Phys.* **1942**,*10*, 51-61.

22. Huggins, M. L. Thermodynamic Properties of Solutions of Long-Chain Compounds *Ann. NY Acad. Sci.* **1942**, *43*, 431-443.

23. Sanchez, I. C.; Lacombe, R. H. Statistical Thermodynamics of Polymer Solutions. *Macromolecules* **1978**, *11*, 1145–1156.

24. Panayiotou, C.; Vera, J.H. Statistical Thermodynamics of r-mer Fluids and Their Mixtures. *Polym. J.* **1982**, *14*, 681-694.

25. Chapman, W. G.; Gubbins, K. E.; Jackson, G.; Radosz, M. SAFT: Equation-of-State Solution Model for Associating Fluids. *Fluid Phase Equilib.* **1989**, *52*, 31–38.

26. Cohen, M. H.; Turnbull, D. Molecular Transport in Liquids and Gases. *J. Chem. Phys.* **1959**, *31*, 1164–1169.

27. Vrentas, J. S.; Duda, J. L. Diffusion in Polymer–Solvent Systems. II. A Predictive Theory for the Dependence of Diffusion Coefficients on Temperature,

Concentration and Molecular Weight. *J. Polym. Sci., Polym. Phys. Ed.* **1977**, *15*, 417–439.

28. Vrentas, J. S.; Duda, J. L.; Ling, H. C. Self Diffusion in Polymer–Solvent–Solvent Systems. *J. Polym. Sci., Polym. Phys. Ed.* **1984**, *22*, 459–469.

29. Alsoy, S.; Duda, J. L. Modeling of Multicomponent Drying of Polymer Films. *AIChE J.* **1999**, *45*, 896–905.

30. Zielinski, J. M.; Hanley, B. F. Practical Friction-Based Approach to Modelling Multicomponent Diffusion. *AIChE J.* **1999**, *45*, 1–12.

31. Price, P. E.; Romdhane, I. H.. Multicomponent Diffusion Theory and its Applications to Polymer–Solvent Systems. *AIChE J.* **2002**, *49*, 309–322.

32. Tanbonliong, J. O.; Prausnitz, J. M. Vapor-Liquid Equilibria for Some Binary and Ternary Polymer Solutions. *Polymer*, **1997**, *38*, 5775-5783.

33. Liu, H.; Huang, Y.; Wang, K.; Ying, H. Vapor-Liquid Equilibria for Mixed Solvent-Polymer Systems, Measurements and Correlation. *Fluid Phase Equilib.*, **2002**,*194–197*, 1067–1075.

34. Surana, R. K.; Danner, R. P.; Duda, J. L. Diffusion and Equilibrium Measurements in Ternary Polymer–Solvent–Solvent Systems Using Inverse Gas Chromatography. *Ind. Eng. Chem. Res*. **1998**, *37*, 3203–3207.

35. Lodge, T. P.; Lee, J. A.; Frick, T. S. Probe Diffusion in Poly(Vinyl Acetate)/Toluene Solutions. *J. Polym. Sci., Polym. Phys. Ed.* **1990**, *28*, 2607-2627.

36 Chapman, B. R.; Paulaitis, M. E.; Gochanour, C. R. Effect of CO2 Plasticization on Azobenzene Diffusion in Glassy Polystyrene Near the Glass Transition. *Macromolecules* **2001**, *34*, 340-342.

37 Gupta, R. R.; RamachandraRao, V. S.; Watkins, J. J. Measurement of Probe Diffusion in CO2-Swollen Polystyrene Using in Situ Fluorescence Nonradiative Energy Transfer. *Macromolecules* **2003**, *36*, 1295-1303.

38 Schabel, W.; Scharfer, P.; Kind, M.; Mamaliga, I. Sorption and Diffusion Measurements in Ternary Polymer–Solvent–Solvent Systems by means of a Magnetic Suspension Balance—Experimental Methods and Correlations with a Modified Flory–Huggins and Free-Volume Theory. *Chem. Eng. Sci.* **2007**,*62*, 2254 – 2266.

39. Zielinski, J. M.; Fry, R.; Kimak, M. F. Probing Multicomponent Thermodynamic Effects by Low- and High-Pressure Capillary Column Inverse Gas Chromatography. *Macromolecules* **2004**, *37*, 10134-10140.

Chapter 2

Predictive Thermodynamic Models for Multicomponent Systems

2.1 Introduction

Knowledge of phase equilibria of a system is critical to polymer-solvent processing applications. Determining how a solvent will distribute through two or more phases is necessary for the design of extruders, reactors, and drying equipment. Because of the broad range of conditions encountered in industrial applications, there is often a lack of experimental data. Therefore, predictive thermodynamic models have been developed to accommodate engineers and scientists in their design of processes. Predictive thermodynamic models can be classified into two categories: activity coefficient models (ACMs) and equations of state (EoS). The benefits of the former are the extensive parameter tables and relatively simple calculation scheme. However, they do not account for volumetric effects and their use is generally limited to low pressure applications. The latter class of models accounts for the full PVT nature of the system although they have found less use and the parameters available are fewer.

The models discussed in this chapter employ group contribution methods for making predictions. In this theory, molecules can be broken into groups, each having characteristic size and energy parameters. By building a molecule using the defined

groups, predictions can be made *a priori* about the phase equilibrium to be expected in physical systems. Probably the most well known group contribution equation is UNIFAC [1]. However, the original UNIFAC neglects free volume effects in the combinatorial term and gives poor predictions for polymer-solvent systems. Oishi and Prausnitz [2]were the first to add a free volume term to UNIFAC to account for the unique behavior in such systems. Their UNIFAC-FV has found widespread application due to its simplicity and predictive capability. Other models either introduced a different free volume term [3,4], recast the combinatorial and free volume terms [5,6], or eliminated the term and accounted for the effect using the combinatorial term [7].

In the case of Kannan et al. [4] it was found that the empirical UNIFAC parameters for the water and -OH groups along with an inadequate free volume term resulted in unsatisfactory predictions for aqueous systems when applying UNIFAC-FV. In order to account for such systems, a revised free volume term was developed and the theoretical hard core volumes of the water and -OH groups were used in calculation of the new term. In their testing of the model they found that not only did the new model, UNIFAC-vdW-FV, predict accurately for aqueous systems, it offered improvement over UNIFAC-FV and Entropic-FV [5] for non-aqueous systems.

The alternative to activity coefficient models is an equation of state. The advantage of this method is that volumetric properties are considered and therefore, systems at high pressure can be studied. High and Danner [8] developed a group contribution form of the Panayiotou-Vera equation of state [9] which can accurately predict phase equilibria in polar and non-polar systems. One of the drawbacks is the limited group parameter listing. Chen et al. [10] developed a group contribution form of

the Flory equation of state which was later revised by Bogdanic and Fredenslund [11]. As shown by Lee and Danner [12] the revised GC-Flory EoS is has almost the same accuracy as UNIFAC-FV but has the benefit of not requiring pure component densities. More recently, there have been efforts to couple ACMs with established cubic equations of state such as the Peng-Robinson and Soave-Redlich-Kwong models. These equation of state/Gibbs energy models are actually a mixing rule for the energy parameter in cubic equations of state. Lastly, there have been efforts to develop a predictive form of the SAFT equation of state, specifically the perturbed chain (PC-SAFT) variant. Some work focused on use of monomer units for predicting the polymer parameters [13]. More recent efforts have attempted to apply group contribution methods [14,15], although the author is unaware of any testing of polymer systems with the proposed group parameters. The complexity of the equation, which is very capable at correlating vapor-liquid equilibria (VLE) and liquid-liquid equilibria (LLE), may prove a hindrance in developing a universally applicable predictive form of the equation.

The models chosen for use in this work were UNIFAC-FV, UNIFAC-vdW-FV, and GCLF-EoS. In this chapter a review of them is provided with a specific focus toward multicomponent applications. They have shown good accuracy in comparisons with other predictive models. Ideally one model could be applied to all the systems in this work. However, given the characteristics and parameter tables, it was necessary to use the ACMs and the EoS. The UNIFAC models contain certain parameters that GCLF-EoS lacks. However, GCLF-EoS is capable of predicting polymer-solvent-high pressure gas systems which was needed in Chapter 3.

2.2 Theory

One of the useful aspects of the UNIFAC-FV and UNIFAC-vdW-FV models is their implicit multicomponent nature. The models predict the activity coefficient of component *i* in a mixture of one or polymers and one or more solvents.

2.2.1 UNIFAC-FV

The UNIFAC-FV model uses a combinatorial expression developed by Staverman [17], a residual term based on Guggenheim's quasichemical theory [18], and a free volume term derived from the Flory equation of state [19]. The combinatorial term accounts for size and shape effects of the molecules, while the residual term accounts for energetic interactions. The free volume term added by Oishi and Prausnitz serves as a correction for the free volume differences between the polymer and solvent molecules. The following shows the activity coefficient represented in terms of the three contributions:

$$\ln \Omega_i = \ln \Omega_i^C + \ln \Omega_i^R + \ln \Omega_i^{FV} \tag{2.1}$$

where Ω_i is the activity coefficient of component *i* in the solution, Ω_i^C is the combinatorial term, Ω_i^R is the residual term, and Ω_i^{FV} is the free volume term. The combinatorial term is given by the following:

$$\ln \Omega_i^C = \ln \frac{\phi_i}{\omega_i} + 5q_i \ln \frac{\theta_i}{\phi_i} + l_i - \frac{\phi_i M_i}{\omega_i} \sum_j \frac{\omega_i l_i}{M_j} \tag{2.2}$$

where ϕ_i is the molecular volume fraction of component *i*, ω_i is the weight fraction of component *i* in the polymer phase, q_i is the surface area parameter of component *i*, θ_i is the molecular area fraction of component *i*, l_i is a parameter for component i, based on the group volume and group area parameters, and M_i is the molecular weight of component *i*. Oishi and Prausnitz recommended the use of the number average molecular weight when specifying the polymer.

The molecular volume fraction is calculated using the following equation:

$$\phi_i = \frac{\frac{r_i \omega_i}{M_i}}{\sum_j \frac{r_j \omega_j}{M_j}} \tag{2.3}$$

where r_i is the volume parameter for component *i*, given by this expression:

$$r_i = \sum_k \nu_k^{(i)} R_k \tag{2.4}$$

where $\nu_k^{(i)}$ is the number of groups of type *k*, in component *i*, R_k is the group volume parameter of group *k*, and *k* is the number of distinct groups in the solution. The values of R_k were determined from the van der Waals group volumes given by Bondi [20] and have been tabulated by Danner and High [21].

The molecular area fraction is calculated using the following equation:

$$\theta_i = \frac{\frac{q_i \omega_i}{M_i}}{\sum_j \frac{q_j \omega_j}{M_j}} \tag{2.5}$$

where q_i is the surface area parameter for component *i*, given by the following:

$$q_i = \sum_k \nu_k^{(i)} Q_k \tag{2.6}$$

where Q_k is the group surface area parameter of group *k*, values of which were determined from the van der Waals group surface areas also given by Bondi [20]. The term l_i is a parameter calculated using the volume and surface area parameters of component *i*, as follows:

$$l_i = 5(r_i - q_i) - (r_i - 1) \tag{2.7}$$

The residual term is given by the following:

$$\ln \Omega_i^R = \sum_k \nu_k^{(i)} \left[\ln \Gamma_k - \ln \Gamma_k^{(i)} \right] \tag{2.8}$$

where Γ_k is the residual activity coefficient of group *k*, in the polymer solution and $\Gamma_k^{(i)}$ is the residual activity coefficient of group *k*, in a reference solution assumed to contain pure component *i*.

The residual activity coefficient is calculated using the following equation:

$$\ln \Gamma_k = Q_k \left[1 - \ln\left(\sum_m \theta_m \psi_{mk} \right) - \sum_m \left(\frac{\theta_m \psi_{km}}{\sum_p \theta_p \psi_{pm}} \right) \right] \tag{2.9}$$

where *m* and *p* are the number of groups in the polymer solution, θ_m is the group surface area fraction of group *m*, and ψ_{mk} is the group interaction parameter between groups *m* and *k*. The group surface area fraction has the following form:

$$\theta_m = \frac{Q_m X_m}{\sum_p Q_p X_p} \tag{2.10}$$

where X_m is the mole fraction of group *m* in the solution. It is calculated by the following expression:

$$X_m = \frac{\sum_j \frac{\nu_m^{(i)} \omega_j}{M_j}}{\sum_j \frac{\omega_j}{M_j \sum_p \nu_p^{(j)}}} \tag{2.11}$$

where $\nu_m^{(j)}$ is the number of groups of type *m* in component *j* and *p* is the number of components in the mixture.

The residual activity component of group *k* in a reference solution containing pure component *i* is calculated with the same equations above, but only considering the groups present in the pure component.

The group interaction parameter function is calculated based on the group interaction parameter, a_{mn} as follows:

$$\psi_{mn} = \exp\left(\frac{-a_{mn}}{T}\right) \tag{2.12}$$

where T is the system temperature in Kelvins. Values for a_{mn} are tabulated [21] and new values for certain *mn* pairs have also been published [22].

The free volume term is given by the following:

$$\ln \Omega_i^{FV} = 3C_i \ln\left[\frac{\widetilde{v}_i^{1/3} - 1}{\widetilde{v}_M^{1/3} - 1}\right] - C_i\left[\left(\frac{\widetilde{v}_i}{\widetilde{v}_M} - 1\right)\left(\frac{1}{1 - \widetilde{v}_i^{-1/3}}\right)\right] \tag{2.13}$$

where C_i is an external degree of freedom parameter taken to be 1.1 for solvents, $\tilde{v}_i$ is the reduced volume of component *i*, and $\tilde{v}_M$ is the reduced volume of the mixture. The reduced volume of component *i* is calculated by the following equation:

$$\tilde{v}_i = \frac{v_i M_i}{0.01517 b r_i} \tag{2.14}$$

where v_i is the specific volume (m^3/kg) of component *i* and *b* is a proportionality factor taken to be 1.28. The reduced volume of the mixture is given as:

$$\tilde{v}_M = \frac{\sum v_i \omega_i}{0.01517 b \sum_i \frac{r_i \omega_i}{M_i}} \tag{2.15}$$

2.2.2 UNIFAC-vdW-FV

Kannan et al. [4] noted that the UNIFAC-FV model gave poor predictions of aqueous systems due to inadequacy of the free volume term based on the Flory EoS. They proposed a new free volume term derived directly from the van der Waals partition function. The original UNIFAC combinatorial and residual terms were retained in their development. The free volume term in UNIFAC-vdW-FV has the following form:

$$\ln \Omega_i^{FV} = \ln\left[\frac{\varphi_i^{FV}}{\varphi_i^h}\right] + \left[\frac{\varphi_i^h - \varphi_i^{FV}}{x_i}\right] \tag{2.16}$$

where the fraction of free-volume associated with component *i* is defined as:

$$\varphi_i^{FV} = \frac{x_i\left(v_i - v_i^*\right)}{\sum_j x_j\left(v_j - v_j^*\right)} \tag{2.17}$$

where v_i^* is the molar hardcore volume of component *i*. The fraction of hardcore volume of component *i* is:

$$\varphi_i^h = \frac{x_i v_i^*}{\sum_j x_j v_j^*} \tag{2.18}$$

Eq. 2.18 combined with Eq. 2.2 and 2.8 respresent the UNIFAC-vdW-FV model. The above equations are written in general form and can therefore be applied to a polymer-mixed solvents system without further modification.

2.2.3 GCLF-EoS

The canonical partition function was used as the starting point for the GCLF-EoS. It is written as:

$$Q = \sum_i \exp\left[-\frac{E_i(V, N_1, N_2, ..., N_n)}{kT} \right] \tag{2.19}$$

From this expression the canonical partition function for a mixture can be expressed in terms of the combinatorial and energetic terms:

$$Q = \left[\prod_i \left(\frac{\delta_i}{\sigma_i} \right)^{N_i} \right] g_c g_{nr} \exp\left(-\frac{E}{kt} \right) \tag{2.20}$$

The first term includes the geometric characteristics of the molecules and does contribute to the mixing properties.

The random combinatorial, g_c, as derived by Guggenheim [18] relates the number of holes, N_h, and molecules, N_i, of r_i-mers on a lattice including N_r total sites and N_q total contact sites. It has the following form:

$$g_c = \frac{N_r!}{N_h! \prod_i N_i!} \left(\frac{N_q!}{N_r!} \right)^{z/2} \tag{2.21}$$

where z is the coordination number which has a fixed value of 10.

Guggenheim [18] also derived the non-random combinatorial term, g_{nr}, which accounts for the effect of local compositions in the solution. It is expressed as:

$$g_{nr} = \frac{\prod_i \overline{N}_{ii}^{0}! \prod_{j>i} \left[\left(\frac{\overline{N}_{ij}^{0}}{2} \right)! \right]^2}{\prod_i \overline{N}_{ii}! \prod_{j>i} \left[\left(\frac{\overline{N}_{ij}}{2} \right)! \right]^2} \tag{2.22}$$

In this expression N_{ii} and N_{ij} are the number of i-i and i-j segment contacts, respectively. The bar over the numbers of contacts indicates that the calculation is made on a hole-free basis. The zero superscript refers to the number of contacts assuming a random lattice of hole and molecules. In their development of the equation of state, Panayiotou and Vera [9] assumed the molecules could be non-randomly distributed but the holes were assumed to be randomly positioned on the lattice. The same approach was adopted by High and Danner [8].

The total lattice energy is the sum of the products of the number of nearest neighbor contacts, expressed as:

$$\begin{aligned} -E &= \frac{1}{N_a} \left(\sum_i N_{ii} \varepsilon_{ii} + \sum_{i=1} \sum_{j>i} N_{ij} \varepsilon_{ij} \right) \\ &= \frac{\theta}{N_a} \left(\sum_i \overline{N}_{ii} \varepsilon_{ii} + \sum_{i=1} \sum_{j>i} \overline{N}_{ij} \varepsilon_{ij} \right) \end{aligned} \tag{2.23}$$

where θ is the total molecular surface fraction and N_a is Avogadro's number. ε_{ii} is the pure component interaction and ε_{ij} is the cross interaction energy.

2.2.3.1 Equation of State

The equation of state for a mixture is derived from the following expression:

$$P = kT\left(\frac{\partial \ln Q}{\partial V}\right)_{T,N_1,\ldots,N_n} \tag{2.24}$$

Substitution of Eq. 2.20 into Eq. 2.24 and differentiation leads to the reduced form of the equation of state as shown below.

$$\frac{\widetilde{P}}{\widetilde{T}} = \ln\left(\frac{\widetilde{v}}{\widetilde{v}-1}\right) + \frac{z}{2}\ln\left(\frac{\widetilde{v}+q/r-1}{\widetilde{v}}\right) - \frac{\theta^2}{\widetilde{T}} \tag{2.25}$$

where the reduced pressure, temperature, and volume are defined as:

$$\widetilde{P} = \frac{2Pv_h}{z\varepsilon^*} \tag{2.26}$$

$$\widetilde{T} = \frac{2RT}{z\varepsilon^*} \tag{2.27}$$

$$\widetilde{v} = \frac{v}{v_h r} \tag{2.28}$$

Simple combining rules are used for the geometric mixture parameters:

$$\theta = \sum_i \theta_i \tag{2.29}$$

$$r = \sum_i x_i r_i \tag{2.30}$$

$$q = \sum_i x_i q_i \tag{2.31}$$

The pure component parameters in Eq. 2.29 - 2.31 are defined as:

$$\theta_i = \frac{z q_i N_i}{z N_q} \tag{2.32}$$

$$r_i = \frac{v_i^*}{v_h} \tag{2.33}$$

$$q_i = \frac{(z-2) r_i + 2}{z} \tag{2.34}$$

In Eq. 2.33, v_h is the volume of a lattice site which was set to a fixed value equal to the volume of a methylene group in polyethylene (9.75×10^{-3} m^3/kmol) The non-randomness parameters, Γ_{ii} and Γ_{ij}, are included in the calculation of the interaction energy of the mixture:

$$\varepsilon^* = \sum_i \bar{\theta}_i^2 \Gamma_{ii} \varepsilon_{ii} + \sum_i \sum_{j>i} 2 \bar{\theta}_i \bar{\theta}_j \Gamma_{ij} \varepsilon_{ij} \tag{2.35}$$

In this expression the molecular surface fraction is defined on a hole-free basis. It is expressed as:

$$\bar{\theta}_i = \frac{\theta_i}{\theta} \tag{2.36}$$

High and Danner [8] developed the GCLF-EoS by introducing group contribution mixing rules for the adjustable parameters in Eq. 2.25. The only input required to make phase equilibrium calculations with the GCLF-EoS is the structure of the molecules.

2.2.3.2 Group Contribution Mixing Rules

The mixing rule for the energetic parameter, ε_{ii}, is expressed as:

$$\varepsilon_{ii} = \sum_k \sum_m \Theta_k^{(i)} \Theta_m^{(i)} \left(e_{kk} e_{mm} \right)^{1/2} \tag{2.37}$$

where e_{kk} is the group interaction energy between like groups *k*. The group surface area fractions, $\Theta_k^{(i)}$, are expressed by:

$$\Theta_k^{(i)} = \frac{n_k^{(i)} Q_k}{\sum_n n_n^{(i)} Q_n} \tag{2.38}$$

where $n_k^{(i)}$ is the number of group *k* in component *i*, and Q_k is the dimensionless surface area parameter of group *k* as used in the UNIFAC method [1].

The cross-interaction energy, ε_{ij}, is represented by the geometric mean of the pure component interaction energies corrected with a binary interaction parameter, k_{ij}:

$$\varepsilon_{ij} = \left(\varepsilon_{ii} \varepsilon_{jj} \right)^{1/2} \left(1 - k_{ij} \right) \tag{2.39}$$

The molecular reference volume parameter is given by the following relation:

$$v_i^* = \sum_k n_k^{(i)} R_k \tag{2.40}$$

where R_k is the group reference volume parameter.

Lee and Danner [16] assigned a quadratic dependence on temperature to the group interaction energies and group reference volume parameters:

$$e_{kk} = e_{0,k} + e_{1,k}\left(\frac{T}{T_0}\right) + e_{2,k}\left(\frac{T}{T_0}\right)^2 \tag{2.41}$$

$$R_k \times 10^3 = R_{0,k} + R_{1,k}\left(\frac{T}{T_0}\right) + R_{2,k}\left(\frac{T}{T_0}\right)^2 \tag{2.42}$$

Here T is the system temperature in kelvin and T_0 is 273.15 K.

The first mixing rule developed for the binary interaction parameter, k_{ij}, by Lee and Danner [16] was expressed as:

$$k_{ij} = \sum_m \sum_n \Theta_m^{(M)} \Theta_n^{(M)} \alpha_{mn} \tag{2.43}$$

where $\Theta_m^{(M)}$ is the surface area fraction of group m in the mixture. It has the following form:

$$\Theta_m^{(M)} = \frac{\sum_i n_m^{(i)} Q_m}{\sum_k \sum_i n_k^{(i)} Q_k} \tag{2.44}$$

An alternative k_{ij} mixing rule was later introduced by Hamedi et al. [23] which only accounted for the interaction of groups of unlike species.

$$k_{ij} = \sum_m \sum_n \Theta_m^{(i)} \Theta_n^{(j)} \alpha_{mn} \tag{2.45}$$

In their formulation $\Theta_m^{(i)}$ and $\Theta_n^{(j)}$ are calculated using Eq. 2.38.

Estimation of the group parameters is described elsewhere [16,24].

2.2.3.3 Non-randomness Parameters

Using Guggenheim's quasi-chemical approach, Panayiotou and Vera introduced the following relationship between the non-randomness parameters and the interchange energy, $\Delta\varepsilon_{ij}$ [25]:

$$\frac{\Gamma_{ii}\Gamma_{jj}}{\Gamma_{ij}^2} = \exp\left(\theta\frac{\Delta\varepsilon_{ij}}{RT}\right) \tag{2.46}$$

where

$$\Delta\varepsilon_{ij} = \varepsilon_{ii} + \varepsilon_{jj} - 2\varepsilon_{ij} \tag{2.47}$$

In addition, conservation of contacts dictates that:

$$\overline{\theta}_i\Gamma_{ii} + \sum_{j\neq i}\overline{\theta}_j\Gamma_{ij} = 1 \tag{2.48}$$

For the case of $\Delta\varepsilon_{ij} = 0$, $\Gamma_{ii} = \Gamma_{ij} = 1$. As pointed out by the author [26], the geometric mixing rule for ε_{ij} introduced by High and Danner prevents satisfying this criterion for a randomly mixed solution. In the Panayiotou-Vera equation of state the enthalpic interaction energy was treated as an adjustable parameter. Therefore, it was possible to adjust the energy parameter such that $\Delta\varepsilon_{ij} = 0$. This is the main theoretical distinction between the PV-EoS and GCLF-EoS. The result of this difference is that the

non-randomness parameters can be omitted when calculating VLE with the GCLF-EoS with little or no effect on the phase equilibria predictions.

2.3 References

1. Fredenslund, Aa.; Jones, R. L.; Prausnitz, J. M. Group-Contribution Estimation of Activity Coefficients in Nonideal Liquid Mixtures. *AIChE J.* **1975**, *21*, 1086-1099.

2. Oishi, T.; Prausnitz, J. M. Estimation of Solvent Activities in Polymer Solutions Using a Group-Contribution Method. *Ind. Eng. Chem. Process Des. Dev.*, **1978**, *17*, 333-339.

3. Liu, Q. L.;, Cheng, Z. F. A Modified UNIFAC Model for the Prediction of Phase Equilibrium for Polymer Solutions. *J. Polym. Sci., Part B: Polym. Phys.* **2005**, *43*, 2541–2547.

4. Kannan, D. C.; Duda, J. L.; Danner, R. P. A Free-Volume Term Based on the van der Waals Partition Function for the UNIFAC Model. *Fluid Phase Equilib.*, **2005**, *228-229*, 321-328.

5. Elbro, H. S.; Fredenslund, Aa.; Rasmussen, P. A New Simple Equation for the Prediction of Solvent Activities in Polymer-Solutions. *Macromolecules* **1990**, *23*, 4707-4714.

6. Kontogeorgis, G. M.; Fredenslund, Aa.; Tassios, D. P. Simple Activity Coefficient Model for the Prediction of Solvent Activities in Polymer Solutions. *Ind. Eng. Chem. Res.* **1993**, *32*, 362-372.

7. Zhong, C.; Sato, Y.; Masuoka, H.; Chen, X. Improvement of Predictive Accuracy of the UNIFAC Model for Vapor-Liquid Equilibria of Polymer Solutions. *Fluid Phase Equilib.* **1996**, *123*, 97-106.

8. High, M. S.; Danner, R. P., Application of the Group Contribution Lattice-Fluid EoS to Polymer Solutions. *AIChE J.* **1990**, *36*, 1625-1632.

9. Panayiotou, C.; Vera, J.H. Statistical Thermodynamics of r-mer Fluids and Their Mixtures. *Polym. J.* **1982**, *14*, 681-694.

10. Chen, F.; Fredenslund, Aa.; Rasmussen, P. Group-Contribution Flory Equation of State for Vapor-Liquid Equilibria in Mixtures with Polymers. *Ind. Eng. Chem. Res.* **1990**, *29*, 875-882.

11. Bogdanic, G.; Fredenslund, A. Prediction of Vapor-Liquid Equilibria for Mixtures with Copolymers. *Ind. Eng. Chem. Res.* **1995**, *34*, 324-331.

12. Lee, B. -C.; Danner, R. P. Prediction of Infinite Dilution Solvent Activity Coefficients in Polymer Solutions: Comparison of Prediction Models. *Fluid Phase Equilib.* **1997**, *128*, 97-114.

13. Kouskoumvekaki, I. A.; von Solms, N.; Lindvig, T.; Michelsen, M. L.; Kontogeorgis, G. M. Novel Method for Estimating Pure-Component Parameters for Polymers: Application to the PC-SAFT Equation of State. *Ind. Eng. Chem. Res.* **2004**, *43*, 2830-2838.

14. Tamouza, S.; Passarello, J.-P.; de Hemptinne, J.-C.; Tobaly, P. Group Contribution Method with SAFT EOS Applied to Vapor Liquid Equilibria of Various Hydrocarbon Series. *Fluid Phase Equilib.* **2004**, *222–223*, 67-76.

15. Thi, T. X. N.; Tamouza, S.; Tobaly, P.; Passarello, J. -P.; de Hemptinne, J. -C. Application of Group Contribution SAFT Equation of State (GC-SAFT) to Model Phase Behaviour of Light and Heavy Esters. *Fluid Phase Equilib.* **2005**, *238*, 254–261.

16. Lee, B. -C.; Danner, R. P. Prediction of Polymer-Solvent Phase Equilibria by a Modified Group-Contribution EOS. *AIChE J.* **1996**, *42*, 837-849.

17. Staverman, A. J. The Entropy of High Polymer Solutions. Generalization of Formulae. *Rec. Trav. Chim. Pays-Bas.* **1950**, *69*, 163-174.

18. Guggenheim, E.A. *Mixtures*; Clarendon Press: Oxford, **1952**.

19. Flory, P. J.; Orwall, R. A.; Vrij, A. Statistical Thermodynamics of Chain Molecule Liquids. I. An Equation of State for Normal Paraffin Hydrocarbons. *J. Am. Chem. Soc.* **1964**, *86*, 3507-3514.

20. Bondi, A. Physical Properties of Molecular Crystals, Liquids and Glasses, Wiley, New York, N.Y., **1968**.

21. Danner, R. P.; High, M. S. *Handbook of Polymer-Solution Thermodynamics*; Design Institute for Physical Property, Data American Institute of Chemical Engineers: New York, **1993**.

22. Wibawa, G.; Takishima, S.; Sato, Y.; Masuoka, H. Revision of UNIFAC Group Interaction Parameters of Group Contribution Models to Improve Prediction Results of Vapor-Liquid Equilibria for Solvent-Polymer Systems. *Fluid Phase Equilib.* **2002**, *202*, 367-383.

23. Hamedi, M.; Muralidharan, V.; Lee, B. -C.; Danner, R. P. Prediction of Carbon Dioxide Solubility in Polymers Based on a Group-Contribution Equation of State. *Fluid Phase Equilib.* **2003**, *204*, 41-53.

24. High, M. S.; Danner, R. P. A Group Contribution Equation of State for Polymer Solutions. *Fluid Phase Equilib.* **1989**, *53*, 323-330.

25. Panayiotou, C.; Vera, J. H. The Quasi-Chemical Approach for Non-Randomness in Liquid-Mixtures - Expressions for Local Surfaces and Local Compositions with an Application to Polymer-Solutions. *Fluid Phase Equilib.* **1980**, *5*, 55-80.

26. Jones, A. T.; Derawi, S.; Danner, R. P.; Duda, J. L. A Simplified Approach to Vapor–Liquid Equilibria Calculations with the Group-Contribution Lattice-Fluid Equation of State. *Fluid Phase Equilib.* **2007**, *In Press*.

Chapter 3

High Pressure Inverse Gas Chromatography

3.1 Introduction

In polymer-solvent systems the diffusion coefficient can decrease several orders of magnitude as the solvent becomes infinitely dilute in the polymer. This can often lead to a mass transfer limited step in the devolatilization of polymers. Plasticization of the polymer by a cosolvent gas can counteract this effect and lead to shorter processing times. In addition, reduced thermodynamic interactions between the polymer-solvent due to a cosolvent gas also aids solvent removal by increasing the thermodynamic driving force for the exit of solvent.

Knowledge of the influence cosolvent gases have on polymer-solvent systems could greatly improve existing devolatilization processes. Replacement of inert gases with ones that influence the mass transport and thermodynamics could result in higher throughput in the manufacture of films, insulating foams, polymers for drug delivery, and bulk plastics. In this work, high pressure IGC (HPIGC) was used to study the influence of CO_2 and ethylene on polymer-solvent transport and thermodynamic behavior in poly(styrene) (PS) and poly(vinyl acetate) (PVAc) systems. The objective of the project was to determine which gas had a stronger influence on the systems. Also, it was desired

to determine if the influence of the gases increased or decreased based on the size of the solvent.

3.2 Background

Gas chromatography is based on the equilibrium partitioning of a solute between a mobile phase and a stationary solid or liquid phase. In traditional gas chromatography it is the mobile solute phase that is of interest. Application of the technique to polymer-solvent systems is referred to as "inverse gas chromatography" (IGC) because the stationary polymer phase is of equal interest.

An inert carrier gas transports a small pulse of solvent through the column and the elution of solvent is measured using a detector. The interactions of the solvent with the polymer affect the retention time. The mass transfer resistance the solvent encounters causes the peak to broaden. The effect of these phenomena is revealed in the elution profile, which can be related to the partition coefficient (thermodynamics) and diffusion coefficient (mass transport). IGC has been proven successful in measuring the partition and diffusion coefficient in polymer-solvent systems [1-7]. In addition to infinite dilution measurements, IGC has been extended to finite concentration measurements [8-14]. Although Brockmeier et al. [11] showed that the technique could be operated at high pressure, there was little interest in its application until recently. Alessi et al. [15] demonstrated that IGC operated with high pressure CO_2 could be used to measure reductions in T_g. More recently, Zielinski et al. [16] showed that IGC could be used to

determine the influence of high pressure gases on the infinite dilution solubility and diffusivity of solvents in polymers.

3.3 Experimental Method

In this section the apparatus is briefly explained and modifications necessary for testing at high pressures are given in detail. The equipment used in this study is similar to that used in analytical GC. The main components are the carrier gas delivery system, injection port, GC oven which houses the column, and a detector of various types (e.g., thermal conductivity, flame ionization, mass spectrometer). A schematic of the experimental setup is shown in Figure 3-1.

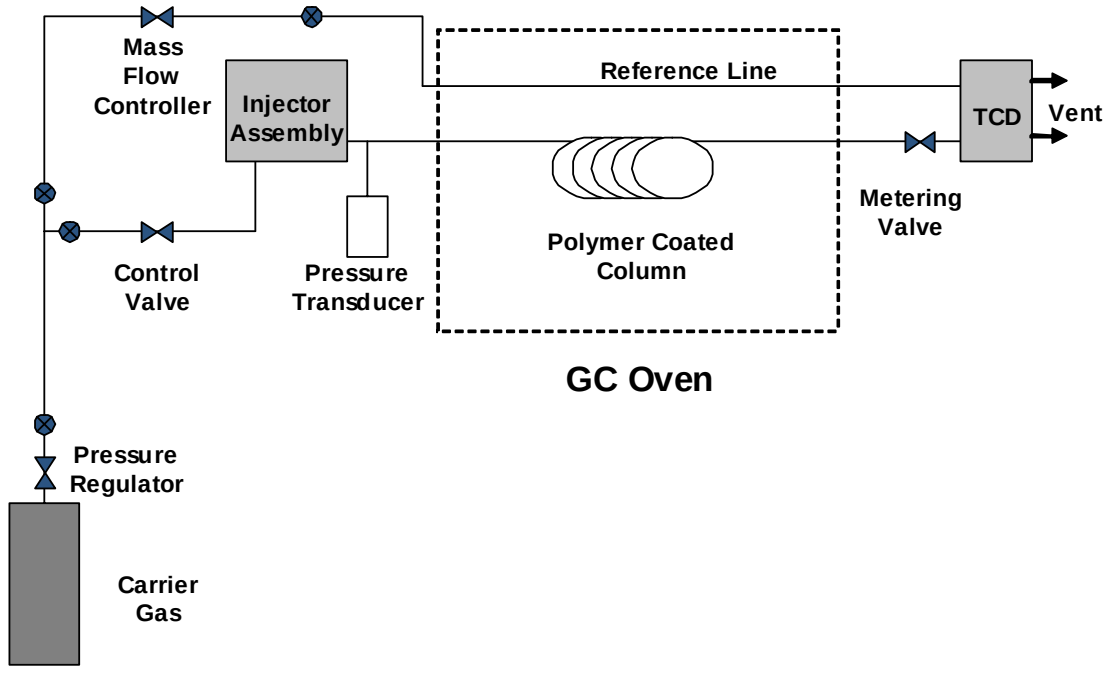

Figure 3-1: Experimental setup for HPIGC.

3.3.1 Modifications for High Pressure Experimentation

An HP 5890 gas chromatograph was used as the main component in design of the high pressure unit. It was equipped with a thermal conductivity detector (TCD). The maximum operating temperature of the oven is around 300°C. A photo of the equipment is shown in Figure 3-2.

Figure 3-2: Photo of the apparatus. The gas delivery system is on the left. The HP 5890 GC appears on the right side with the injector temperature zone controller to the far right of the photo. The Tylan mass flow controller interface sits between the GC and gas delivery system. Overhead vents are used to remove exhaust gases generated during experimentation.

The key modifications for testing at high pressures involved the injection port, gas delivery system, and flow and pressure regulation in the column.

3.3.1.1 Injection Assembly

The typical IGC apparatus employs a rubber septa fitted injection port that cannot withstand high pressures. Therefore, a Rheodyne model number 7410 sample injector was installed for uninterrupted injection of the solvent to the carrier gas at high pressures. The sample injector had an upper pressure limit of 7000 psia. The injection volume of the sample injector loop was 0.5 μL. During an experiment the loop was filled with solvent while in the load position and the injector was then pneumatically switched to the inject position to introduce the solvent onto the column.

3.3.1.2 Carrier Gas Delivery System

A gas delivery system was designed for controlling pressures and flows through the capillary column and reference lines. The gas source was a typical cylinder and controlled by a regulator. The line from the regulator was split with one line supplying high pressure gas to the capillary column and the other line supplying gas to the reference line flow control system.

A Tescom (maximum operating pressure of 4000 psig) regulator was used to control the pressure inside the column. The pressure was monitored using a Heise pressure transducer rated up to 3000 psig. To control the flow through the column, a

Swagelok metering valve (model no. SS-SS1-MH) was fitted to the column exit tubing. This valve was installed outside the GC oven to permit testing systems at high temperatures. The line from the metering valve was run back inside the oven and into the detector inlet. Testing was performed to ensure the additional dead volume added by the valve placement did not contribute to peak spreading and erroneous diffusion results. The existing thermal conductivity detector (TCD) of the HP 5890 was used without modification. The lines from the sample injector to the column were heated with heating tape. Temperatures in that zone were controlled with a Watlow Series 935A temperature controller. A standard Windows-based personal computer was used for control of the TCD and GC temperatures zones, as well as collection of data.

A Tylan model FC-260 mass flow controller along with a Tylan RO-28 controller module was used for delivery of gas to the reference line. The upper pressure limit of 150 psig precluded use of the mass flow controller for use with the column supply lines.

Prior to carrying out an injection, the system was allowed to equilibrate for 30 minutes after any change in pressure or temperature so that equilibrium was reached between the carrier gas and polymer.

3.3.2 Materials

The poly(styrene) (PS) coated column was provided and coated by Restek (Bellefonte, PA) with a 10μm thick coating. The poly(vinyl acetate) (PVAc) coated column was coated in the Center for the Study of Polymeric Systems at Penn State University. The column specifications are listed in Table 3-1.

Table 3-1: Capillary column specifications

Polymer	Length (cm)	Inner diameter (cm)	Coating thickness (μm)
PS	1562	0.053	10
PVAc	925	0.053	5

Solvents used in this work were received from Sigma Aldrich and used without further purification. Helium, CO_2, and ethylene gases were UHP, bone dry, and chemically pure grade, respectively.

3.4 Analysis of Data

Macris [17] modeled the capillary column as a straight cylindrical tube with an annular film of polymer deposited on the inner wall. One of the assumptions was that a uniform coating existed. Pawlisch modified the model developed by Macris and provided a detailed description of the model for capillary columns [18]. The following expression (in the Laplace domain) for the concentration profile at the exit of the column was developed:

$$\frac{\overline{C}L}{C_0 v} = \exp\left[\frac{1}{2\gamma}\right]\exp\left[-\left(\frac{1}{4\gamma^2}+\frac{s}{\gamma}+\frac{2\sqrt{s}}{\alpha\beta\gamma}\tanh\left(\beta\sqrt{s}\right)\right)^{1/2}\right] \tag{3.1}$$

where

$$\alpha = \frac{R}{K\left(1-y_1\right)\tau} \tag{3.2}$$

$$\beta^2 = \frac{\tau^2 v}{D_p L} \tag{3.3}$$

$$\gamma = \frac{D_g}{vL} \tag{3.4}$$

In the above expressions, $\overline{C}$ is the eluent concentration, C_0 is the initial concentration, L is the length of the capillary column, τ is the thickness of the polymer coating, R is the radius of the column from the centerline to the surface of the polymer coating (i.e., column radius minus polymer thickness), D_g is the diffusion coefficient of solvent in the carrier gas, v is the velocity of carrier gas, D_p is the mutual diffusion coefficient for the polymer-solvent system, K is the partition coefficient, and y_1 is the concentration of solvent in the carrier gas.

Methods of obtaining parameter estimates for Eq. 3.1 from elution profiles fall into one of four categories: method of moments, time-domain fitting, Laplace domain fitting, or Fourier domain fitting. The merits of each method were discussed by Pawlisch et al. [3]. Moment analysis works well when the elution profile is nearly symmetric with well-defined end points. However, the use of the method for response curves with significant tailing was found to be unreliable. Estimation of the model parameters in the time domain avoids these difficulties and is preferred for its increased accuracy and reliability. In this work a fast Fourier inverse transform was used to invert the solution at the column exit from the Laplace domain to the time domain. A nonlinear regression routine was then performed on the data to obtain α and β.

The key assumption in traditional IGC that is no longer valid is that the carrier gas is insoluble in the polymer phase. The finite solubility of the carrier gas in the polymer results in swelling which changes the film thickness of the polymer. In addition the gas phase pressure could affect the regressed parameters for the polymer-solvent interactions. One of the initial efforts was to examine that behavior. The solubility and diffusivity of methanol at infinite dilution was measured at increasing pressures of the helium carrier gas. Helium is not appreciably soluble in PVAc and therefore is not expected to influence the partitioning of methanol in the polymer. This is verified in Figure 3-3.

The diffusion shows a slight decrease with increasing pressure of helium. This may be due to increased mass transfer resistance in the gas phase. Zielinski et al. [16] observed similar behavior for PVAc-vinyl acetate at elevated helium pressures. However, this trend is within experimental error and the existing IGC model was used without modification for analysis of the elution profile data obtained in the experiments.

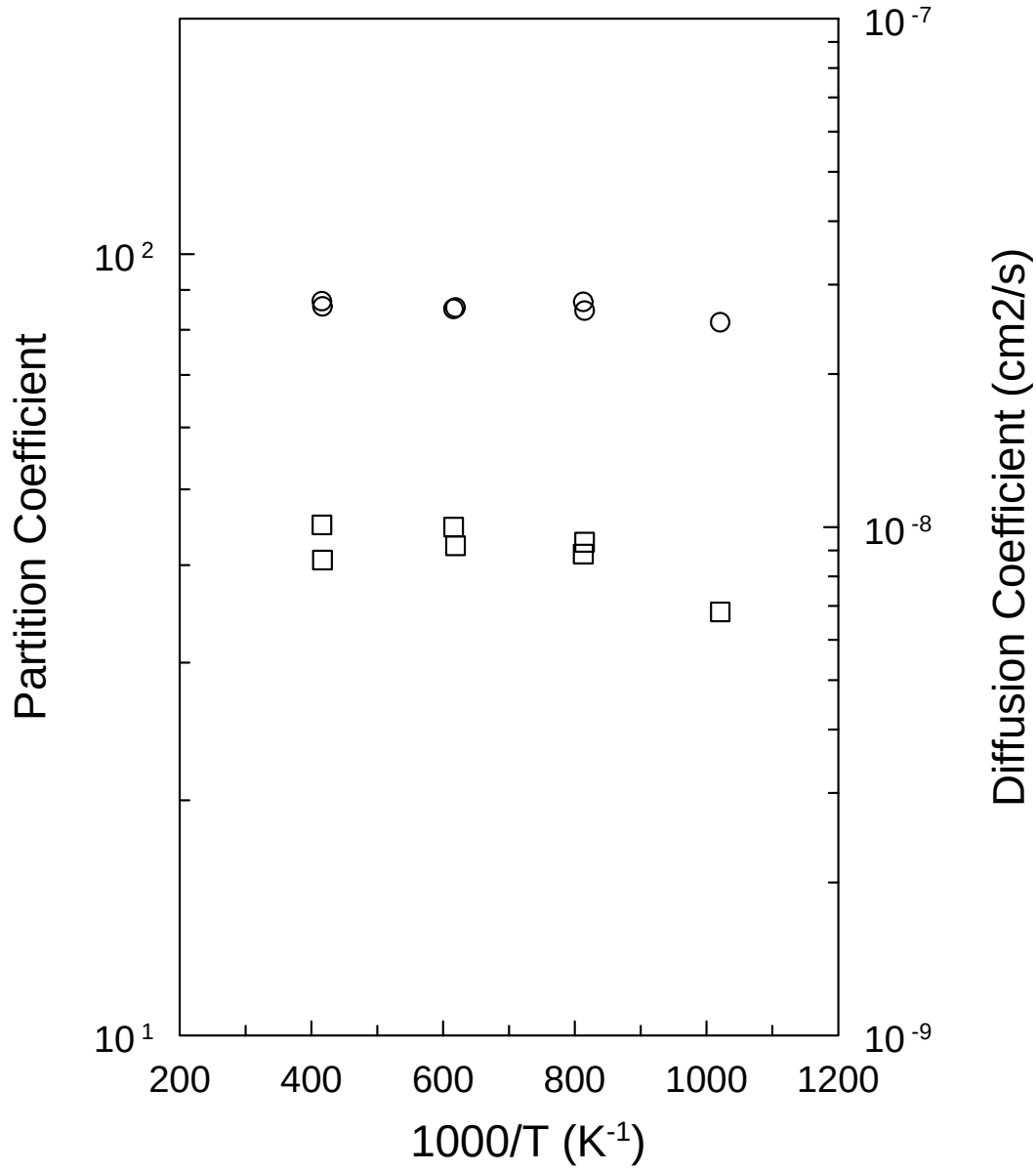

Figure 3-3: Diffusion (□) and partition coefficient (○) of PVAc-methanol system at 60°C as a function of helium carrier gas pressure.

Table 3-2: Partition and diffusion coefficients of methanol in PVAc at 60°C and varying pressures of helium carrier gas.

Helium Pressure (psia)	**K**	**D_p (10^9 cm2/s)**
417	85.8	8.62
416	87.1	10.1
616	85.1	10.0
619	85.4	9.19
815	84.7	9.34
813	86.9	8.85
1021	81.8	6.81

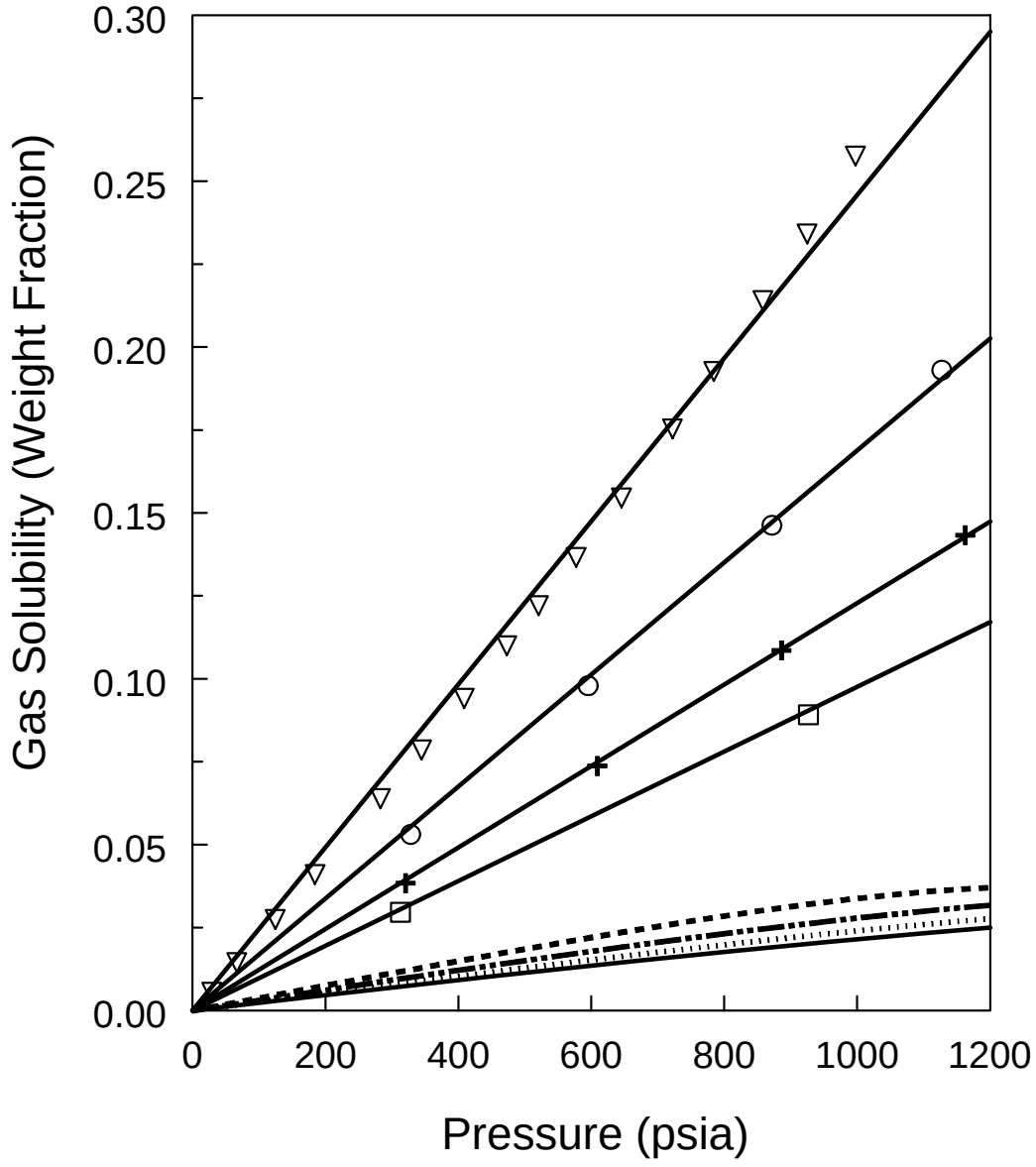

Figure 3-4: Solubility of the carrier gases in PVAc. Experimental data for CO_2 at 40 (▽), 60 (○), 80 (✚), and 100°C (□) taken from Sato et al. [19]. Lines through data are Henry Law correlations. Solubility of ethylene in PVAc was predicted with GCLF-EoS with a single binary interaction parameter (k_{ij} = 0.0264) for all temperatures and concentrations. Predictions were made at 40 (– – –), 60 (— · ·), 80(·····), and 100°C (———) for comparison with CO_2 data at those temperatures.

The film thickness was corrected by determining the binary solubility of the interacting carrier gases in the polymers. Experimental data from Sato et al. [19] was used for CO_2 with PVAc and PS. Due to the lack of experimental data for ethylene in those polymers, the density and solubility were estimated at the experimental conditions using the GCLF-EoS. The solubility of the carrier gases in PVAc and PS is shown in Figures 3-4 and 3-5, respectively. CO_2 has a higher solubility than ethylene in both polymers. CO_2 is considerably more soluble than ethylene in PVAc at a given temperature and pressure. However, the solubility of the two gases is comparable in PS.

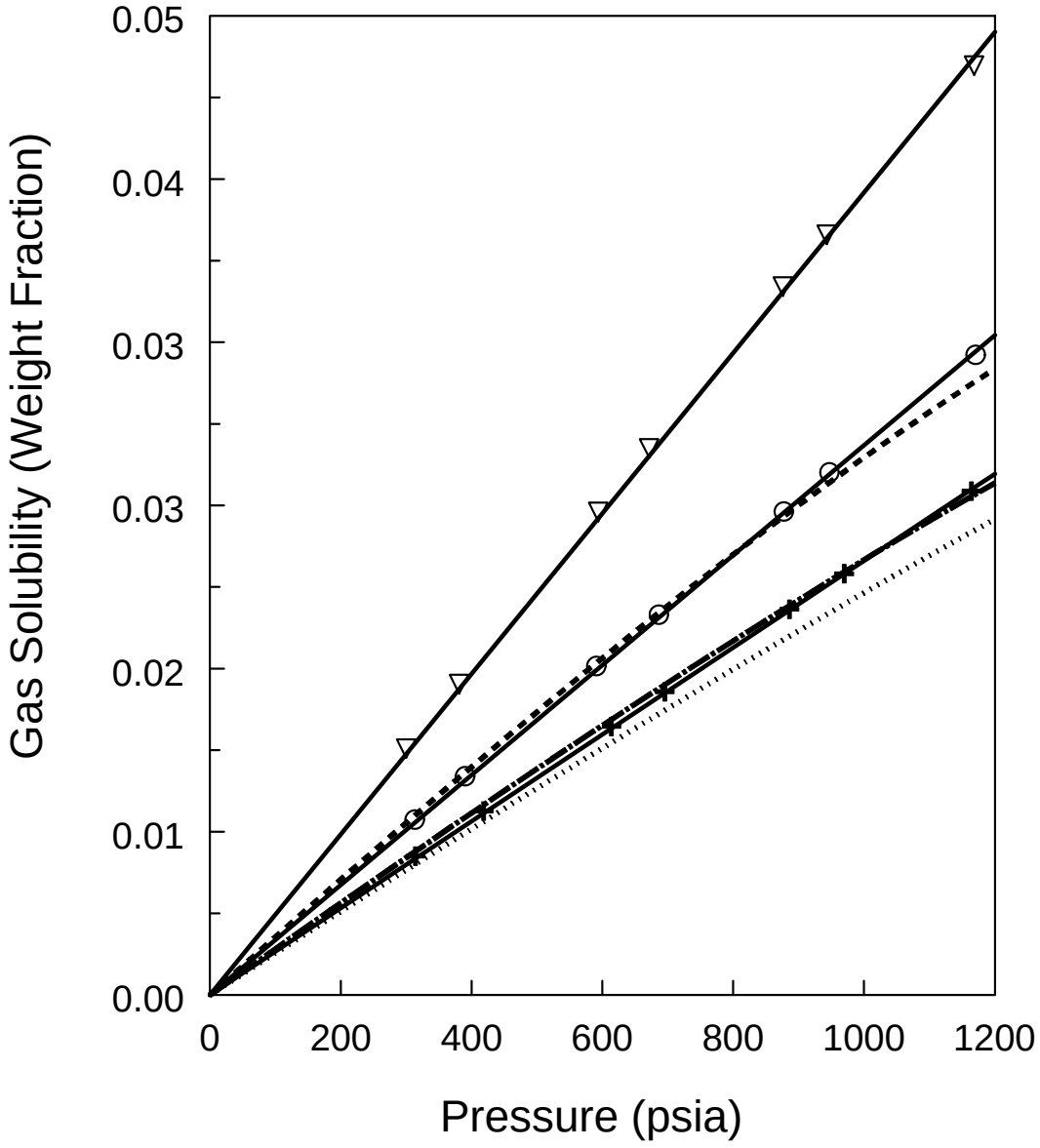

Figure 3-5: Solubility of the carrier gases in PS. Experimental data for CO_2 at 100 (▽), 150 (○), and 200°C (✚) taken from Sato et al. [19]. Lines through data are Henry Law correlations. Solubility of ethylene in PS was predicted with GCLF-EoS with a single binary interaction parameter (k_{ij} = 0.0081) for all temperatures and concentrations. Predictions were made at 100 (— — —), 150 (—— · ·), and 200°C (·····) for comparison with CO_2 data at those temperatures.

Henry's Law constants were used to determine the solubility of CO_2 at different temperatures used in this work. In addition, k_{ij} was regressed using the experimental data to calculate the density of the polymers with CO_2 using the GCLF-EoS. For the ethylene experiments, the solubility and density were both predicted with the GCLF-EoS.

The film thickness when swollen is determined by the following:

$$V_{swollen} = V_{column} - V_{inner} \tag{3.5}$$

where $V_{swollen}$ is the volume of swollen polymer in the capillary column, V_{column} is the total volume of the column, and V_{inner} is the volume inside the column not occupied by polymer. Note that the polymer is assumed to be non-porous and form a uniform coating on the column wall.

The volume of the swollen polymer can be written in terms of known variables.

$$V_{swollen} = \frac{m_{gp} + m_p}{\rho_{so\ln}} \tag{3.6}$$

where m_{gp} is the mass of carrier gas in the polymer, m_p is the mass of polymer in the column, and $\rho_{so\ln}$ is the density of the polymer-gas mixture at the experimental conditions.

The volume of the column depends on its dimensions:

$$V_{column} = \pi R^2 L \tag{3.7}$$

where R is the column radius and L is the length of the column (see Table 3-1).

The volume of the inside of the column depends on the swollen film thickness:

$$V_{inner} = \pi\left(R - \tau_{swollen}\right)^2 L \tag{3.8}$$

where $\tau_{swollen}$ is the swollen film thickness.

Substitution of Eqs. 3.6-3.8 into Eq. 3.5 and rearrangement leads to the following expression for the swollen film thickness:

$$\tau_{swollen} = R - \left[R^2 - \frac{m_{gp} + m_p}{\pi L \rho_{so\ln}} \right]^{1/2} \tag{3.9}$$

The largest swelling occurred in PVAc-CO_2, where the film thickness changed as much as 17% at the highest pressures and lowest temperatures used in this study. For PS-CO_2 the largest change was around 5%. Because the solubility of ethylene in the polymers is lower than that of CO_2, the swelling was lower. In PVAc, the change was about 3% while in PS the change was only about 1%.

3.5 Results

3.5.1 Ambient Pressure Benchmarking

The first step in this work was to verify the accuracy of the apparatus in obtaining low pressure non-interacting carrier gas data. This was necessary because the equipment was also used to obtain normal IGC data for comparison with the high pressure data. In addition, one of the important features of the design is the external metering valve that controls the flow through the capillary column. The valve was placed outside the GC oven to permit testing at high temperatures. However, it was unclear if the dead volume

of tubing and valve space between the end of the column and the detector would affect the data obtained.

In these experiments, the pressure of helium in the column was typically 150 psia or less. That is well below the level at which it is expected to see any influence on the results, as indicated by Figure 3-3.

3.5.1.1 PVAc Systems

The partition and diffusion coefficients of methanol, toluene, methyl acetate, and vinyl acetate were measured at temperatures in the range of 40-100°C. The results for PVAc with toluene and methanol are shown in Figures 3-6 and 3-7. The data show the expected trends. The diffusion coefficient increases with increasing temperature while the partition coefficient decreases with increasing temperature. As expected the apparent activation energy of diffusion for methanol is lower than that of the bulkier toluene species. There is good agreement between the results from the HPIGC and literature. Slightly more scatter is observed in the values of the diffusion coefficients compared to the partition coefficients.

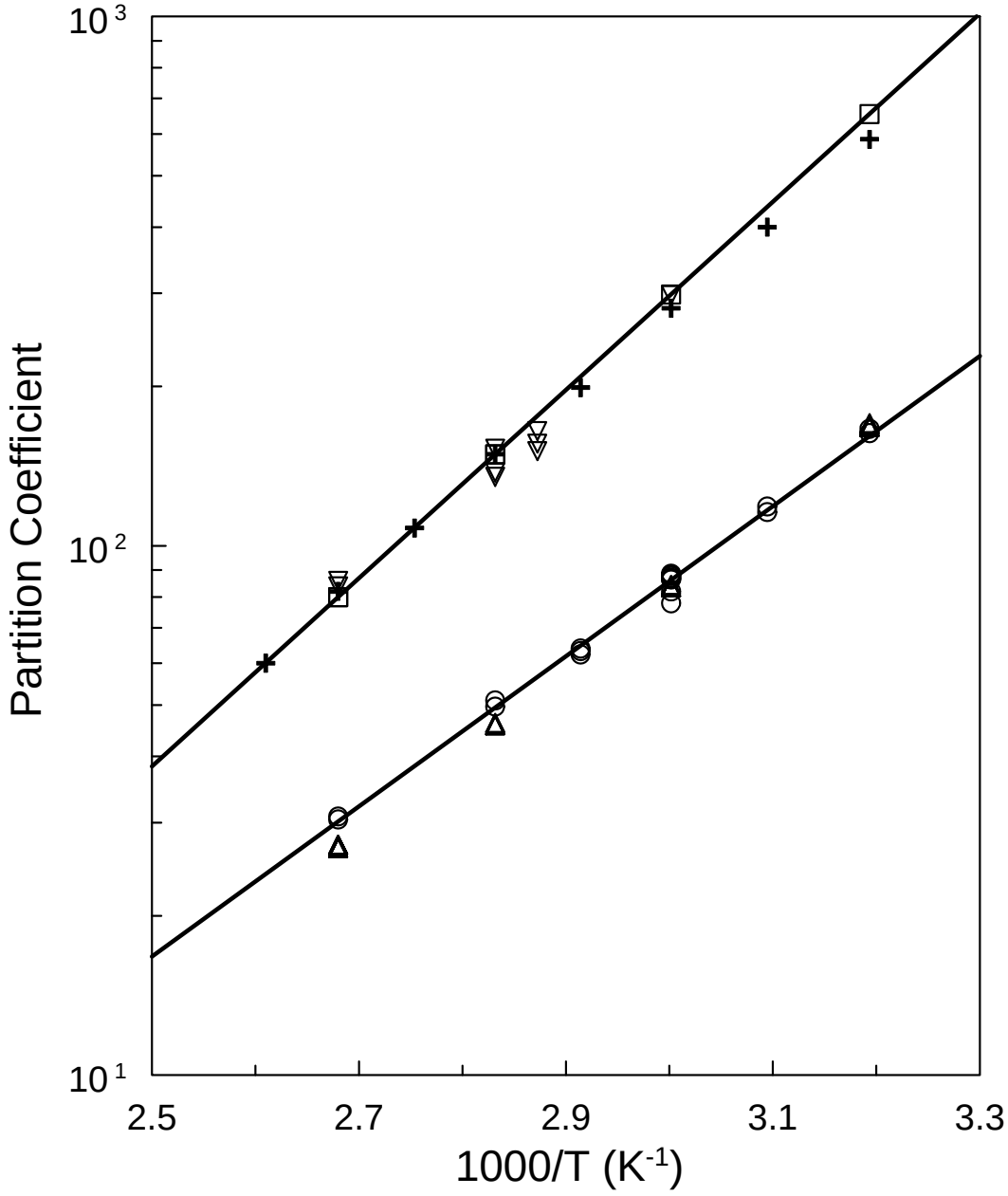

Figure 3-6: Partition coefficients as a function of inverse temperature. PVAc-methanol results from this work (○) are compared with those of Zielinski et al. (△) [16]. PVAc-toluene results from this work (▽) are compared with those of Zielinski et al. (□) [16] and Tihminlioglu et al. (+) [13].

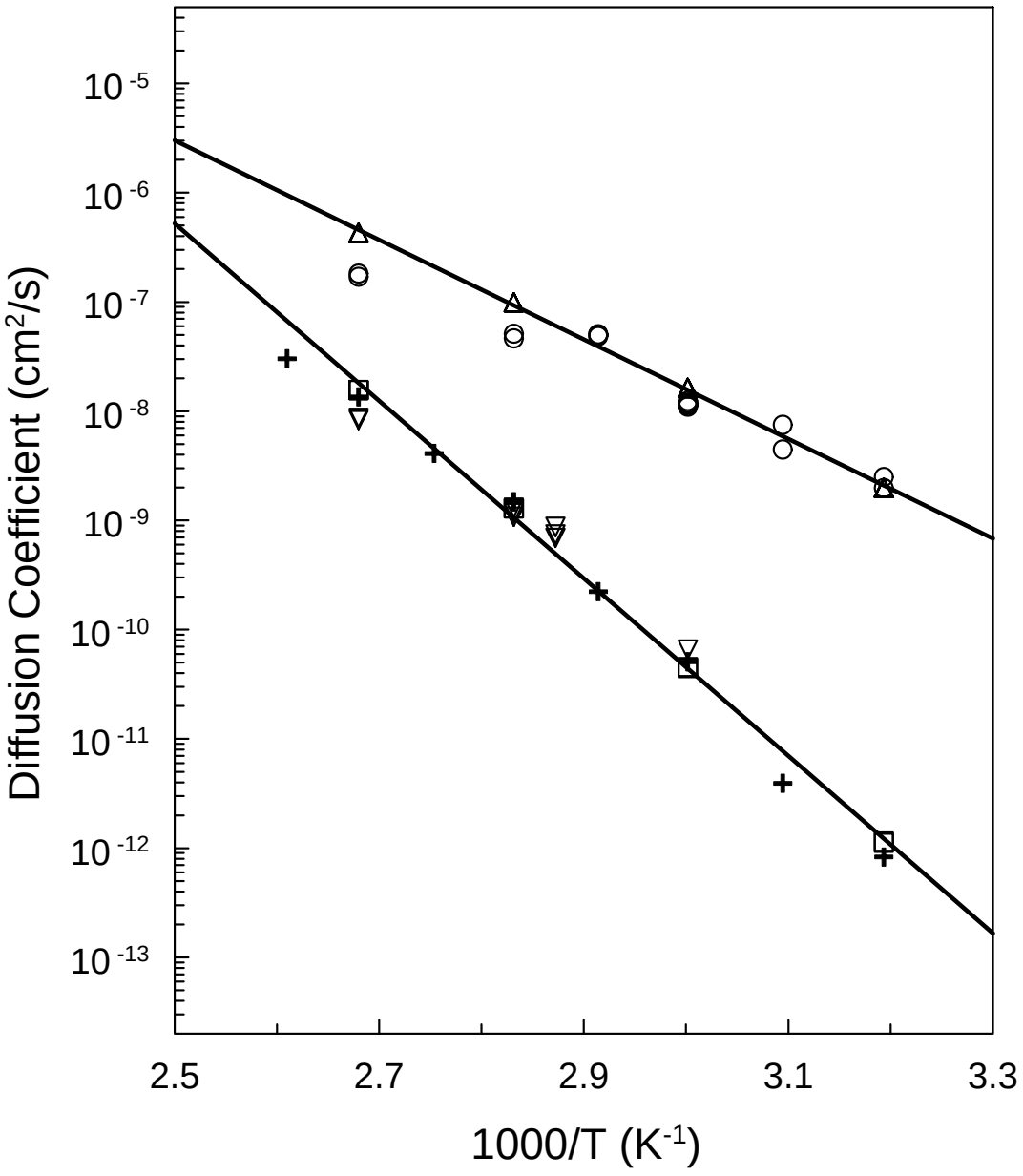

Figure 3-7: Diffusion coefficients as a function of inverse temperature. PVAc-methanol results from this work (○) are compared with those of Zielinski et al. (△) [16]. PVAc-toluene results from this work (▽) are compared with those of Zielinski et al. (□) [16] and Tihminlioglu et al. (✚) [13].

Table 3-3: Partition and diffusion coefficients of toluene in PVAc measured with the HPIGC using low pressure helium carrier gas.

T (°C)	K	D_p (10^{10} cm^2/s)
60	298.	0.657
75	156.	6.92
75	165.	7.44
75	151.	8.73
80	138.	13.1
80	135.	11.7
80	153.	10.8
100	83.8	87.1
100	85.9	82.8

Table 3-4: Partition and diffusion coefficients of methanol in PVAc measured with the HPIGC using low pressure helium carrier gas.

T (°C)	K	D_p (10^9 cm^2/s)
40	163.	2.50
40	166.	1.98
50	116.	7.50
50	119.	4.46
60	77.9	11.9
60	82.0	12.4
60	87.9	11.4
60	88.0	11.9
60	86.8	11.4
60	87.1	11.4
60	86.6	11.5
60	86.4	11.0
60	87.8	11.5
60	88.6	11.5
70	62.4	50.6
70	63.3	50.0
70	64.0	48.6
80	51.0	46.4
80	49.7	51.2
100	30.8	170.
100	30.4	182.

Data were also collected on methyl acetate and vinyl acetate in PVAc. Values of the partition coefficient are plotted as a function of inverse temperature in Figure 3-8.

Vinyl acetate shows slightly higher solubility than methyl acetate. However, methyl acetate has a higher diffusivity as shown in Figure 3-9. Good agreement is again observed between the results obtained in this work and those from literature sources.

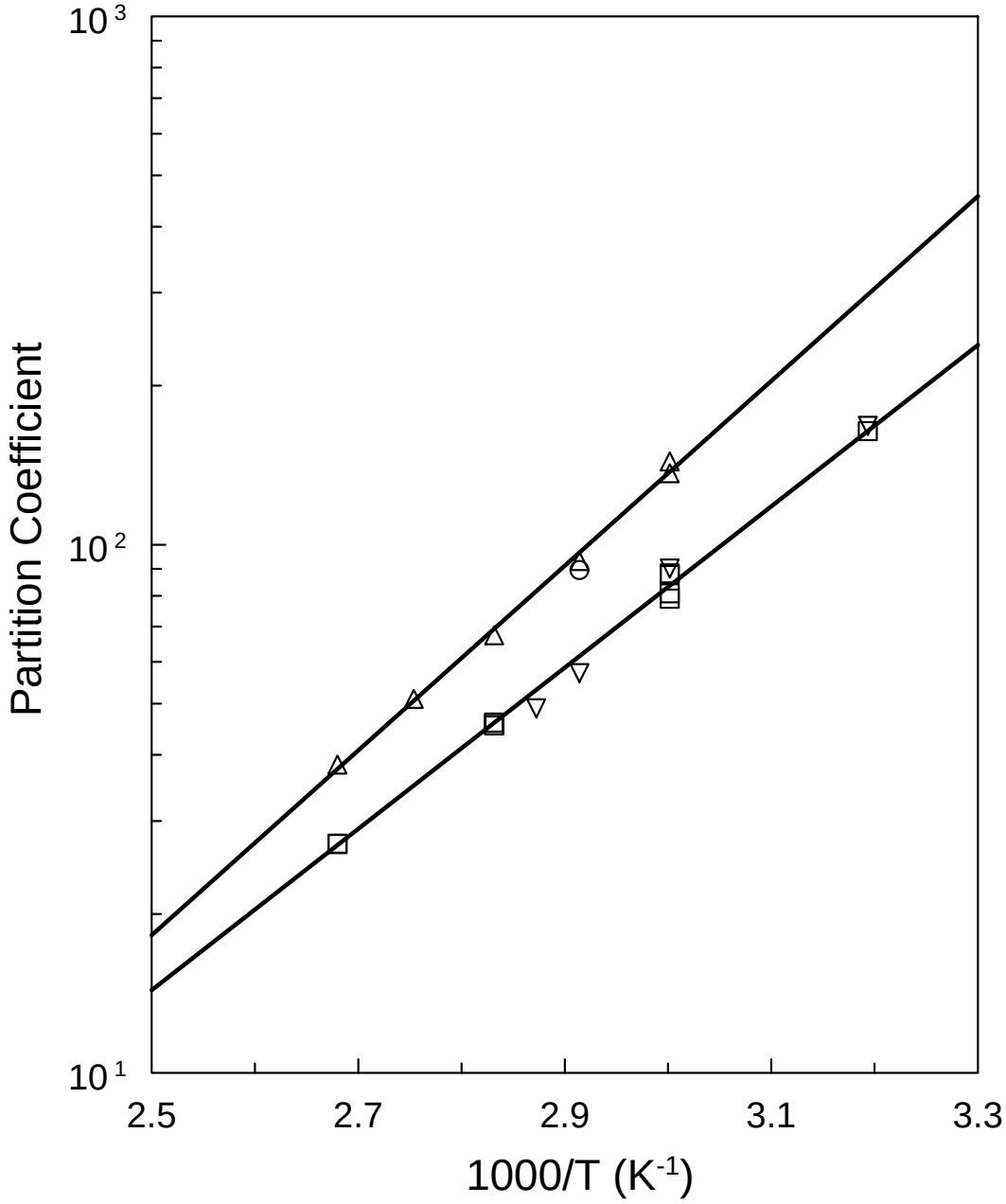

Figure 3-8: Partition coefficients as a function of inverse temperature. PVAc-vinyl acetate results from this work (○) are compared with those of Zielinski et al. (△) [16]. PVAc-methyl acetate results from this work (▽) are compared with those of Zielinski et al. (□) [16].

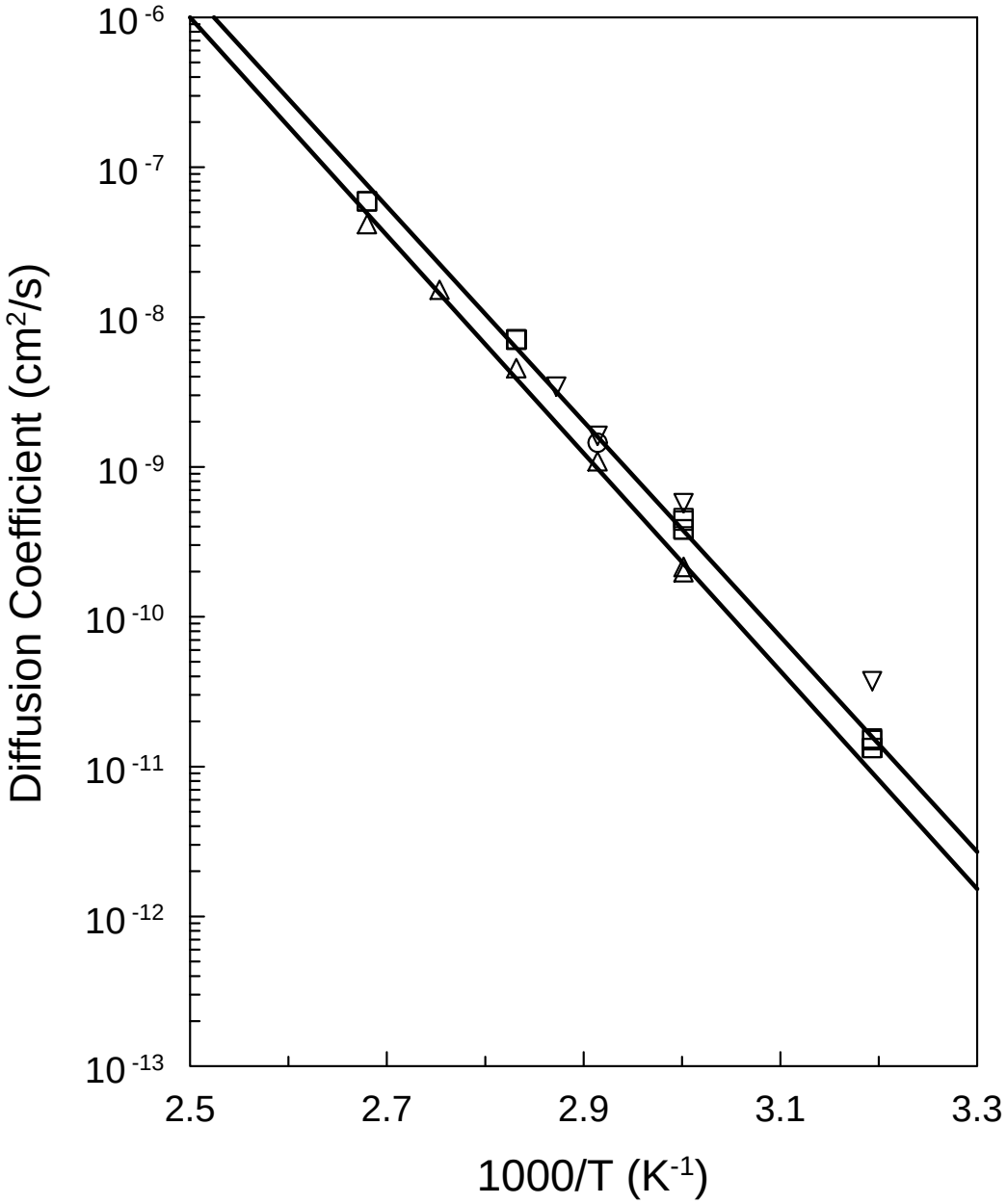

Figure 3-9: Diffusion coefficients as a function of inverse temperature. PVAc-vinyl acetate results from this work (○) are compared with those of Zielinski et al. (△) [16]. PVAc-methyl acetate results from this work (▽) are compared with those of Zielinski et al. (□) [16].

Table 3-5: Partition and diffusion coefficients of methyl acetate and vinyl acetate in PVAc measured with the HPIGC using low pressure helium carrier gas.

T (°C)	Methyl Acetate		Vinyl Acetate	
	K	D_p (10^{11} cm^2/s)	K	D_p (10^{11} cm^2/s)
40	168.	3.71	-	-
60	90.1	57.3	-	-
70	57.1	161.	89.5	145.
75	49.0	343.	-	-

3.5.1.2 PS Systems

Another aspect of the low pressure testing was to insure that temperature drops in the column stream did not influence the results obtained with the HPIGC. In the actual design, the column stream exits the oven and flows through the metering valve where the pressure is stepped down to atmospheric. The temperature also drops quickly due to the small diameter tubing used in the system. After passing through the metering valve the line is routed back into the GC oven and into the detector. Testing at temperatures well above room temperature indicated that the design did not affect the data. The partition and diffusion coefficients of benzene and toluene in PS were measured at temperatures in the range of 115-175°C. The data are shown in Figures 3-10 and Figure 3-11. The results show good agreement with literature sources.

These results along with those on the PVAc systems indicate the HPIGC is reliable for obtaining accurate normal IGC data. Clearly the additional dead volume and temperature drops between the column and detector do not impact the data.

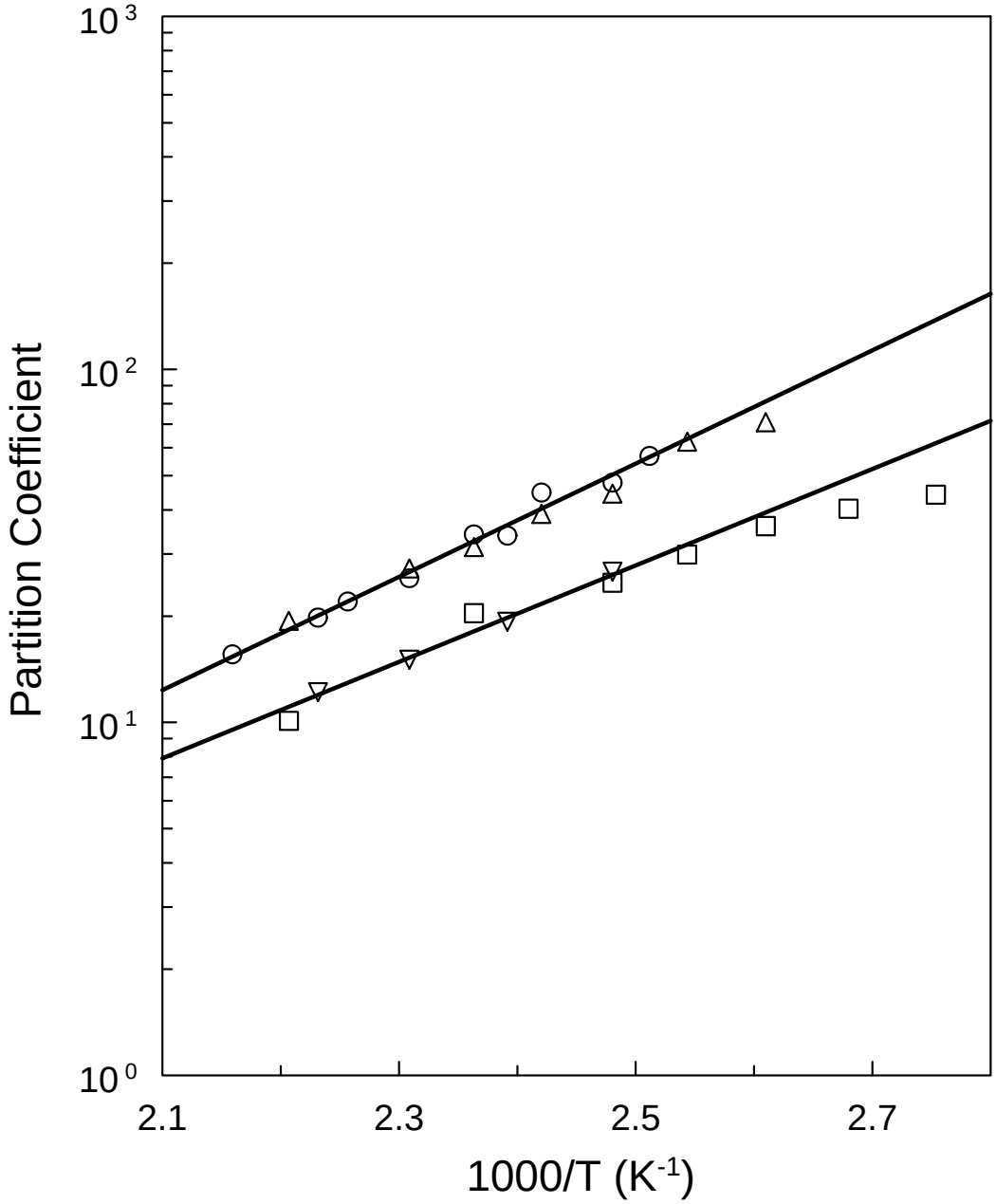

Figure 3-10: Partition coefficients as a function of inverse temperature. PS-toluene results from this work (○) are compared with those of Tihminlioglu et al. (△) [13]. PS-benzene results from this work (▽) are compared with those of Tihminlioglu et al. (□) [13].

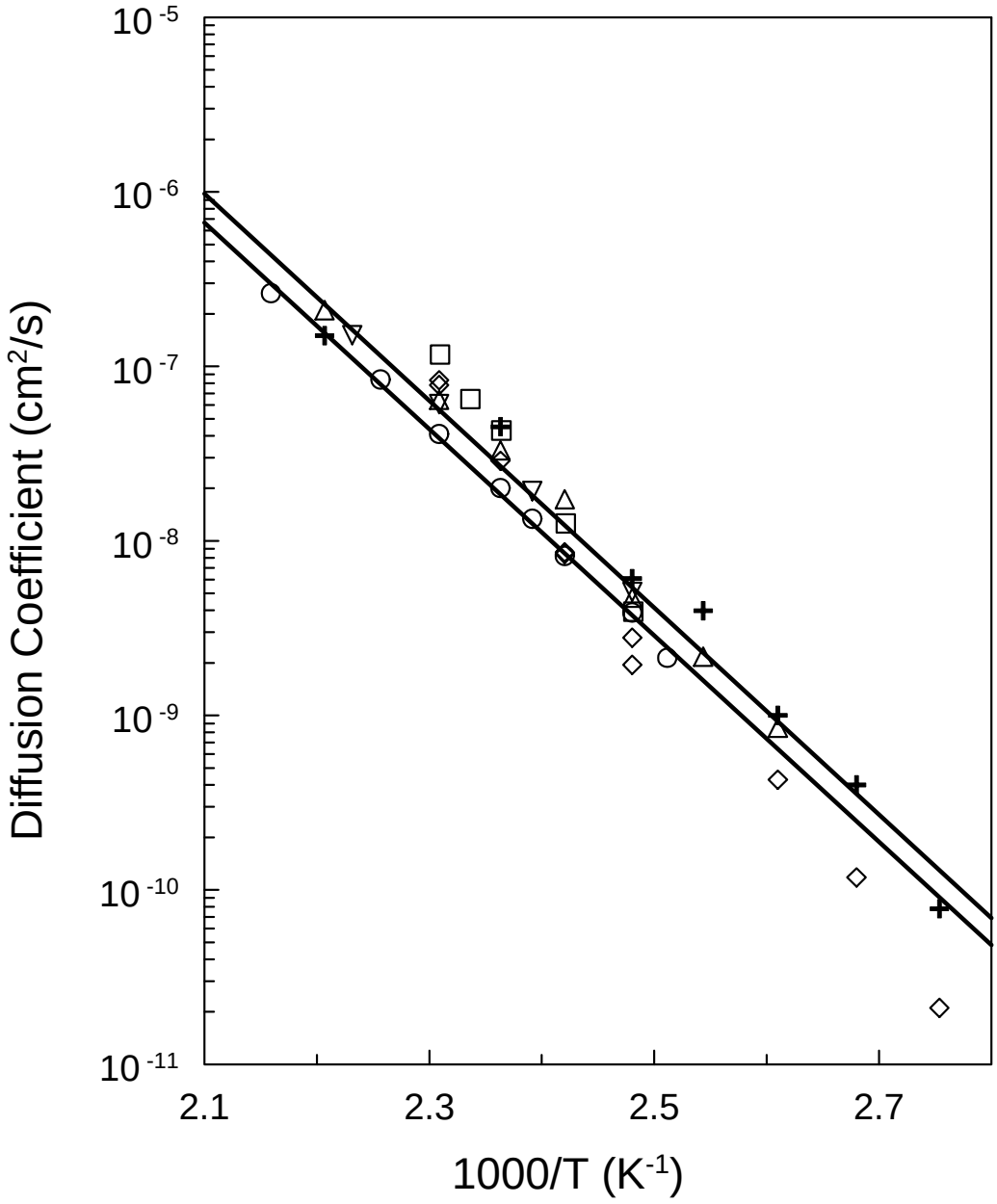

Figure 3-11: Diffusion coefficients as a function of inverse temperature. PS-toluene results from this work (○) are compared with those of Tihminlioglu et al. (△) [13] and Hadj-Romdhane et al. [6] (◇). PS-benzene results from this work (▽) are compared with those of Tihminlioglu et al. (□) [13] and Hadj-Romdhane et al. [6] (+).

Table 3-6: Partition and diffusion coefficients of benzene and toluene in PS measured with the HPIGC using low pressure helium carrier gas.

T (°C)	Benzene		Toluene	
	K	D_p (10^9 cm^2/s)	K	D_p (10^9 cm^2/s)
125	-	-	56.9	2.14
130	26.7	5.11	47.8	3.89
140	-	-	44.8	8.21
145	19.3	19.3	33.8	13.4
150	-	-	34.1	20.1
160	15.1	60.8	25.6	41.0
170	-	-	22.0	84.1
175	12.2	151.	19.8	119.
190	-	-	15.6	263.

3.5.2 High Pressure Results

In general when a polymer absorbs gas it becomes plasticized resulting in a liquid of higher total free volume. With few exceptions this is true. It was expected that both CO_2 and ethylene would plasticize the polymer to varying degrees and increase the diffusion coefficient. However, it was unknown whether the solvents would have stronger or weaker interactions in the polymer-gas mixtures compared to the polymer itself.

3.5.2.1 PVAc Systems

Data were first obtained on PVAc-vinyl acetate with CO_2 and ethylene as a high pressure carrier gas. Zielinski et al. [16] have observed that ethylene and CO_2 both led to lower partition coefficients of vinyl acetate in PVAc. Also they observed that the diffusion coefficients increased with both gases.

The partition coefficient results at 60 and 75°C are shown in Figure 3-12. Values indicated as being at zero pressure were obtained at ambient conditions with the HPIGC unit. The data are plotted as a function of carrier gas pressure in the column. Within experimental error the data collected in this work appear to follow the same trend exhibited by values obtained at other pressures. Notice that the partition coefficient of vinyl acetate decreases as the pressure of CO_2 is increased. This indicates that vinyl acetate has less favorable interactions in the polymer-gas mixture. The trend appears to be linear with pressure up to 600 psia.

Values of the diffusion coefficient at 60 and 75°C are shown Figure 3-13. The influence of pressure on diffusivity is much greater. The additional free volume added to the system by CO_2 results in an increase of several orders of magnitude in the diffusion coefficient of vinyl acetate. Although the data point at 75°C obtained in this work seems to follow the same trend, the value at 60°C is lower than expected based on the results Zielinski et al. [16].

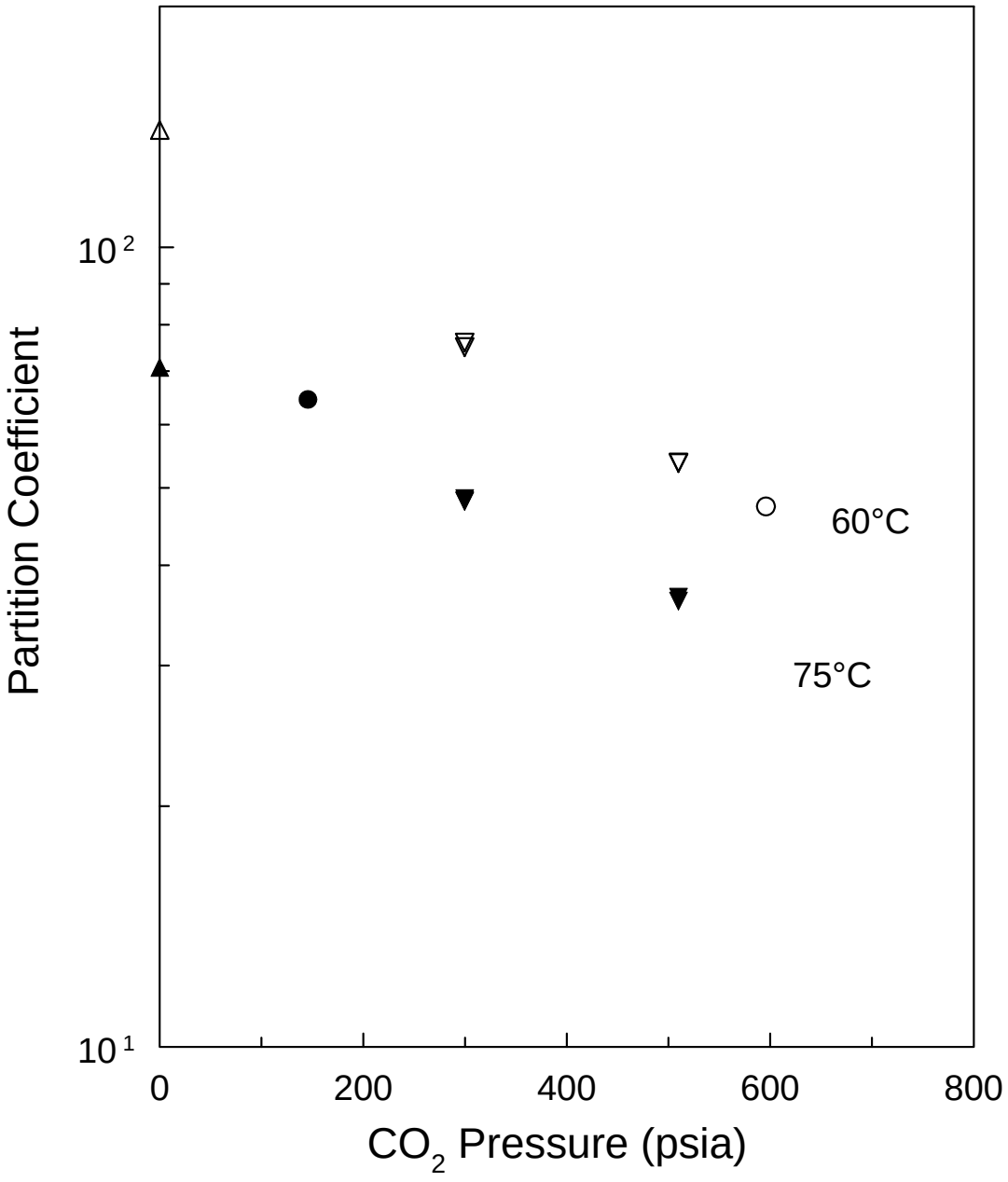

Figure 3-12: The partition coefficient of vinyl acetate on PVAc as function of CO_2 carrier gas pressure. Data from this work at 60 (○) and 75°C (●) were collected with the high pressure IGC unit. Results are compared with results from Zielinski et al. [16] at 60 (▽) and 75°C (▼). Data at 0 pressure from Zielinski et al. [16] at 60 (△) and 75°C (▲).

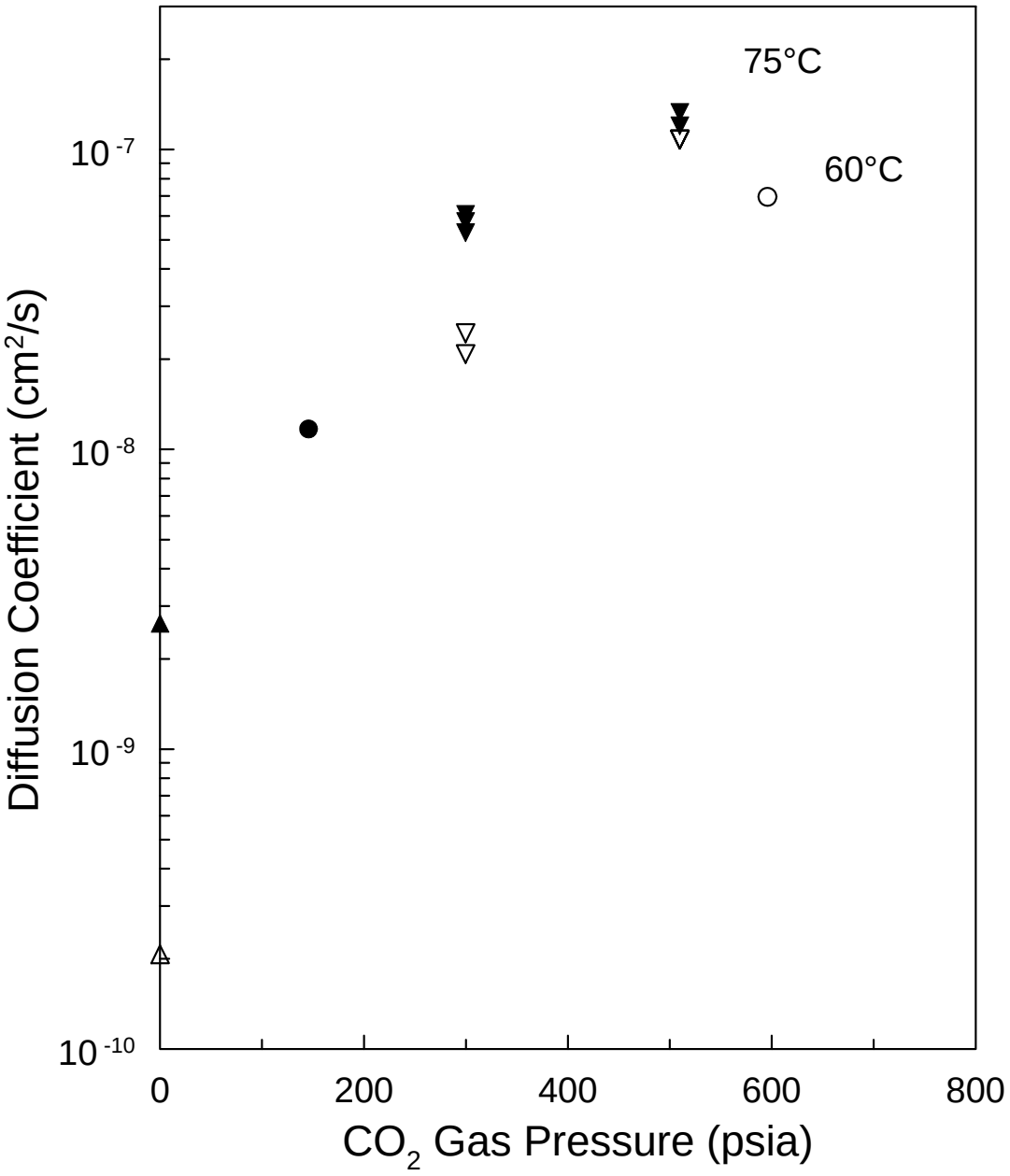

Figure 3-13: The diffusion coefficient of vinyl acetate on PVAc as function of CO_2 carrier gas pressure. Data from this work at 60 (○) and 75°C (●) were collected with the HPIGC. Results are compared with results from Zielinski et al. [16] at 60 (▽) and 75°C (▼). Data at 0 pressure from Zielinski et al. [16] at 60 (△) and 75°C (▲).

Table 3-7: Partition and diffusion coefficients of vinyl acetate in PVAc measured with the HPIGC using high pressure carrier gas.

T (°C)	Carrier Gas	Pressure (psia)	K	D_p (10^9 cm2/s)
60	CO_2	596	47.4	69.6
70	CO_2	97	83.1	5.91
70	CO_2	123	81.9	7.40
70	CO_2	146	64.5	11.7
70	CO_2	246	67.6	8.67
70	CO_2	247	64.5	9.69
70	CO_2	596	37.1	74.6
70	CO_2	810	28.3	62.2
70	**C_2H_4**	**310**	**54.3**	**9.75**
75	CO_2	146	64.5	11.7

In Figure 3-14 data are presented using CO_2 and ethylene as carrier gases. A similar trend is observed. The partition coefficient of vinyl acetate decreases with increasing pressure of carrier gas. Values were obtained in this work up to 810 psia using the HPIGC at 70°C. The data follow a linear trend with pressure at least up to that level. Figure 3-15 presents the results of the diffusion coefficient of vinyl acetate in the polymer-gas mixture. The dependence of the diffusion coefficient on ethylene pressure appears comparable to that observed by Zielinski et al. [16]. However, the data obtained in the presence of CO_2 do not seem to show such a strong influence as they observed. In particular the data point at 810 psia of CO_2 is slightly lower than the points at 596 psia. This illustrates the limitations of applying the existing IGC model to the data. The influence of the mass transfer resistance in the gas phase illustrated in Figure 3-3 likely

becomes significant at pressures of 600 psia and higher and the apparent increase in diffusion within the polymer is lower.

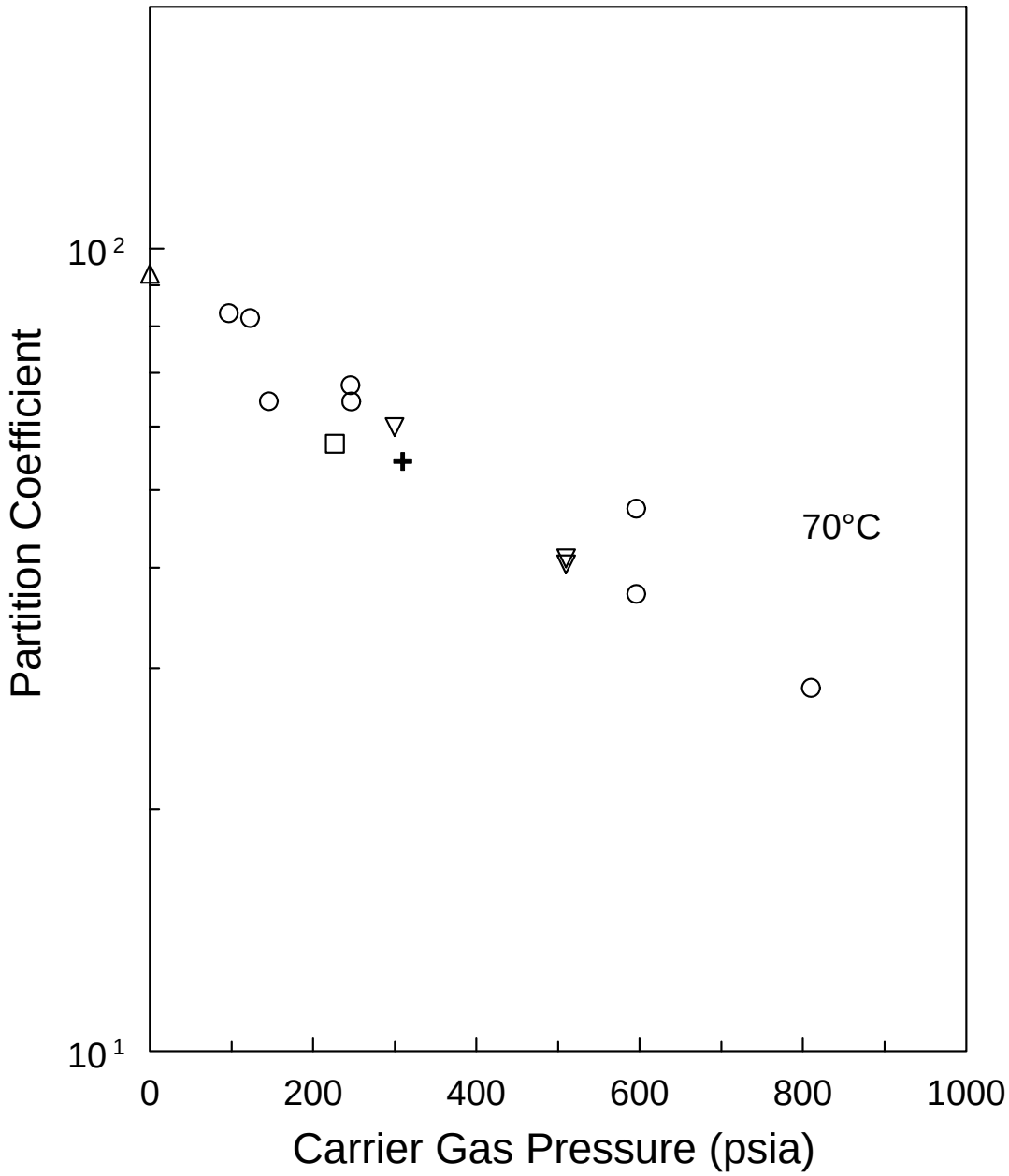

Figure 3-14: The partition coefficient of vinyl acetate on PVAc at 70°C as function of carrier gas pressure. Value at 0 pressure (△) was taken with HPIGC using helium at low pressure. Data collected using CO_2 carrier gas from this work (○) are compared with results from Zielinski et al. [16] (▽). Value measured using ethylene carrier gas from this work (+) is compared with that from Zielinski et al. [16] (□).

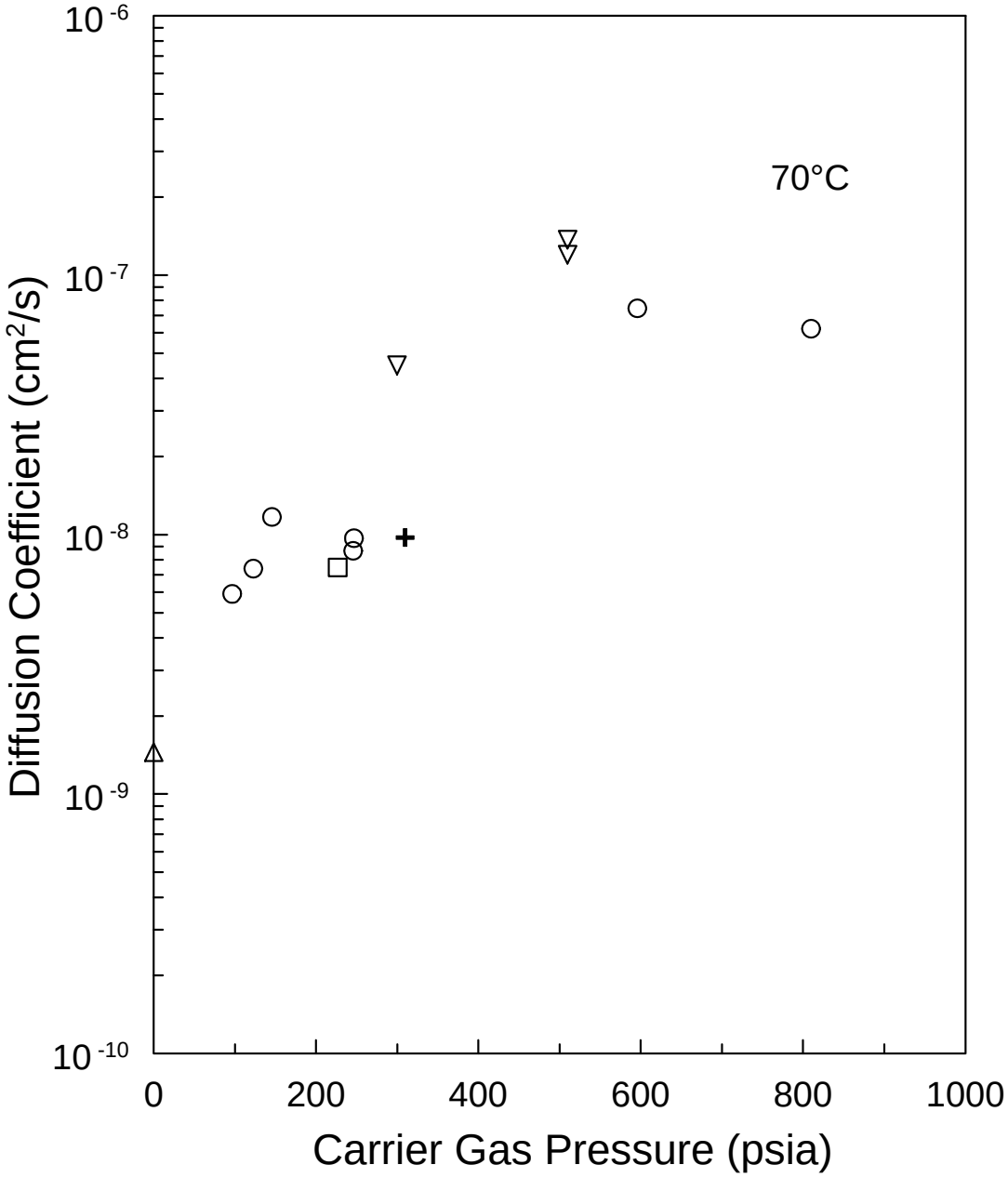

Figure 3-15: The diffusion coefficient of vinyl acetate on PVAc at 70°C as function of carrier gas pressure. Data collected using CO_2 carrier gas from this work (○) are compared with results from Zielinski et al. [16] (▽). Value measured using ethylene carrier gas from this work (✚) is compared with that from Zielinski et al. [16] (□). Value at 0 pressure (△) was taken with HPIGC using helium at low pressure.

The next system studied was PVAc-methanol using CO_2 as the carrier gas. Methanol is the smallest molecule tested and was expected to show a minimal diffusion influence. This is because the free volume necessary for diffusion is lower for smaller molecules.

Values of the partition coefficient as a function of temperature and CO_2 pressure are plotted in Figure 3-16. Interestingly, at ~133 psia of CO_2 the partition coefficient shows essentially no influence but the value at 147 psia at the same temperature shows a marked decrease. At higher pressures the partition coefficient shows further decrease.

Figure 3-17 presents a similar plot of the diffusion coefficients for this system. There is a marked increase at ~133 psia compared to the values obtained at ambient conditions. However, the values at ~247 psia do not show further increase. This is likely due to experimental error. The value at 596 psia indicates that even for a small molecule such as methanol, the additional free volume brought to the system by CO_2 has a strong influence on the diffusion of the solvent in the system.

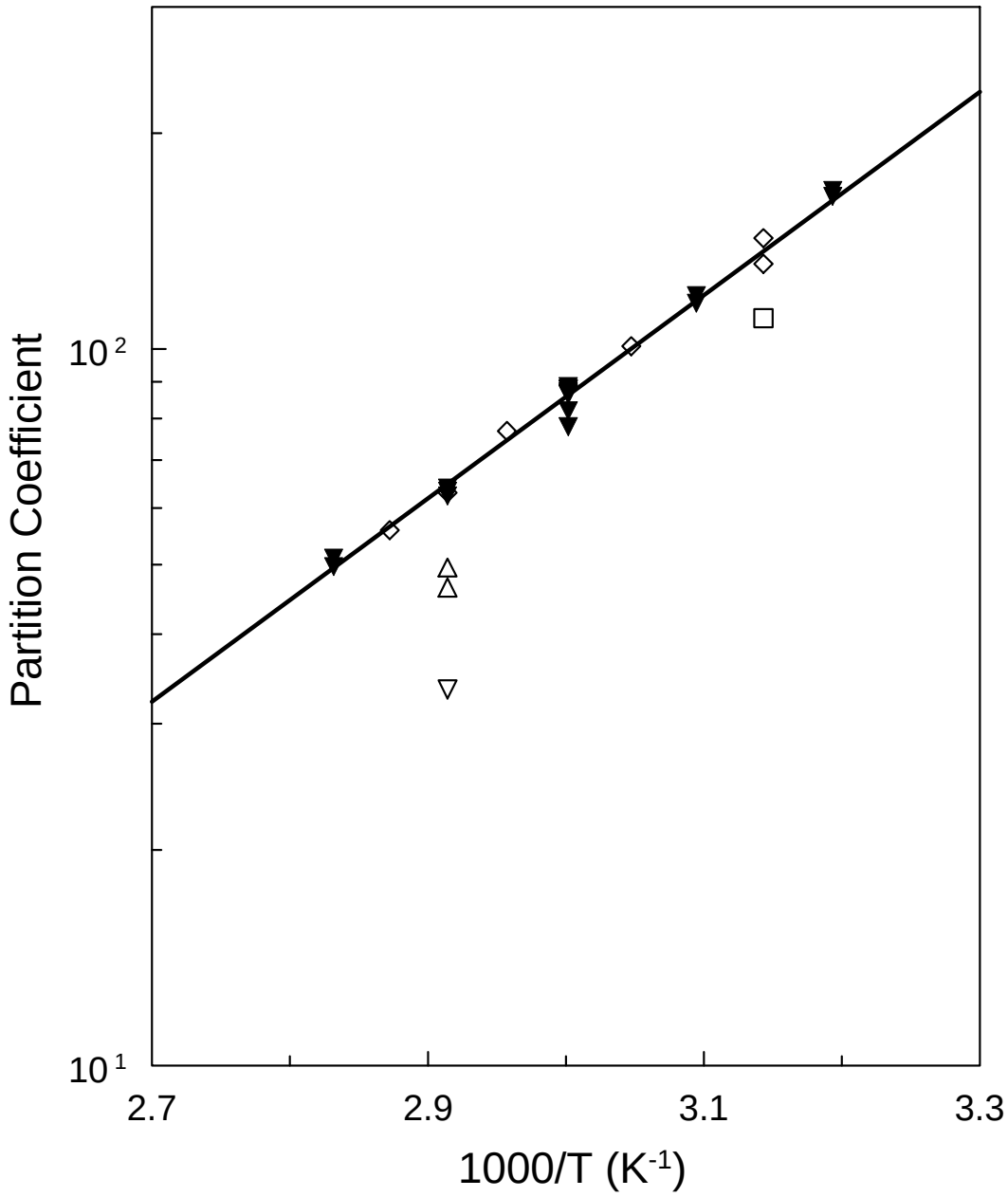

Figure 3-16: Partition coefficients of PVAc-methanol as a function of inverse temperature and CO_2 carrier gas pressure. Results at ambient conditions (▼) are compared with values obtained in the presence of CO_2 at ~133 (◇), 147(□), ~246 (△), and 596 psia (▽).

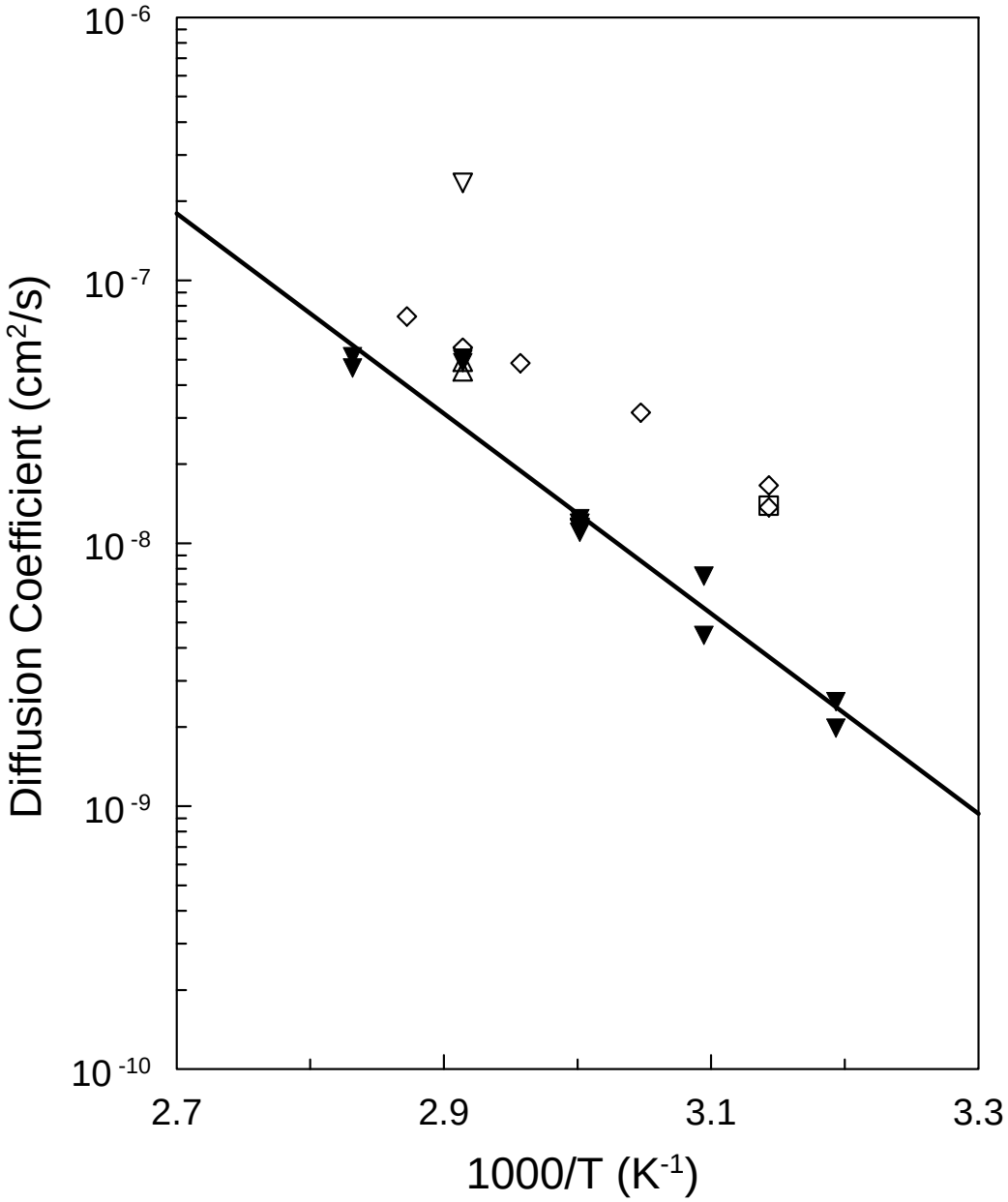

Figure 3-17: Diffusion coefficients of PVAc-methanol as a function of inverse temperature and CO_2 carrier gas pressure. Results at ambient conditions (▼) are compared with values obtained in the presence of CO_2 at ~133 (◇), 147(□), ~246 (△), and 596 psia (▽).

Table 3-8: Partition and diffusion coefficients of methanol in PVAc measured with the HPIGC using high pressure CO_2 carrier gas.

T (°C)	Pressure (psia)	K	D_p (10^8 cm^2/s)
45	128	143.	1.37
45	137	131.	1.66
45	147	110.	1.39
55	133	101.	3.14
65	133	76.8	4.84
70	133	63.0	5.55
70	246	46.5	4.90
70	247	49.5	4.51
70	596	33.5	23.5
75	133	55.9	7.29

Data were also collected on PVAc-methyl acetate using CO_2 and ethylene as carrier gases. The partition coefficients for the system with CO_2 are shown in Figure 3-18. Data were collected at four pressures of CO_2 up to 810 psia. The results indicate that, like vinyl acetate, the partition shows a continued decrease with increasing pressure up to that level. In addition, the influence is somewhat higher at the lower temperatures. This is because at a given pressure the uptake of CO_2 is higher at lower temperatures and the influence on the partition and diffusion coefficient is more pronounced.

Results of the diffusion coefficient measurements with CO_2 as the carrier gas are shown in Figure 3-19. Again, the diffusion coefficient shows a proportional increase with increasing pressure up to 414 psia. The value of the diffusion coefficient measured at 810 psia is quite low compared to that at 414 psia. At 810 psia, mass transfer resistance in the gas phase is likely a significant factor with CO_2. Notice that the plasticization effect

starts to dominate the temperature effect at moderate pressures of CO_2. Typically, the diffusion coefficient decreases with decreasing temperature. However, the uptake of CO_2 with decreasing temperature counteracts the temperature effect and produces this unique effect. The apparent activation energy of diffusion for the data at 247 psia is lower than that at 120 psia (i.e., the slope of the data at 247 is smaller). At 3.19×10^{-3} T^{-1} (40°C) and 247 psia the value of the diffusion coefficient is about two orders of magnitude higher than that observed in the normal polymer-solvent system.

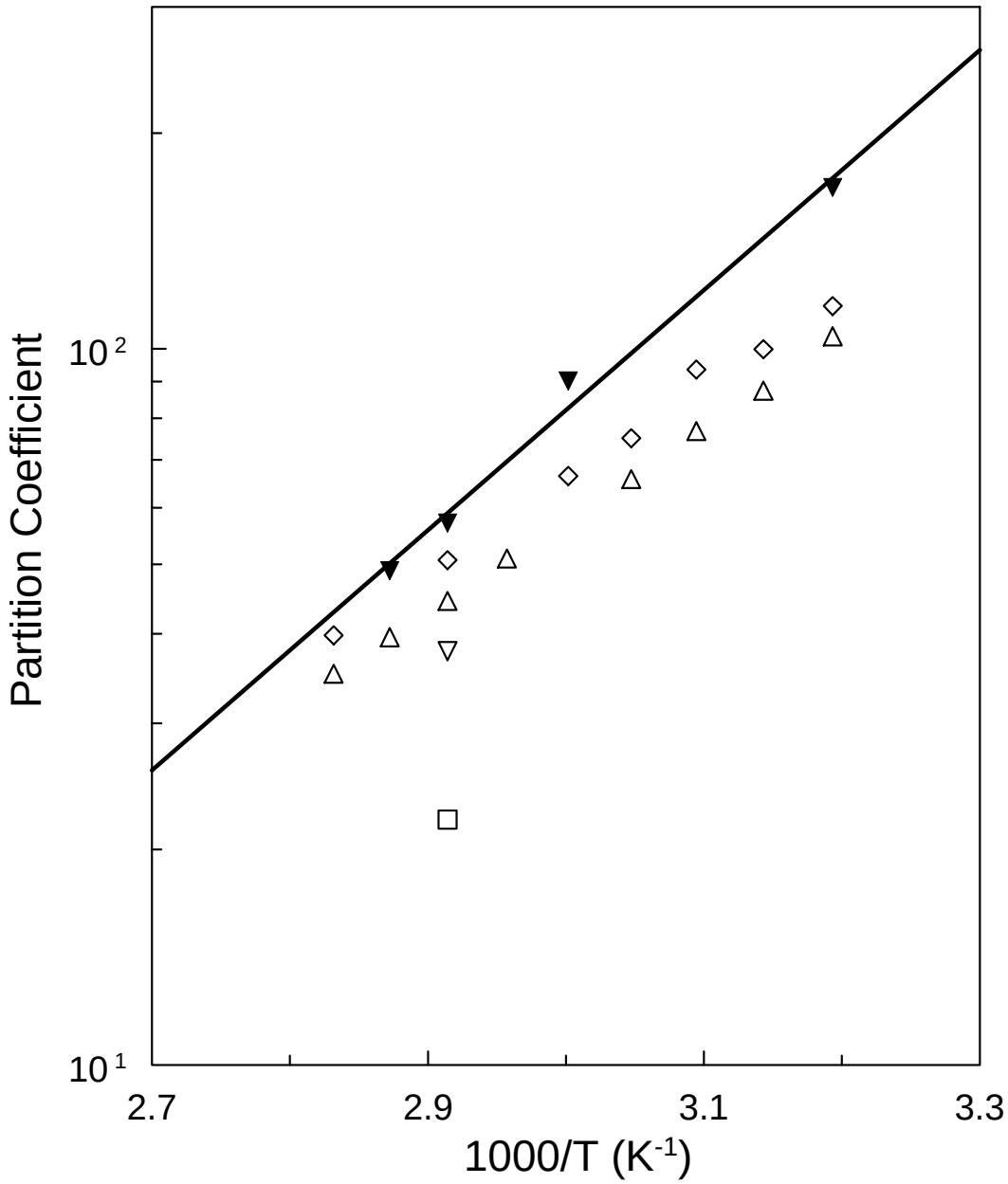

Figure 3-18: Partition coefficients of PVAc-methyl acetate as a function of inverse temperature and CO_2 carrier gas pressure. Results at ambient conditions (▼) are compared with values obtained in the presence of CO_2 at 120 (◇), 247 (△), 414 (▽), and 810 psia (□).

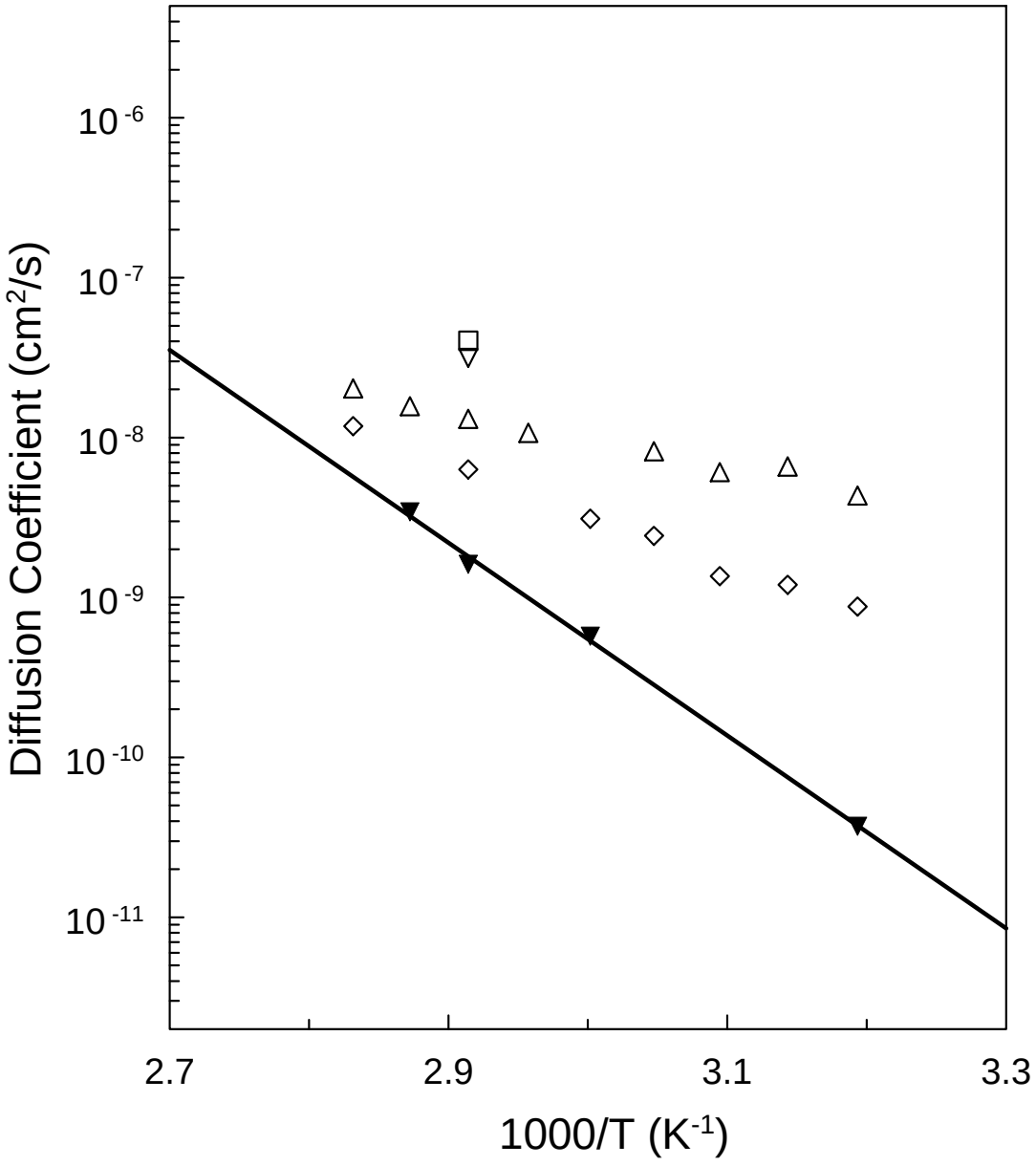

Figure 3-19: Diffusion coefficients of PVAc-methyl acetate as a function of inverse temperature and CO_2 carrier gas pressure. Results at ambient conditions (▼) are compared with values obtained in the presence of CO_2 at 120 (◇), 247 (△), 414 (▽), and 810 psia (□).

Results in Figure 3-20 show the dependence of the partition coefficient in PVAc-methyl acetate on temperature and ethylene pressure. The results are similar to those observed with CO_2 for this same system. Ethylene strongly hinders the interactions of methyl acetate with PVAc. The decrease again increases with increasing pressure of ethylene.

Figure 3-21 gives the values of the diffusion coefficient for this system with ethylene. The effect as a function of temperature does not appear as pronounced as with CO_2. However, the influence on the diffusion is still quite large with a change of nearly two orders of magnitude observed at the lower temperatures.

Table 3-9: Partition and diffusion coefficients of methyl acetate in PVAc measured with the HPIGC using high pressure carrier gases.

T	CO_2			C_2H_4		
(°C)	P (psia)	K	D_p (10^{10} cm^2/s)	P (psia)	K	D_p (10^{10} cm^2/s)
40	120	115.	8.78	225	85.4	8.40
	247	104.	43.4	310	86.2	13.4
	-	-	-	394	67.7	18.8
45	120	100.	12.0	175	79.5	11.2
	247	87.4	66.0	225	74.7	12.7
	-	-	-	310	75.4	17.6
	-	-	-	394	61.3	24.7
50	120	93.5	13.6	225	69.4	17.1
	247	76.7	60.8	310	66.9	27.4
		-		394	58.2	32.8
55	120	75.0	24.3	175	64.2	20.3
	247	65.8	82.1	-	-	-
60	120	66.4	31.1	175	56.6	29.5
	-	-	-	225	54.4	37.9
	-	-	-	310	51.7	52.2
	-	-	-	394	43.3	66.5
65	247	50.9	107.	175	51.1	43.4
	-	-	-	225	48.5	56.7
	-	-	-	310	45.2	86.0
70	120	50.7	63.3	175	44.5	65.0
	247	44.4	131.	225	41.7	84.5
	414	37.8	315.	310	38.9	114.
	810	22.0	403.	-	-	-
75	247	39.6	157.	175	39.0	101.
	-	-	-	225	36.6	119.
	-	-	-	310	35.4	152.
	-	-	-	394	31.9	172.
80	120	39.8	118.	175	34.6	148.
	247	35.2	203.	225	33.7	183.
	-	-	-	310	31.5	195.
	-	-	-	394	27.2	263.

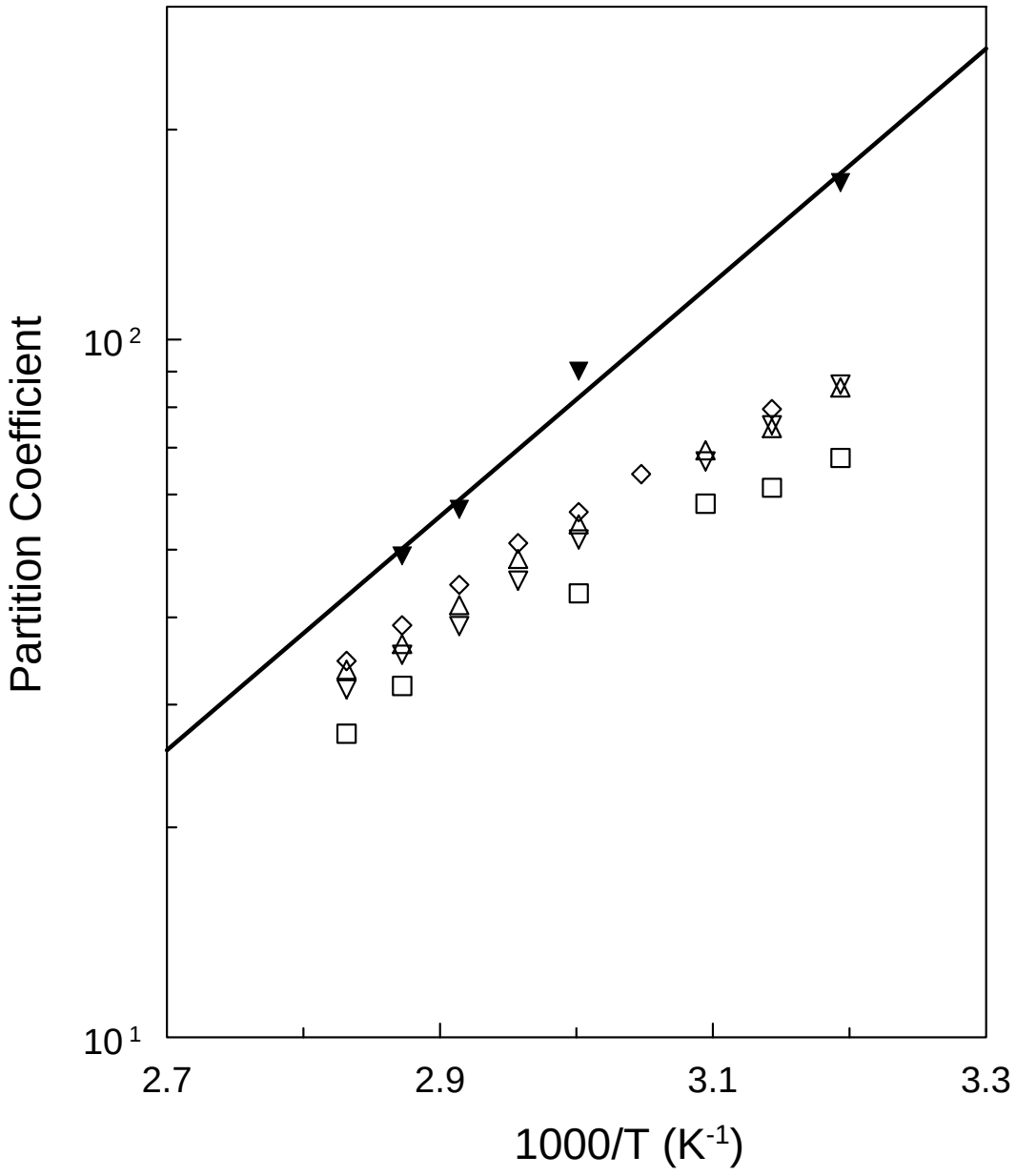

Figure 3-20: Partition coefficients of PVAc-methyl acetate as a function of inverse temperature and ethylene carrier gas pressure. Results at ambient conditions (▼) are compared with values obtained in the presence of ethylene at 175 (◇), 225 (△), 310 (▽), and 394 psia (□).

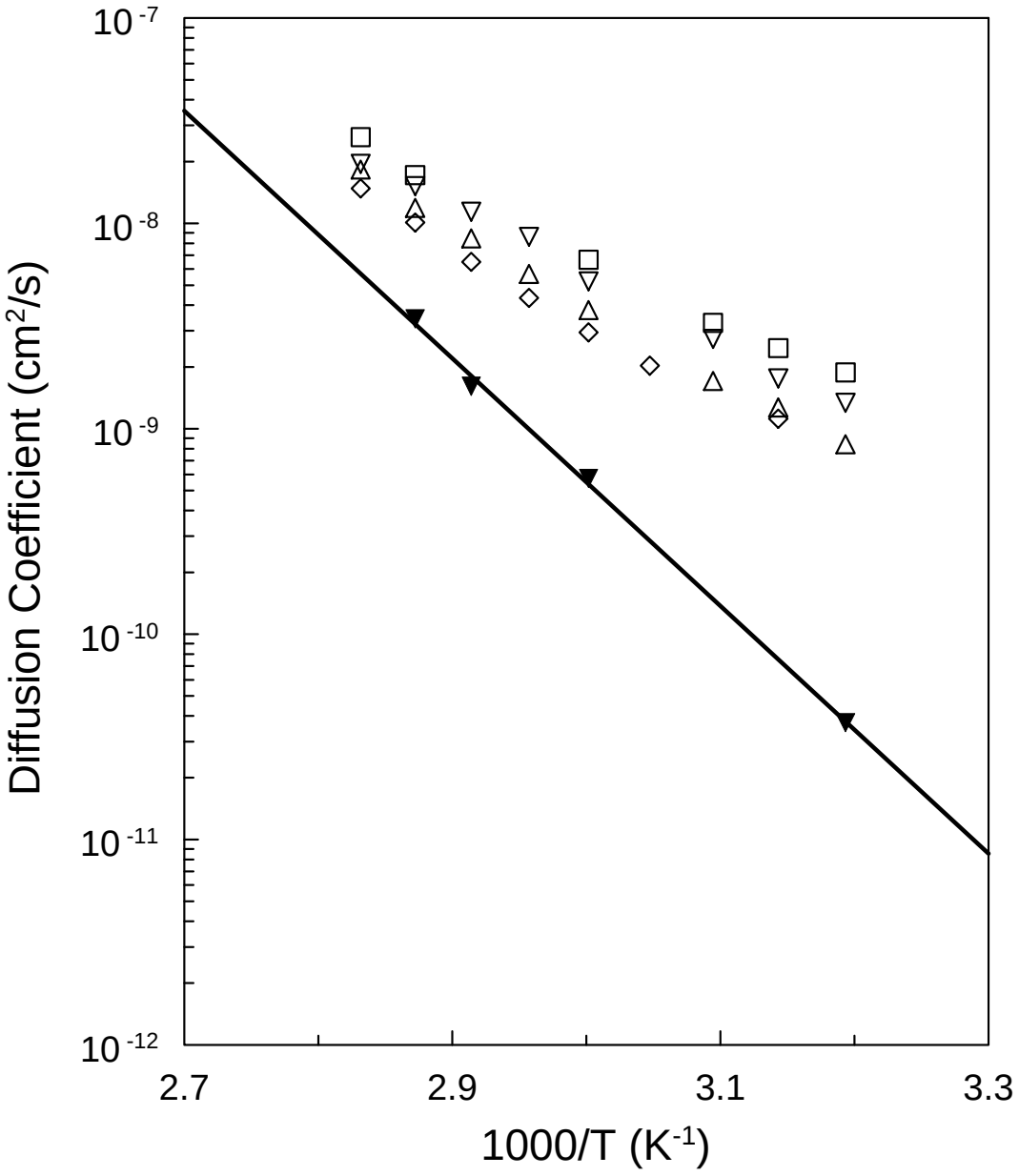

Figure 3-21: Diffusion coefficients of PVAc-methyl acetate as a function of inverse temperature and ethylene carrier gas pressure. Results at ambient conditions (▼) are compared with values obtained in the presence of ethylene at 175 (◇), 225 (△), 310 (▽), and 394 psia (□).

Another of the objectives of this work was to determine if a strong correlation exists between solvent size and the influence of the carrier gases on the system. Solvents of different molar volumes were tested at the same temperature and pressure. The solvents and their molar volume at 70°C are listed in Table 3-10. The relative influence of the carrier gas on the thermodynamics was defined as the ratio of the partition coefficient at ambient conditions to that obtained in the presence of the high pressure gas. Because all the systems tested showed reduced interactions in the presence of high pressure gases (lower K values), the values are greater than unity, as shown in Figure 3-22.

Table 3-10: Data on PVAc-solvent systems at 70°C with low pressure (helium) and high pressure (CO_2) carrier gases. All data were collected with the HPIGC.

Solvent	Molar Volume (cm^3/mol)	Helium		CO_2		
		K	D_p (10^9 cm^2/s)	P (psia)	K	D_p (10^9 cm^2/s)
Methanol	43.1	See Tables 3-4 and 3-8				
Isopropanol	81.5	78.9	1.46	246	68.8	6.98
				247	68.4	8.37
				596	49.1	55.7
				810	37.0	47.2
Methyl Acetate	85.5	See Tables 3-5 and 3-9				
Benzene	94.5	99.7	0.876	246	85.3	4.12
				247	80.0	5.77
				596	47.8	49.8
				810	37.5	50.9
Vinyl Acetate	99.2	See Tables 3-5 and 3-7				
Ethyl Acetate	105.1	85.3	1.28	246	66.1	5.47
				-	-	-
				-	-	-
				810	29.5	50.4
Toluene	112.1	202.	0.535	-	-	-
				247	154.	4.00
				-		
				810	61.6	29.6
Ethyl Benzene	128.7	356.	0.403	-	-	-
				-	-	-
				-	-	-
				810	99.4	24.4
p-Xylene	129.8	378.	0.420	-	45.0	-
				-	-	-
				-	-	-
				810	100.	29.3

GCLF-EoS was used to predict the influence on the partition coefficient. Values were calculated at 70°C and three pressures (247, 596, and 810 psia) of CO_2. At the lowest pressure there appears to be no correlation with solvent size. However, at 596 and 810 psia, there appears to be a general increase in the influence on the partition

coefficient with increasing solvent size. GCLF-EoS predicts that the influence of the high pressure gas on the solubility of the solvent will increase as the solvent size increases. The trend at 247 psia is not as strong as predicted, but there is good agreement between the model and experimental results for isopropanol and methyl acetate (molar volumes 81.5 and 85.5 cm^3/mol, respectively). At 596 psia there is quite good agreement between the predictions and the observed influence, with the exception of the methanol results. Interestingly, GCLF-EoS predicts that there should be slightly higher solubility of methanol (molar volume 43.1 cm^3/mol) in the presence of the high pressure gas compared to the binary polymer-solvent system at the higher temperatures. This was not observed experimentally in the PVAc systems, although at 810 psia methanol does show the lowest influence of the carrier gas on the partition coefficient. The results at 810 show generally good agreement with GCLF-EoS. The same trend with solvent size is predicted with the predicted values being just slightly lower than the experimental ones.

Figure 3-23 shows a similar plot at 70°C of the partition coefficient ratios obtained with ethylene. Values used to calculate the ratios are provided in Table 3-11. The correlation between influence of the interacting gas and solvent size is quite clear in this plot. The increase in the partition coefficient in the presence of the high pressure gas shows a steady increase over the range of solvents tested. The effect that the gas has on the system is higher with bulkier molecules than smaller ones. However, GCLF-EoS predicts a much stronger dependence on solvent size than observed. The general trend is the same but the experimental values indicate that the partition coefficient in the presence of high pressure gas is only about 50% of the predicted values.

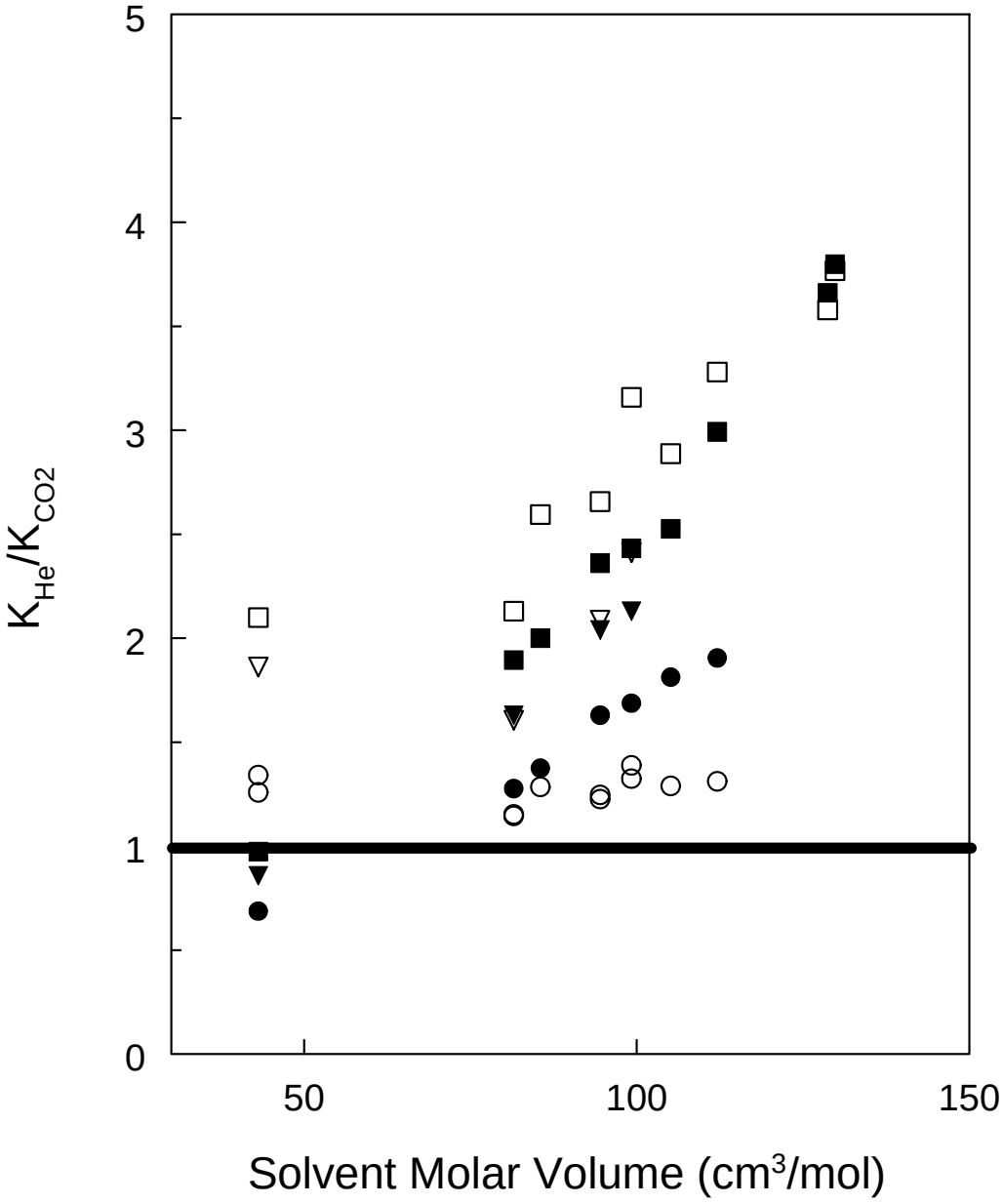

Figure 3-22: Carrier gas influence as determined by influence on partitioning of solvents of different sizes. Comparison was made for solvents in PVAc at 70°C with CO_2 carrier gas at ~247 (○), 596 (▽) and 810 psia (□). GCLF-EoS was used to predict the influence of CO_2 on the partition coefficient at ~247 (●), 596 (▼) and 810 psia (■).

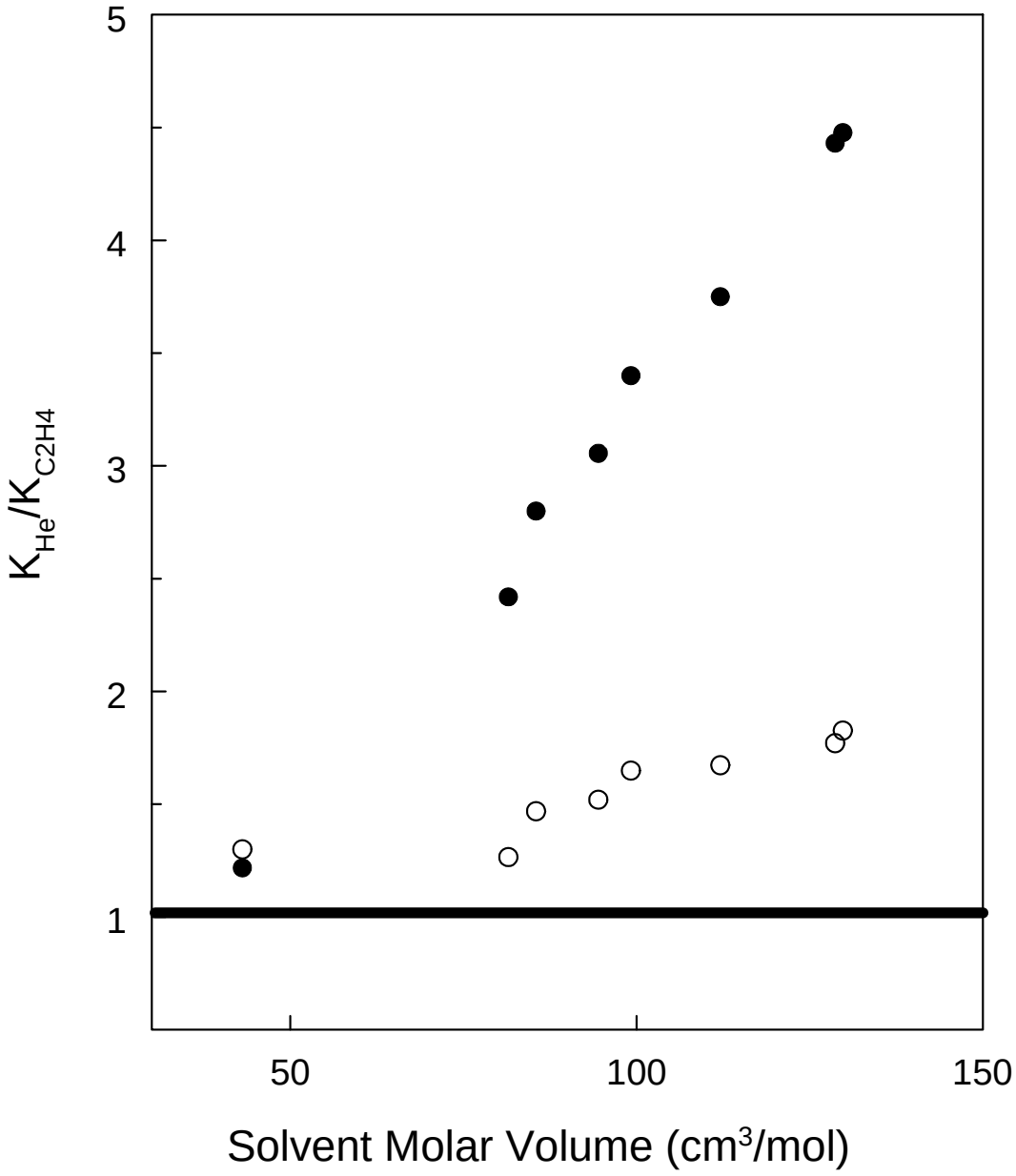

Figure 3-23: Carrier gas influence as determined by influence on partitioning of solvents of different sizes. Comparison was made for solvents in PVAc at 70°C with ethylene carrier gas at 310 psia (○). GCLF-EoS was used to predict the influence of ethylene on the partition coefficient at 310 psia (●).

The influence of solvent size on the diffusion behavior was also determined. In this case the ratio of the diffusion coefficient in the presence of the high pressure gas to that obtained at ambient conditions was calculated. In almost all cases the diffusion was observed to increase in the presence of the plasticizing gas, and therefore this ratio was greater than unity.

Table 3-11: Data on PVAc-solvent systems at 70°C with high pressure ethylene carrier gas.

Solvent	**Molar Volume (cm^3/mol)**	**C_2H4**		
		P (psia)	**K**	**D_p (10^9 cm^2/s)**
Methanol	43.1	310	48.1	37.8
Isopropanol	81.5	310	62.3	6.47
Methyl Acetate	85.5	See Table 3-9		
Benzene	94.5	310	65.4	4.91
Vinyl Acetate	99.2	See Table 3-7		
Toluene	112.1	310	121.	3.58
Ethyl Benzene	128.7	310	201.	2.69
p-Xylene	129.8	310	207.	2.94

The results obtained with CO_2 as the high pressure gas are shown in Figure 3-24. Again the results at ~247 psia do not show a strong correlation. However, there is a clear trend with solvent size at higher pressures. The bulkier molecules are able to take advantage of the additional free volume brought to the system by CO_2. The smaller molecules which require less free volume for a diffusion "jump" are not as highly influenced by the additional free volume in the system.

Figure 3-25 indicates a similar trend for the data obtained in the presence of ethylene. Interestingly, values above 100 cm^3/mol all show similar behavior. The point

for methanol falls below unity indicating slightly slower diffusion in the presence of methanol. The peak of methanol was by far the narrowest and slightly higher error was observed compared to other solvents. It is not expected that the PVAc-methanol-ethylene system would exhibit anti-plasticization behavior. Therefore, it is concluded that within experimental error there appears to be no influence of ethylene on the diffusion of methanol.

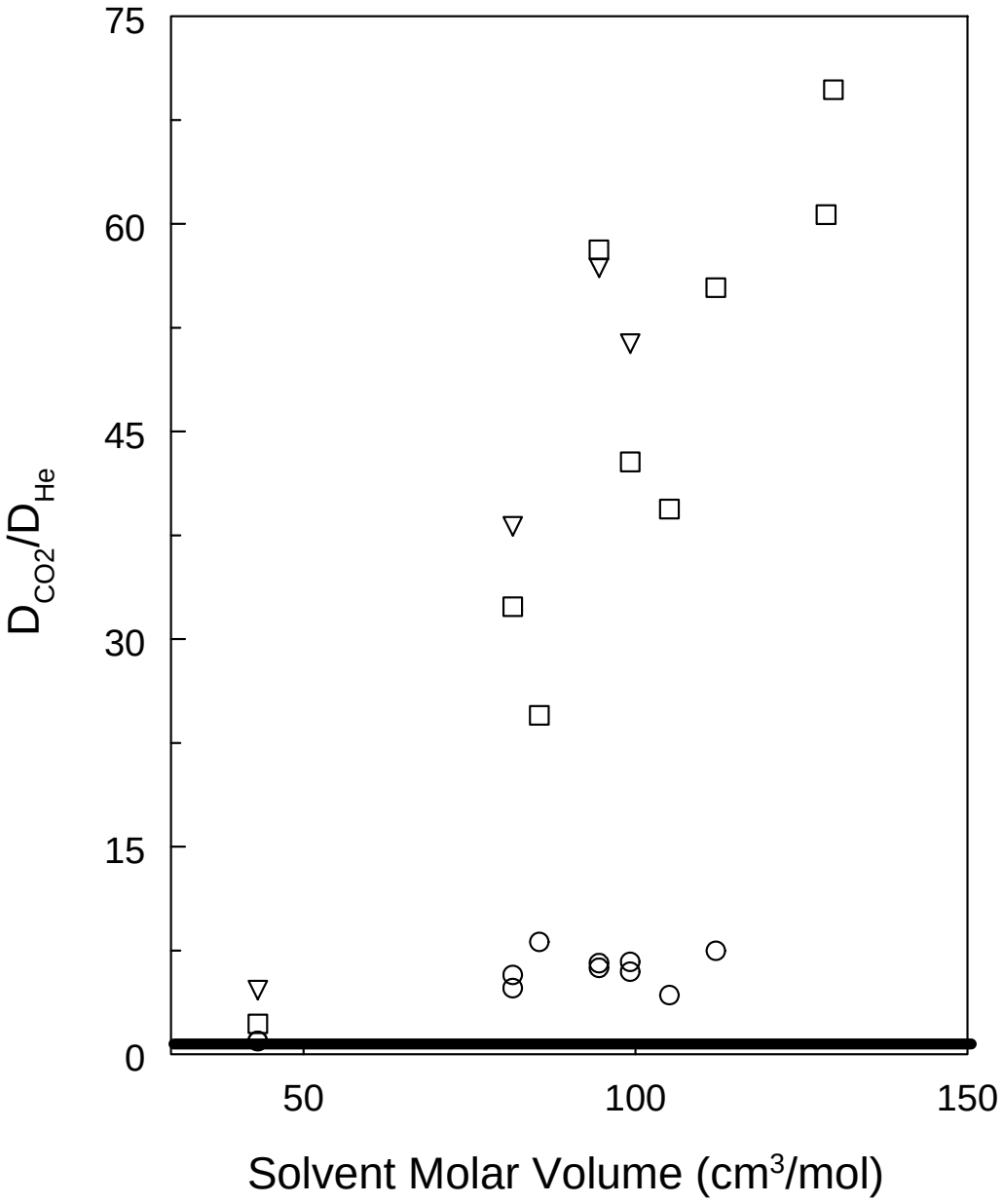

Figure 3-24: Carrier gas influence as determined by influence on diffusion of solvents of different sizes. Comparison was made for solvents in PVAc at 70°C with CO_2 carrier gas at ~247 (○), 596 (▽) and 810 psia (□).

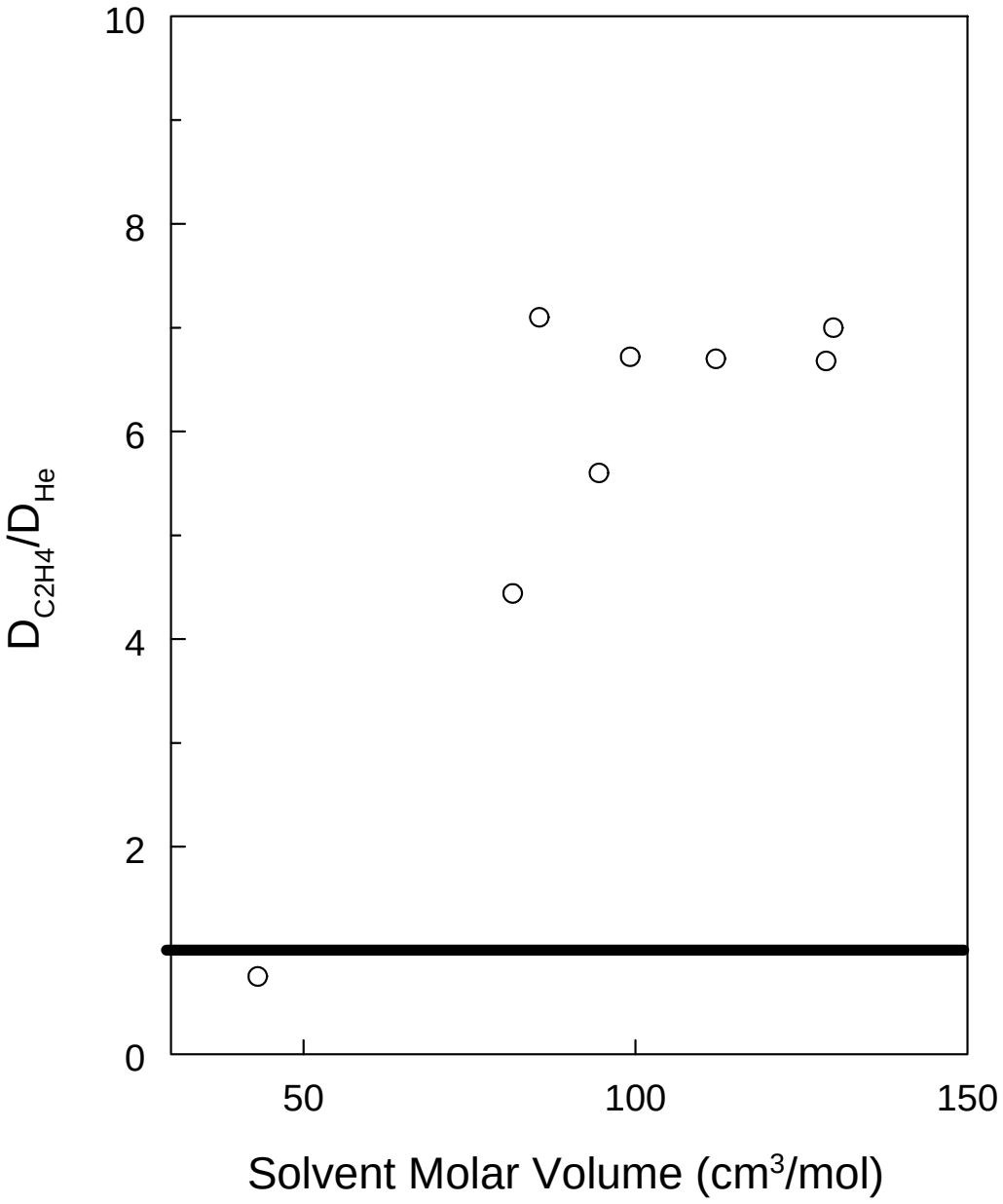

Figure 3-25: Carrier gas influence as determined by influence on diffusion of solvents of different sizes. Comparison was made for solvents in PVAc at 70°C with ethylene carrier gas at 310 psia (○).

3.5.2.2 PS Systems

Comparing the Henry's Law constants determined from the experimental data of Sato et al. [19] indicates that the solubility of CO_2 in PS is significantly lower than in PVAc. However, the solubility of ethylene in PS is about the same as that in PVAc. Overall the uptake of the gases was lower compared to the PVAc systems because of the higher temperatures of the experiments for PS.

Data were obtained for benzene in PS with CO_2 and ethylene as carrier gases. Partition coefficients are presented in Figure 3-26 at two pressures for each carrier gas. Both gases have a pronounced influence on the thermodynamics of the system, with a significant reduction in the interactions between benzene and PS. The data indicates that ethylene at 340 psia has the same influence on the partition coefficient as CO_2 does at 590 psia. Considering that CO_2 has roughly 25% higher solubility than ethylene in PS at a given pressure it is clear ethylene has a stronger influence on the thermodynamics of this system.

Diffusion coefficients are presented in Figure 3-27 at two pressures for each carrier gas. Again ethylene at 340 psia and CO_2 at 590 psia have the largest influence. The strong temperature effect observed in PVAc-methyl acetate is not present in this system because of the lower overall solubilities of the gases at the higher temperatures.

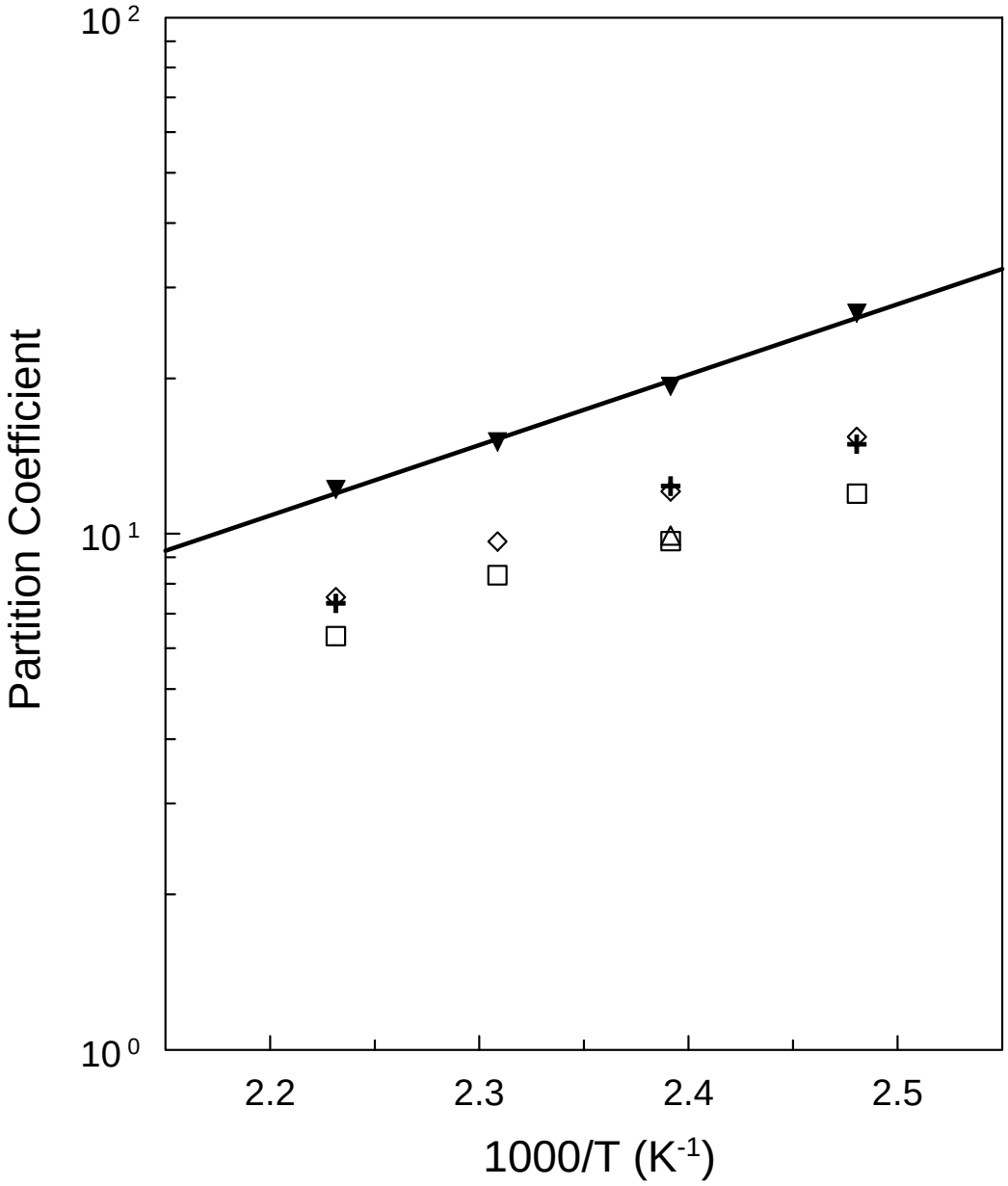

Figure 3-26: Partition coefficients of PS-benzene as a function of inverse temperature and carrier gas pressure. Results at ambient conditions (▼) are compared with values obtained in the presence of CO_2 at 360 (◇) and 599 psia (△). Data collected in the presence of ethylene were at 200 (✚) and 340 psia (□).

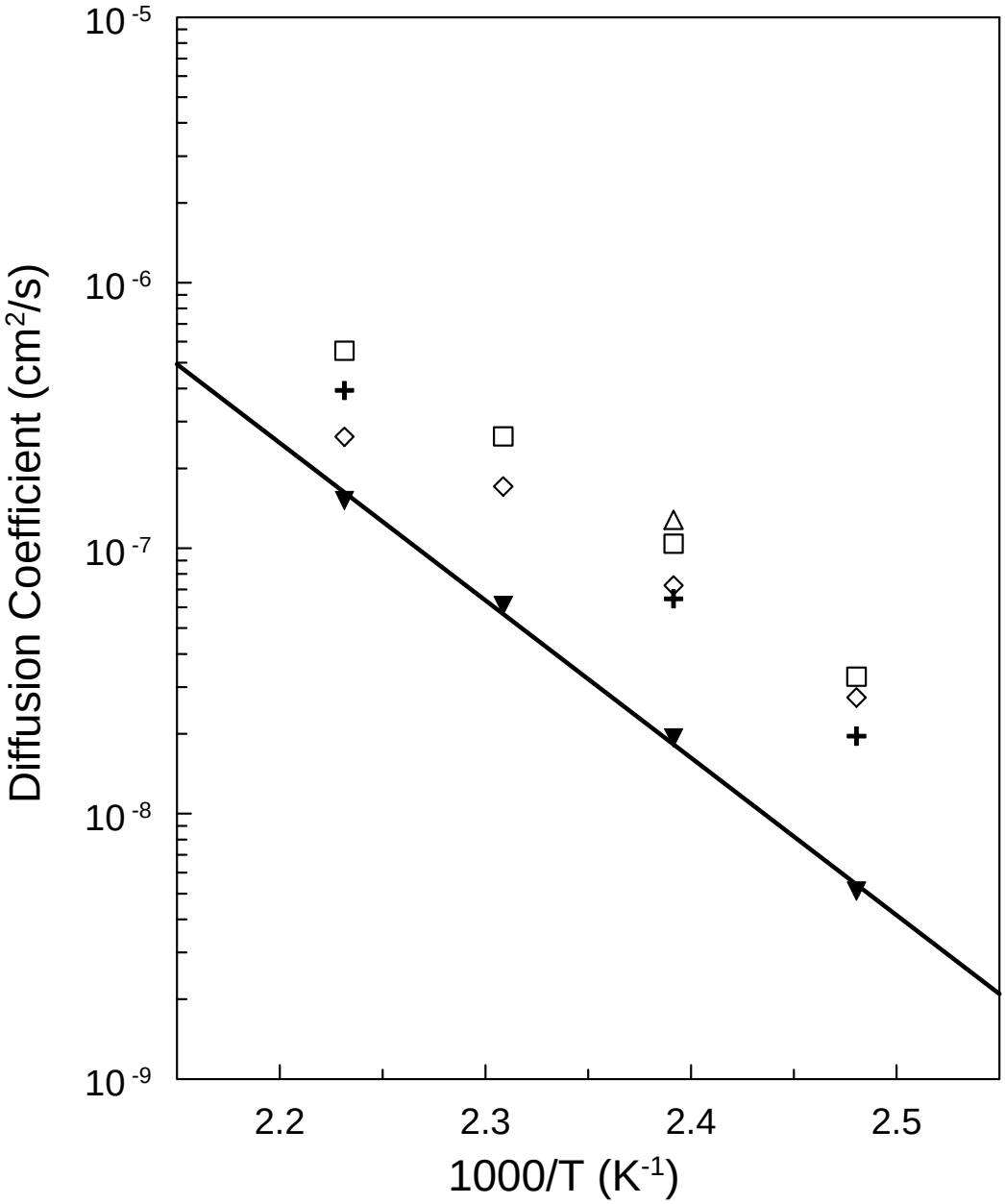

Figure 3-27: Diffusion coefficients of PS-benzene as a function of inverse temperature and carrier gas pressure. Results at ambient conditions (▼) are compared with values obtained in the presence of CO_2 at 360 (◇) and 599 psia (△). Data collected in the presence of ethylene were at 200 (✚) and 340 psia (□).

Table 3-12: Partition and diffusion coefficients of benzene in PS measured with the HPIGC using high pressure carrier gases.

T (°C)	CO_2			C_2H_4		
	P (psia)	K	Dp (10^8 cm^2/s)	P (psia)	K	Dp (10^8 cm^2/s)
130	360	15.4	2.74	200	14.9	1.96
	-	-	-	340	12.0	3.28
145	360	12.1	7.24	200	12.4	6.45
	599	9.92	12.8	340	9.67	10.4
160	360	9.66	17.1	340	8.31	26.4
175	360	7.54	26.3	200	7.33	39.3
	-	-	-	340	6.33	55.5

Table 3-13: Partition and diffusion coefficients of solvents in PS measured with the HPIGC using low pressure helium carrier gas. All D_p values have units of (10^9 cm^2/s).

T(°C)	Methanol		Benzene		Toluene		Ethyl Benzene		p-Xylene	
	K	D_p	K	D_p	K	D_p	K	D_p	K	D_p
130	3.83	266.	26.7	5.11	55.8	3.02	88.0	1.71	-	-
145	3.10	861.	19.3	19.3	33.8	13.4	54.7	6.69	60.6	6.36
160	2.67	680.	15.1	60.8	25.6	41.0	40.3	30.4	43.0	25.2

The influence of solvent size on the thermodynamics was also examined for PS with several solvents. The solvents tested were benzene, toluene, methanol, ethyl benzene, and p-xylene (see Tables 3-13 and 3-14). Values were calculated at 160°C for

CO_2 at 360 psia and ethylene at 340 psia. Unfortunately, it was not possible to obtain reliable results for ethyl benzene and p-xylene in PS with ethylene as a high pressure carrier gas. Figure 3-28 does not show a clear trend with solvent size for the ethylene results. In this graph K_{Gas} refers to the partition coefficient with either CO_2 or ethylene as the carrier gas. Values calculated for the solvents in the presence of CO_2 indicate a higher influence in the bulkier molecules compared to methanol. However, there is no clear indication that the thermodynamic influence increases with increasing solvent size for the PS systems. GCLF-EoS indicates that the influence of the high pressure gas on the partition coefficient should increase for bulkier molecules. Other than the PS-benzene-CO2, there is little agreement between the model and the experimental results. This could be due to inaccurate pure component parameters at the higher temperatures of the PS systems study.

The influence of solvent size on the diffusion behavior is shown in Figure 3-29. Results were only obtained for the solvents in PS with CO_2 as a carrier gas. There appears to be a clear trend with solvent size which supports the results observed in the PVAc system.

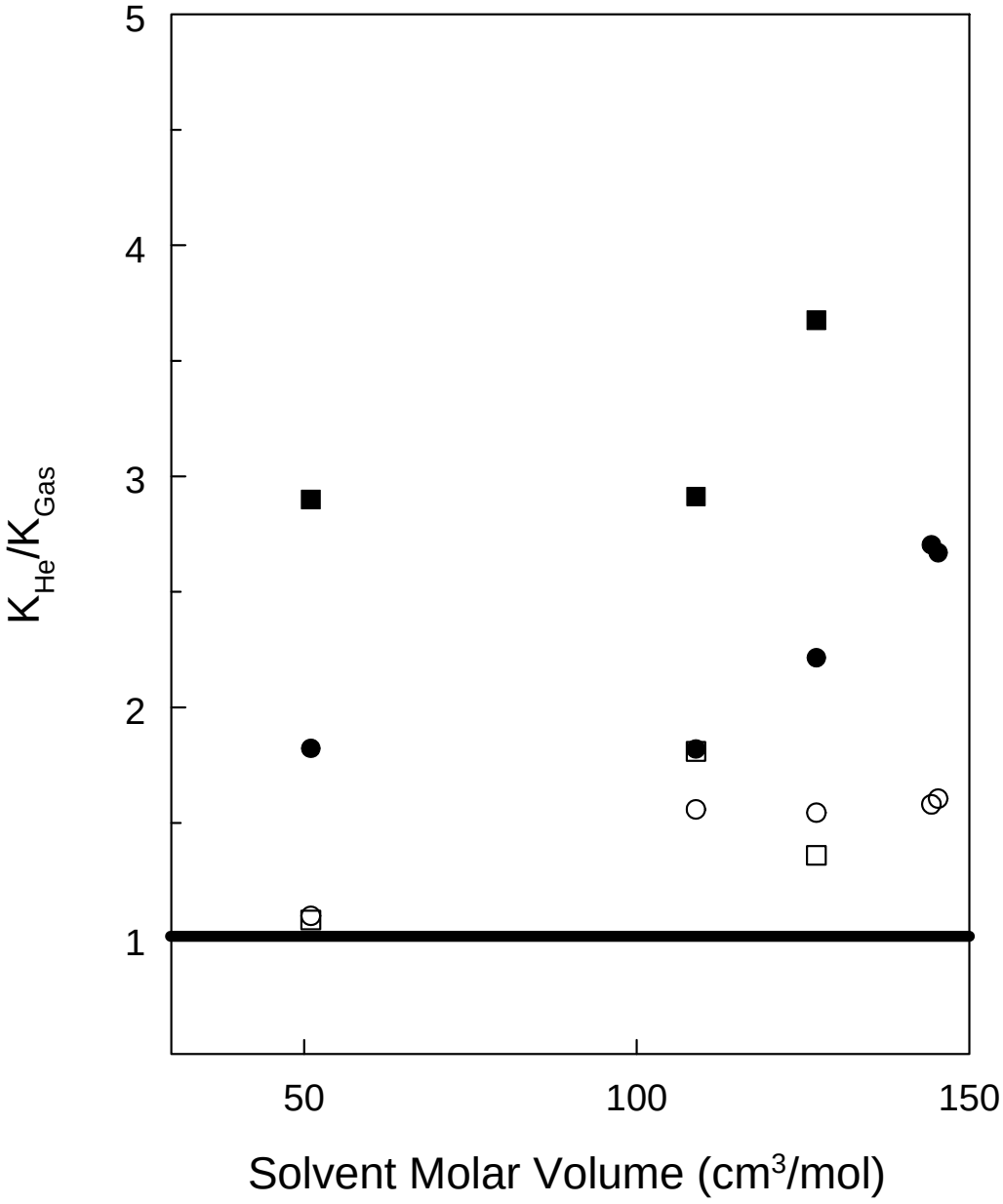

Figure 3-28: Carrier gas influence as determined by influence on partitioning of solvents of different sizes. Comparison was made for solvents in PS at 160°C with CO_2 carrier gas at 360 psia (○) and ethylene at 340 psia (□). GCLF-EoS was used to predict the influence of ethylene on the partition coefficient at 360 psia (●) of CO_2 and 340 psia (■) of ethylene.

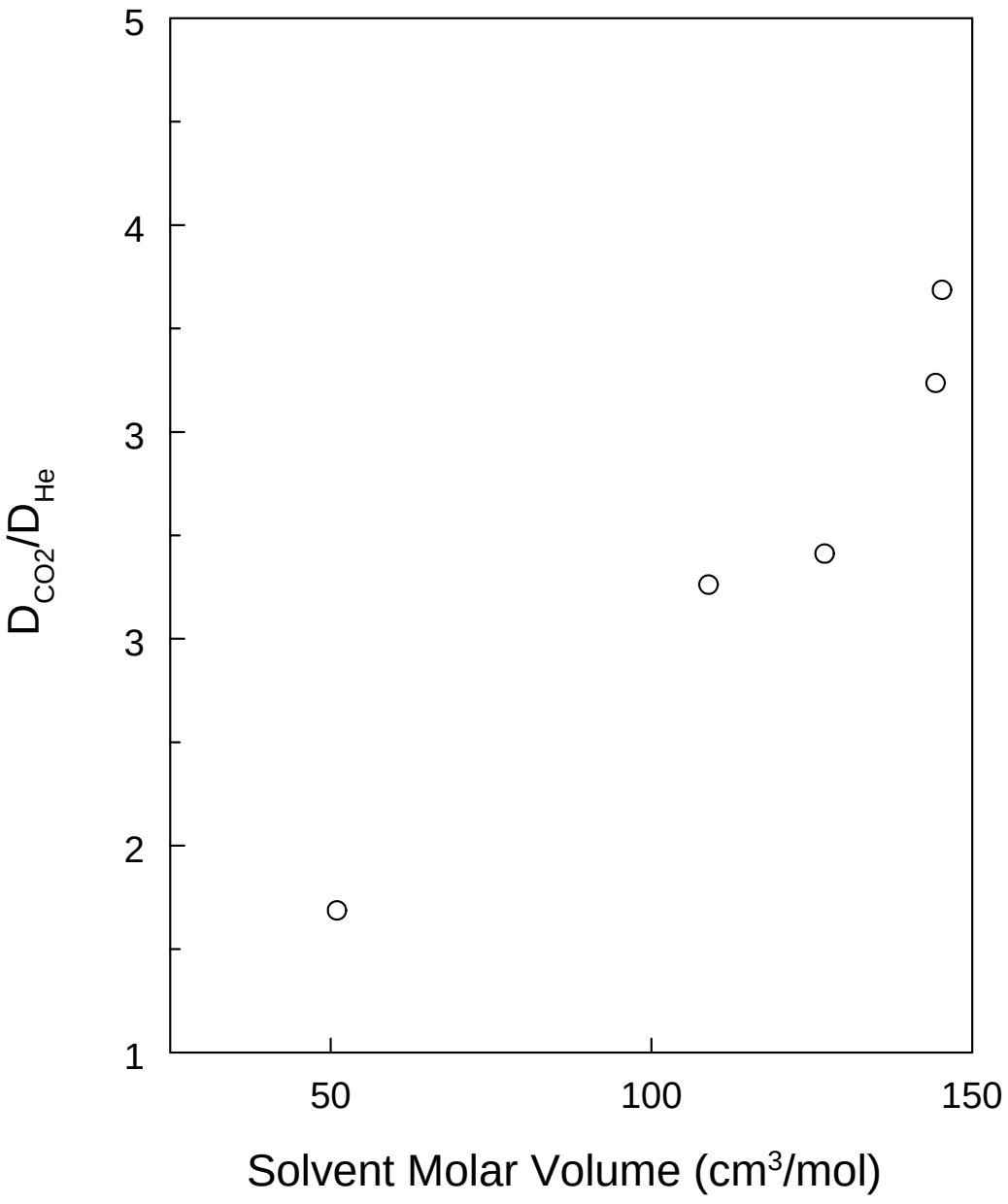

Figure 3-29: Carrier gas influence as determined by influence on diffusion of solvents of different sizes. Comparison was made for solvents in PS at 160°C with CO_2 carrier gas at 360 psia (○).

Table 3-14: Partition and diffusion coefficients of solvents in PS at 160°C measured with the HPIGC using high pressure carrier gases. All D_p values have units of (10^8 cm^2/s).

Solvent	Molar Volume (cm^3/mol)	CO_2			C_2H_4		
		P (psia)	K	D_p	P (psia)	K	D_p
Methanol	51.0	360	2.43	106.	340	2.47	-
Benzene	108.9	See Table 3-12					
Toluene	127.0	360	16.6	12.0	340	18.9	-
Ethyl Benzene	144.3	360	25.5	10.9	-	-	-
p-Xylene	145.3	360	26.8	9.94	-	-	-

The last step in this project was to evaluate the carrier gas potential in terms of the thermodynamic and diffusion influences on a per mole basis. To do so, the partition and diffusion coefficient ratios were plotted as a function of carrier gas concentration in the polymer. For the case of CO_2, the concentration was determined from the data of Sato et al. [19]. For the ethylene data, GCLF-EoS was used to estimate the concentration at the experimental temperature and pressure. It is assumed this calculation may have contributed up to 10% error in the results. However, as will be shown, despite the error assumption the results clearly indicate the more efficient gas.

Figure 3-30 shows a plot of the partition coefficient ratios for PVAc-methyl acetate as a function of carrier gas pressure at 70°C. The slope of the data indicates the strength of the carrier gas in terms of influence on the thermodynamic behavior of the

polymer-solvent system. It is clear that ethylene has a strong influence per molecule on the thermodynamics than CO_2.

Figure 3-31 shows a plot of the diffusion coefficient ratios for PVAc-methyl acetate as a function of carrier gas pressure. The slope of the data indicates the strength of the carrier gas in terms of influence on the diffusion behavior of the polymer-solvent system. Again, based on these results it appears ethylene has a strong plasticization potential. This is expected from the free volume theory of diffusion. Generally, a larger molecule will bring more free volume to the system and have a larger influence. The data in this study support that theory.

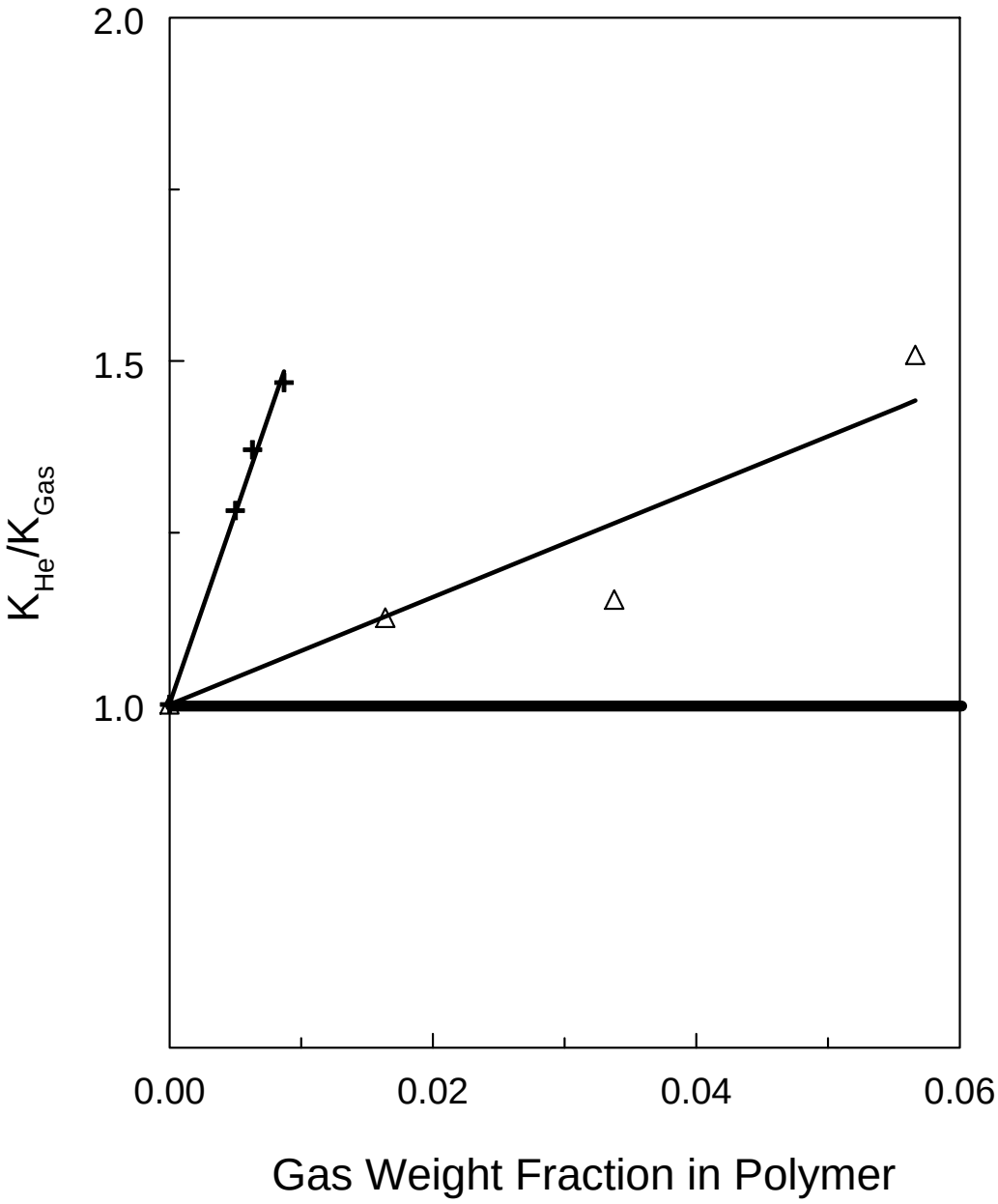

Figure 3-30: Comparison of carrier gas influence of ethylene (+) and CO_2 (△) on partitioning of PVAc-methyl acetate at 70°C. The weight fraction of CO_2 in PVAc was determined from experimental data of Sato et al. [19]. The weight fraction of ethylene in PVAc was calculated using the GCLF-EoS.

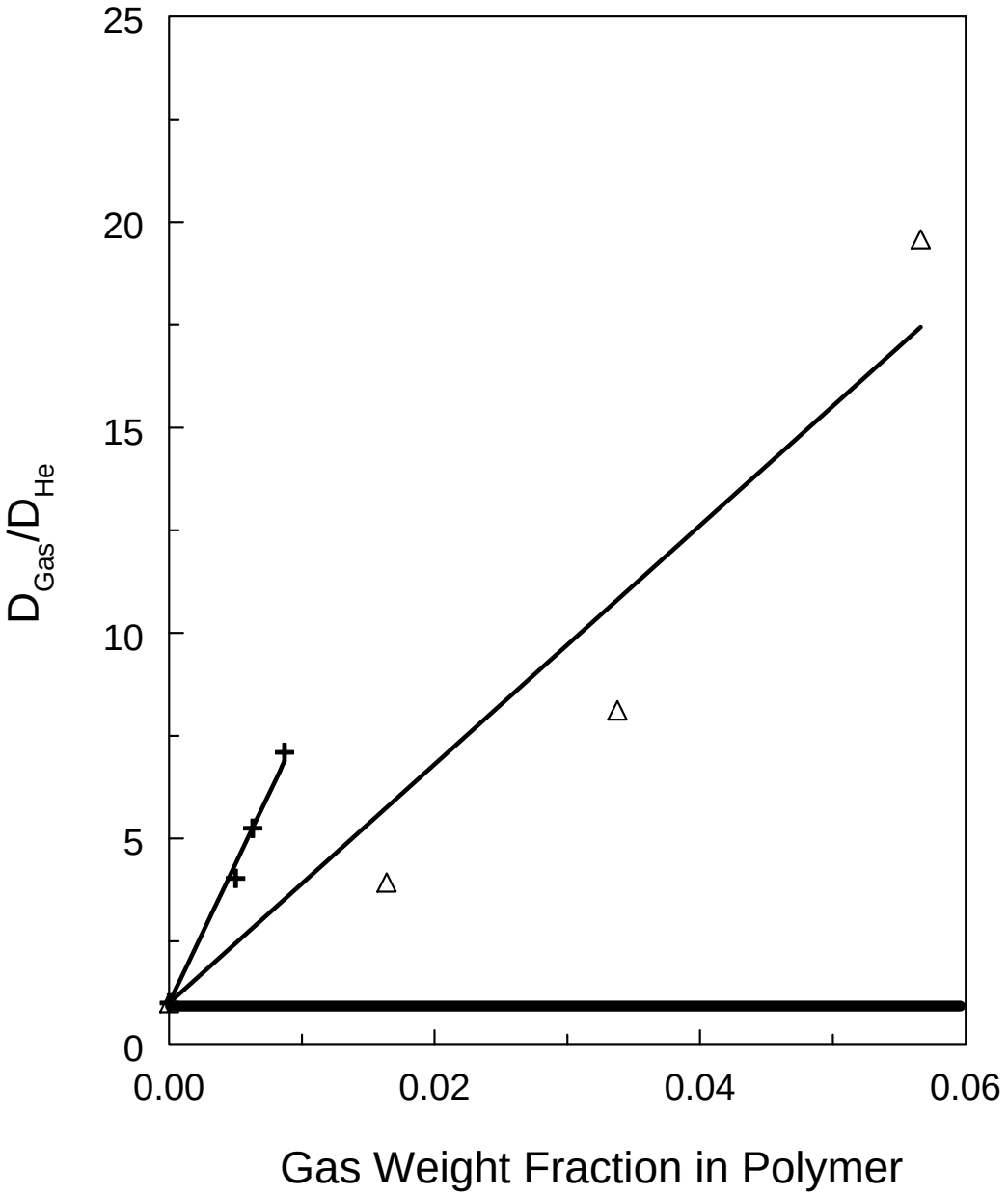

Figure 3-31: Comparison of carrier gas influence of ethylene (+) and CO_2 (△) on diffusion of PVAc-methyl acetate at 70°C. The weight fraction of CO_2 in PVAc was determined from experimental data of Sato et al. [19]. The weight fraction of ethylene in PVAc was calculated using the GCLF-EoS.

Figure 3-32 shows a similar comparison for the system PS-benzene at 145°C. Again the trend of the data indicates that ethylene has a strong influence per molecule on the thermodynamics than CO_2.

Figure 3-33 shows a plot of the diffusion coefficient ratios for PS-benzene as a function of carrier gas pressure. The slope of the data indicates the strength of the carrier gas in terms of influence on the diffusion behavior of the polymer-solvent system. Again, based on these results it appears ethylene has a strong plasticization potential.

The data on two different polymer-solvent systems both indicate that ethylene has the strongest potential for influencing the thermodynamics and mass transport behavior.

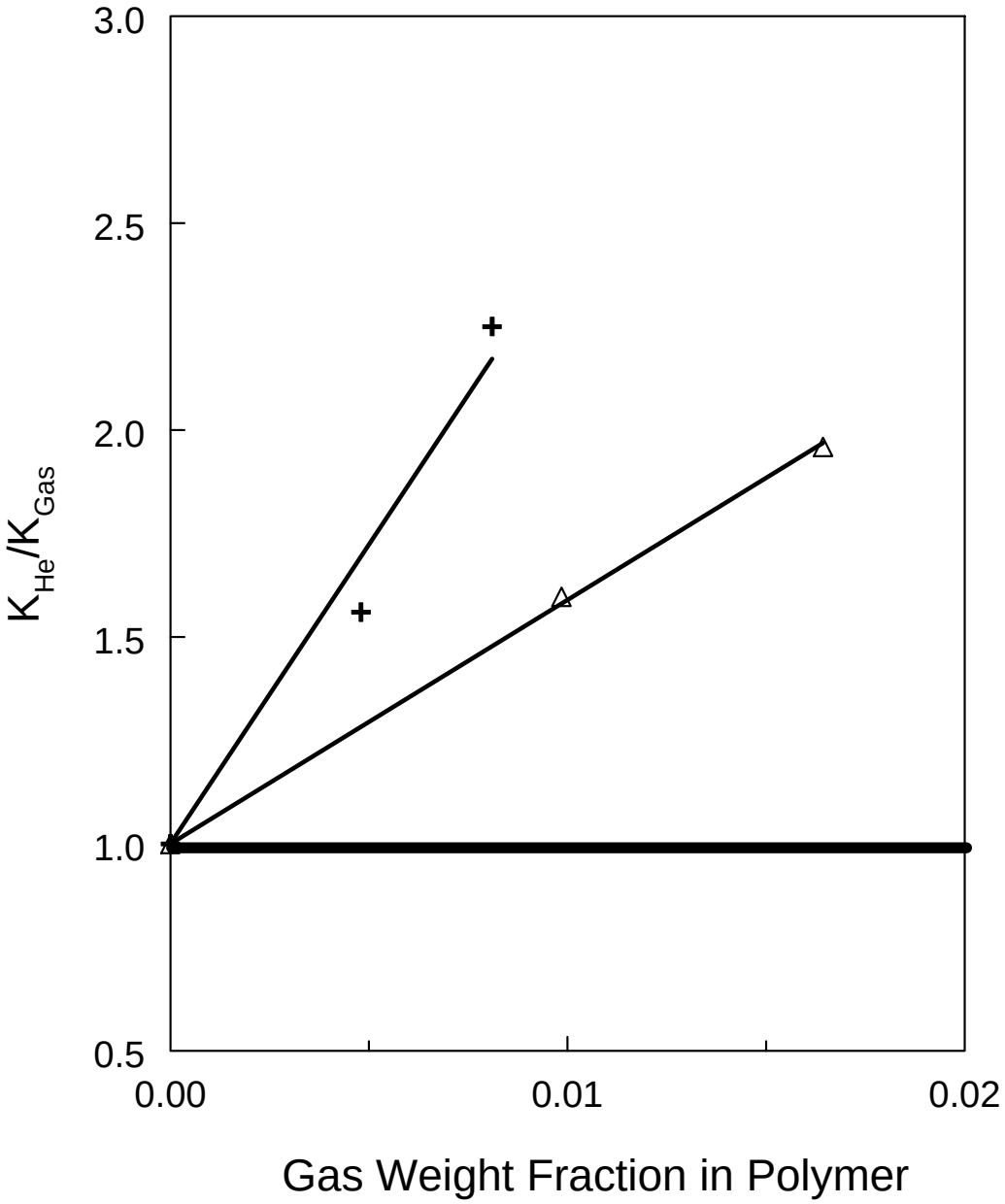

Figure 3-32: Comparison of carrier gas influence of ethylene (+) and CO_2 (△) on partitioning of PS-benzene at 145°C. The weight fraction of CO_2 in PS was determined from experimental data of Sato et al. [19]. The weight fraction of ethylene in PS was calculated using the GCLF-EoS.

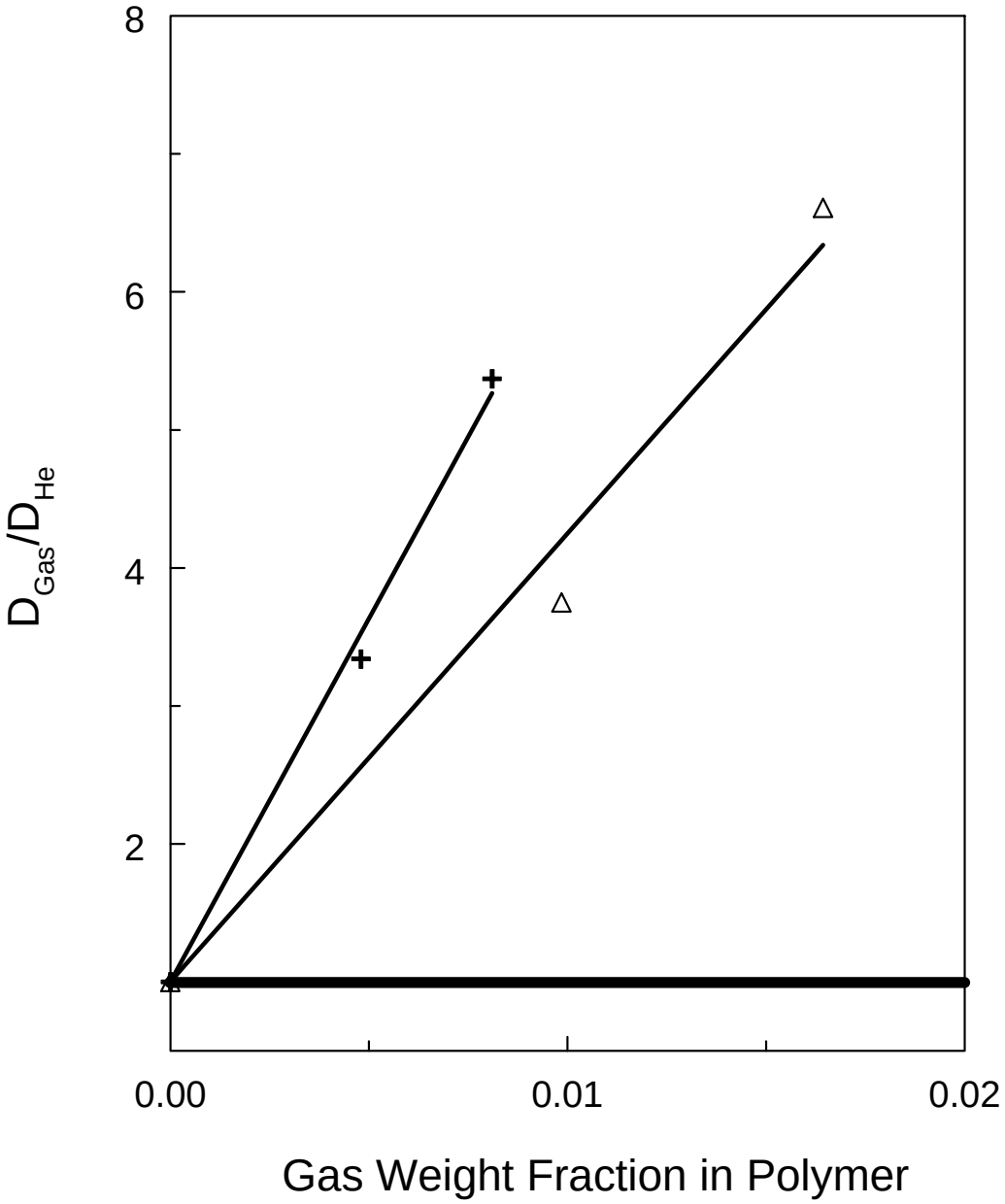

Figure 3-33: Comparison of carrier gas influence of ethylene (+) and CO_2 (△) on diffusion of PS-benzene at 145°C. The weight fraction of CO_2 in PS was determined from experimental data of Sato et al. [19]. The weight fraction of ethylene in PS was calculated using the GCLF-EoS.

3.6 Conclusions

IGC has been shown to be a useful tool for examining the effects of high pressure gases on polymer-solvent behavior. In this work it was determined that ethylene (on a per mole basis) has a stronger influence on polymer-solvent solubility and diffusivity compared to CO_2. GCLF-EoS was used to predict the influence of the high pressure gases on the thermodynamic behavior. The model predicts that the influence of the gases is higher for larger molecules. The experimental results for the PVAc systems confirm that the influence of these gases on the thermodynamics increases with increasing solvent size. Free volume theory of diffusion predicts that molecules having larger free volume will plasticize the polymer to a higher extent. The comparison of carrier gases in Figures 3-31 and 3-33 indicate that the influence of the gases on the diffusion behavior almost certainly increases for bulkier solvent molecules. The implications of this work are that CO_2 and ethylene have a pronounced effect on the thermodynamics and mass transport of polymer-solvent systems and devolatilization processes involving removal of higher molecular weight species such as aromatics and long chain paraffins will benefit the most from their use in those processes.

3.7 References

1. Gray, D. G.; Guillet, J. E. Studies of Diffusion in Polymers by Gas-Chromatography. *Macromolecules* **1973**, *6*, 223-227.

2. Price, G. J.; Guillet, J. E., The Use of Gas-Chromatography to Study Solubility in Polymeric Systems. *J. Solution Chem.* **1987**, *16*, 605-613.

3. Pawlisch, C. A.; Macris, A.; Laurence, R. L., Solute Diffusion in Polymers .1. The Use of Capillary Column Inverse Gas-Chromatography. *Macromolecules* **1987**, *20*, 1564-1578.

4. Pawlisch, C. A.; Bric, J. R.; Laurence, R. L. Solute Diffusion in Polymers .2. Fourier Estimation of Capillary Column Inverse Gas-Chromatography Data. *Macromolecules* **1988**, *21*, 1685-1698.

5. Arnould, D.; Laurence, R. L. Size Effects on Solvent Diffusion in Polymers. *Ind. Eng. Chem. Res.* **1992**, *31*, 218-228.

6. Romdhane, I. H.; Danner, R. P. Polymer-Solvent Diffusion and Equilibrium Parameters by Inverse Gas-Liquid-Chromatography. *AIChE J.* **1993**, *39*, 625-635.

7. Xie, L.Q. Measurement of Solute Diffusion in Polymers by Inverse Gas-Chromatography using Fused-Silica Open-Tubular Columns. *Polymer* **1993**, *34*, 4579-4584.

8. Brockmeier, N. F.; McCoy, R. W.; Meyer, J. A. Gas Chromatographic Determination of Thermodynamic Properties of Polymer Solutions. I. Amorphous Polymer Systems. *Macromol.* **1972**, *5*, 464-470.

9. Brockmeier, N. F.; McCoy, R. W.; Meyer, J. A. Gas Chromatographic Determination of Thermodynamic Properties of Polymer Solutions. *Macromol.* **1972**, *5*, 130-132.

10. Brockmeier, N. F.; McCoy, R. W.; Meyer, J. A. Gas Chromatographic Determination of Thermodynamic Properties of Polymer Solutions. II. Semicrystalline Polymer Systems. *Macromol.* **1973**, *6*, 176-180.

11. Brockmeier, N. F.; Carlson, R. E.; McCoy, R. W. Gas-Chromatographic Determination of Thermodynamic Properties of Polymer-Solutions at High-Pressure. *AIChE J.* **1973**, *19*, 1133-1139.

12. Price, G. J.; Guillet, J. E., The Determination of Thermodynamic Properties of Polymer-Solutions by Finite-Concentration Gas-Chromatography *J. Macromol. Sci. Chem.* **1986**, *A23*, 1487-1502.

13. Tihminlioglu, F; Surana, R. K.; Danner, R. P.; Duda, J. L. Finite Concentration Inverse Gas Chromatography: Diffusion and Partition Measurements. *J Polym. Sc.i Pol. Phys.* **1997**, *35*, 1279-1290.

14. Surana, R. K.; Danner, R. P.; Duda, J. L. Diffusion and Equilibrium Measurements in Ternary Polymer-Solvent-Solvent Systems Using Inverse Gas Chromatography. *Ind. Eng. Chem. Res.* **1998**, *37*, 3203-3207.

15. Alessi, P.; Cortesi, A.; Kikic, I.; Vecchione, F. Plasticization of Polymers with Supercritical Carbon Dioxide: Experimental Determination of Glass-Transition Temperatures. *J. Appl. Polym. Sci.* **2003**, *88*, 2189-2193.

16. Zielinski, J. M.; Fry, R. F.; Kimak, M. F. Probing Multicomponent Thermodynamic Effects by Low- and High-Pressure Capillary Column Inverse Gas Chromatography. *Macromolecules* **2004**, *37*, 10134-10140.

17. Macris, A. Measurement of Diffusion and Thermodynamic Interactions in Polymer-Solvent Systems Using Capillary Column Inverse Gas Chromatography. M.S. Thesis, University of Massachusetts, Amherst, MA, **1979**.

18. Pawlisch, C. A. Measurement of the Diffusivity and Thermodynamic Interaction Parameters of a Solute in a Polymer Melt Using Capillary Column Inverse Gas Chromatography. Ph.D. Thesis, University of Massachusetts, Amherst, MA, **1985**.

19. Sato, Y.; Takikawa, T.; Takishima, S.; Masuoka, H. Solubilities and Diffusion Coefficients of Carbon Dioxide in Poly(Vinyl Acetate) and Polystyrene. *J. Supercrit. Fluid.* **2001**, *19*, 187-198.

Chapter 4

Effect of Water on Polyethylene-Ethylene Transport and Thermodynamic Behavior

4.1 Introduction

In the production of polymers, the resulting product typically retains residual solvent and/or monomer which must be removed through a process step referred to as devolatilization. Gas or steam stripping is one of the common techniques used. Steam stripping offers benefits over gas stripping such as easy recovery of volatile organic compounds (VOCs) through condensation of the steam, higher operating temperatures, and improved economics due to smaller stripping columns and the absence of air blowers and equipment. In addition, use of air or nitrogen poses potential problems such as formation of dangerous gas mixtures, difficulty in separation of VOCs from the gas, and poor heat transfer [1].

Much of the work on devolatilization has dealt with either latex processes [2-5] or poly (vinyl chloride) systems [6,7]. In such systems the polymer particles are relatively small and thus diffusion within the particle can be neglected. However, in the devolatilization of polyethylene pellets of considerable dimension diffusion of the solvent or monomer within the polymer is often the limiting step. Therefore, knowledge of

thermodynamic and mass transfer effects that water may have on the system is vital to properly designing stripping units. Two possible effects of water on the system are:

1) lower solubility of solvents and monomers in polyethylene-water mixture which offers larger thermodynamic driving force for exit of ethylene from polymer
2) plasticization of polyethylene by water resulting in increased diffusion rates

An early claim indicated that the use of steam could have a significant effect on the equilibrium of residual cyclohexane in high density polyethylene (HDPE) [8]. Subsequent work by Matthews et al. [9] found that water hindered the diffusion of hexane in ethylene-propylene elastomers. In addition, they found that the stripping rate of elastomer particles was not influenced by the formation of a liquid film surrounding the particles. The goal of this work was to examine whether water would influence the diffusion and solubility of ethylene in polyethylene and determine if an increased stripping rate might be expected.

4.2 Experimental

Data were collected using two independent gravimetric techniques. The first is the static sorption capsule technique (referred to as the capsule method from hereon) which was developed by Palamara and coworkers [10]. Originally designed with a single sorption chamber (“capsule”) for solubility measurements, Palamara et al. [11] later extended the method to diffusion studies through the addition of more capsules. It is a relatively simple experiment in which polymer charged capsules are weighed before and

after solvent loading. The total mass uptake is experimentally measured and the partitioning of solvent is calculated to determine the uptake of solvent within the polymer. In this work, the method was modified to probe the influence of water on binary polyethylene-ethylene sorption and diffusion behavior.

The second technique is a pressure decay method developed by Davis et al. [12]. The method has proven useful in the measurement of sorption and diffusion of gases in polymers at high pressures. Pressure decay was used primarily to insure the binary polyethylene-ethylene data obtained with the capsule method was an accurate baseline prior to testing the influence of water on the system.

The details of the pressure decay technique for study of binary systems have been well described elsewhere [12]. Important details of the capsule method are highlighted and modifications necessary for testing the influence of water are described in the following sections.

4.2.1 Capsule Method Apparatus

A schematic diagram of the static sorption capsule apparatus is shown in Figure 4-1. For pressure measurement, a Druck PMP Model 4010 pressure transducer was used which had a sensitivity of ±1.6 psi. A custom-built aluminum heating block was machined with four chambers for housing of the sorption capsules during experimentation. A Fuji Electric PXZ-4 temperature controller was used to regulate the temperature of the aluminum block. The sorption capsules were machined from high-strength aluminum alloy 7075. The chamber of each capsule had a volume of

approximately 5.5 cm^3. Swagelok valves were used to open and close the capsules during an experiment. The balance used for weight measurements was an Ohaus Analytical Plus electronic balance with an upper limit of 210 g and accuracy to 0.1 mg.

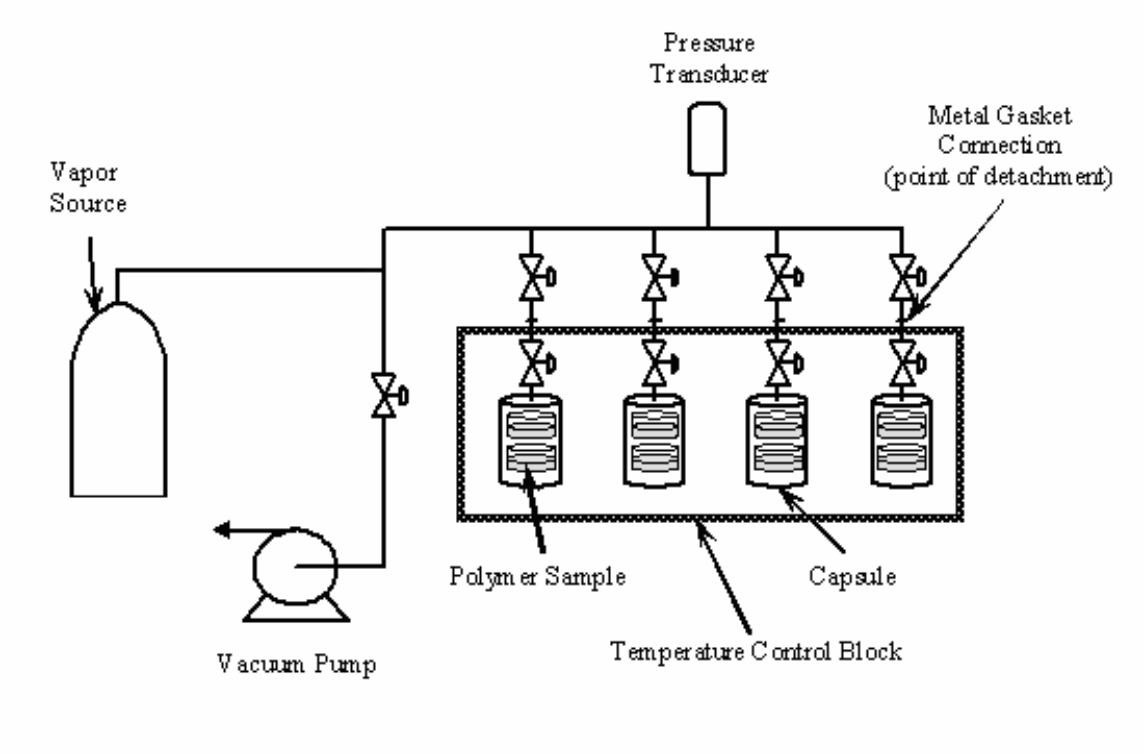

Figure 4-1: Static sorption capsule apparatus

4.2.2 Experimental Procedure

Prior to an experiment, volumes of the empty capsules were determined by charging them with argon, measuring the weight change, and calculating the volume based on the gas density.

The capsules were packed with polyethylene pellets in their native form. The plug at the base of the capsule was not removed after capsule volumes were determined. This

reduced the error introduced in later calculations involving the capsule volume. For collection of wet data, a needle port was welded to the valves used for opening and closing the capsules to minimize the flux of water vapor from the capsules during exposure to ethylene. This is shown in Figure 4-2.

Figure 4-2: Photo of capsule body. In the upper right-hand corner is a full assembled capsule. At top left, is the plug which fits into the bottom of the capsule body (upper middle of photo). At bottom left is a picture of the valve assembly with attached needle port.

Following loading of the polymer, 0.3 mL of water was added to each capsule. The valve was then replaced and the capsules were connected to vacuum. The capsules were evacuated at room temperature for less than a minute to prevent appreciable loss of water. The capsules were then closed and brought up to temperature. Next, the capsules were opened and exposed to ethylene for the prescribed amount of time. The capsules are weighed twice during an experiment: at early times when diffusion is occurring and once the system has reached equilibrium. This provides a total of eight data, as shown in Figure 4-3. Using the solution of Crank [14] (described in next section), the initial slope of the mass uptake curve can be used to obtain the diffusion coefficient. To prevent bias, the capsules were randomized by leaving different ones open for different lengths of time during diffusion experiments.

The capsule method and pressure decay techniques have been shown to give good agreement with other gravimetric techniques [10-12]. In addition, Figure 4-4 indicates that the two techniques give good agreement with each other [15,16].

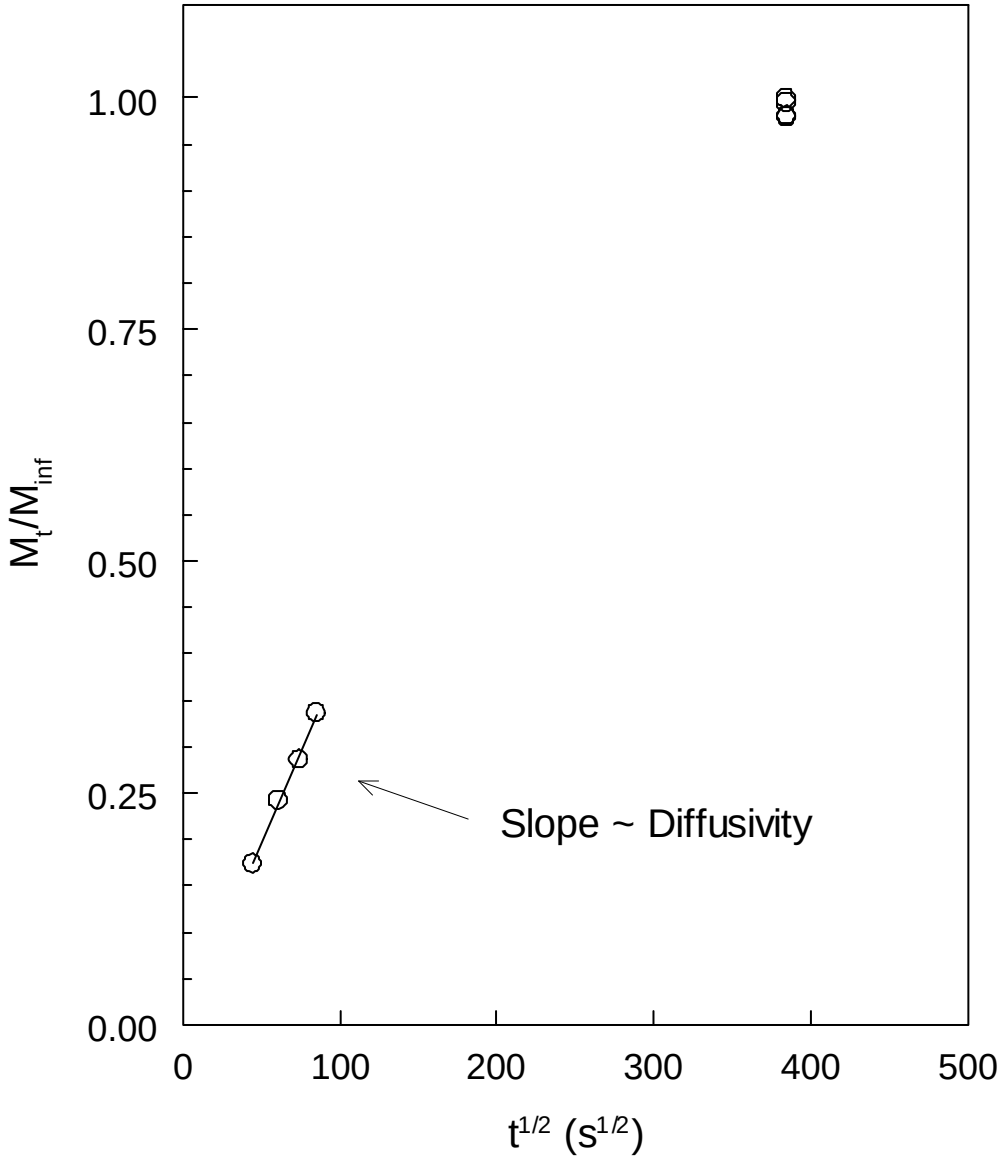

Figure 4-3: Sample mass uptake curve obtained from the static sorption capsule method [13].

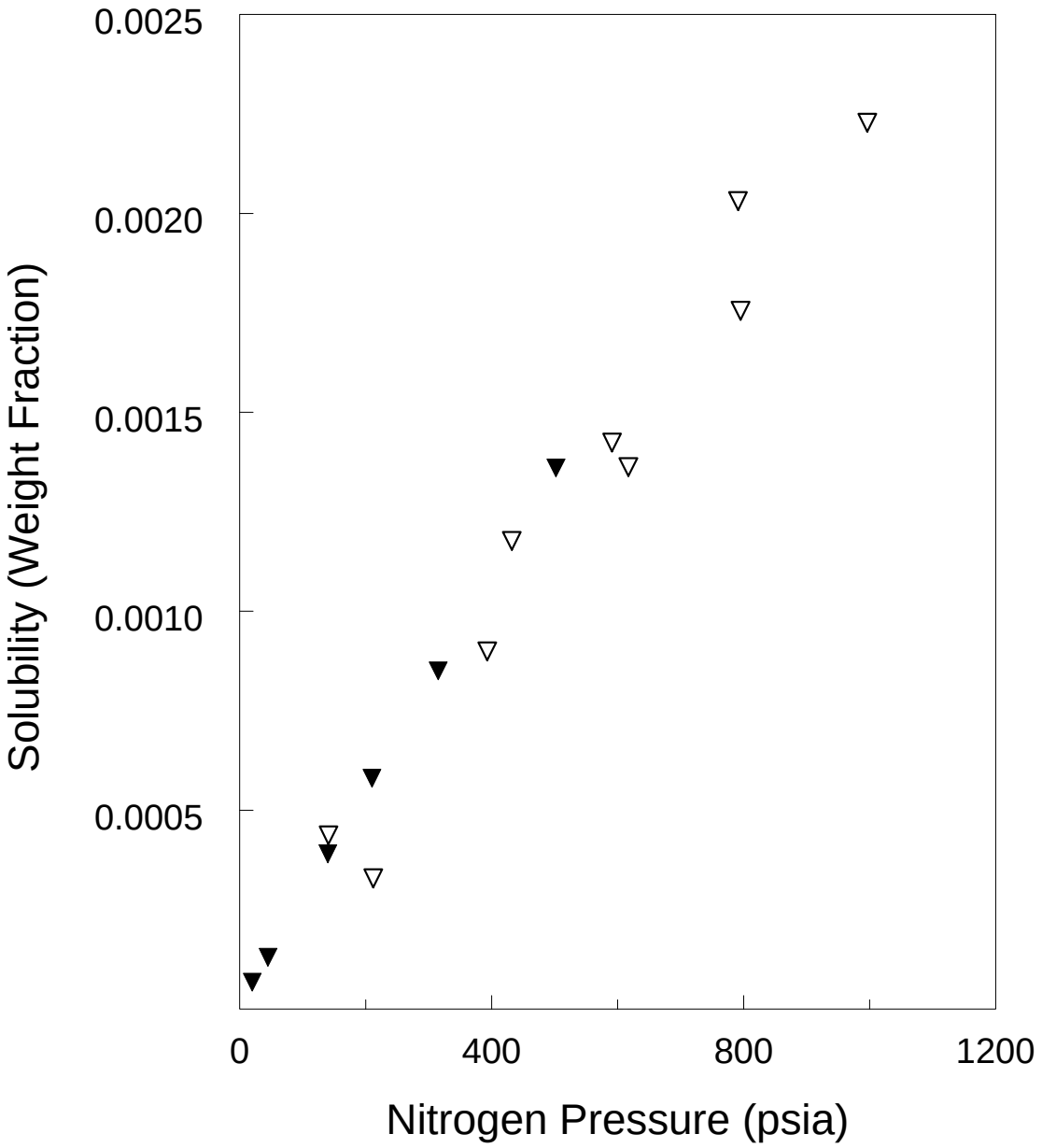

Figure 4-4: Comparison of solubility data for nitrogen in poly(vinyl acetate) (PVAc) at 40°C collected with the capsule method (▽) [15] and pressure decay technique (▼) [16].

4.2.3 Materials

Low-density polyethylene (LDPE) pellets were provided by NOVA Chemicals and had a spherical geometry with average diameter of 3.33 ± 0.04 cm. Differential scanning calorimetry (DSC) was used to determine the crystallinty of the sample. Figure 4-5 shows the results of the test. Using a suggested value [17] of 293 J/g for the standard heat of fusion resulted in a crystallinity of 49 wt%. Other properties of the sample are provided in Table 4-1.

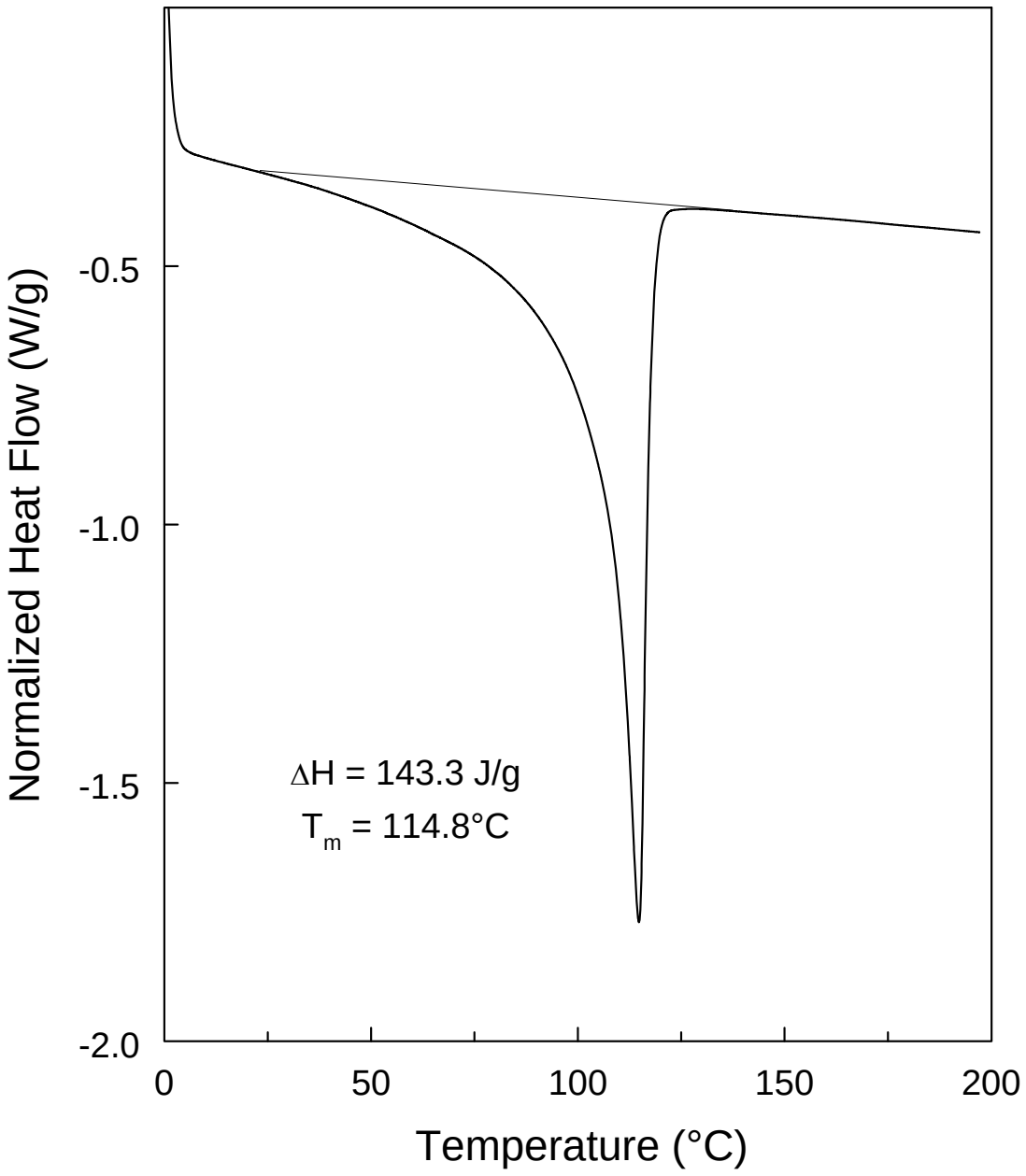

Figure 4-5: DSC results for LDPE used in this study.

Ethylene was provided by Valley National Gas Company and had purity greater than 99.5%. Distilled water was used as provided by in-house supply lines.

Table 4-1: LDPE Properties

M_w	Polydispersity	T_m (°C)	Crystallinity (wt%)
145600	5.5	114.8	49

4.3 Theory

4.3.1 Analysis of Data

The analysis used for the pressure decay technique was described in [12]. Analysis of the capsule method data and changes necessary when water is present in the capsule are provided here.

The goal of the experiment was to determine the mass of ethylene in LDPE during the diffusion step and at equilibrium. To calculate the mass of ethylene in the polymer, a mass balance is carried out on the static sorption capsule. The capsule is weighed before and after exposure to the gas. Based on the weight difference and knowledge of the headspace volume, the ethylene gas present in the polymer phase is determined at the experimental conditions. The primary benefit of the experiment is that weighing is performed at ambient conditions and the distribution of mass within the capsule is calculated at the experimental conditions. This permits use of a standard analytical

balance for weighing of the capsule. The calculation of ethylene gas in the polymer at given temperature and pressure is given by the following:

$$m_{gp} = M_g - V_{HS}\rho_g(T,P) \tag{4.1}$$

where m_{gp} is the mass of ethylene gas in the polymer, M_g is the total mass of ethylene in the capsule, V_{HS} is the volume of the vapor headspace, and ρ_g is the ethylene gas density calculated using an extended BWR equation of state[18]. Table 4-2 lists the constants used in this work.

Table 4-2: Parameters for the extended BWR [18] equation of state

A_1	$-0.99440284 \times 10^{-2}$
A_2	$0.15538290 \times 10^{-4}$
A_3	0.17517303×10^{3}
A_4	$-0.81264911 \times 10^{7}$
A_5	$0.14945133 \times 10^{-4}$
A_6	$-0.17142165 \times 10^{-7}$
A_7	-0.47193713
A_8	0.29932596
A_9	$-0.64351593 \times 10^{4}$
A_{10}	$0.43850930 \times 10^{-13}$
A_{11}	0.89877298×10^{7}
A_{12}	$-0.19440328 \times 10^{5}$
B	0.26×10^{-4}

The second term on the right side of Eq. 4.1 represents the mass of ethylene present in the vapor headspace. Therefore, any remaining gas must be present in the polymer phase. In terms of measured variables Eq. 4.1 can be recast as:

$$m_{gp} = M_{tot} - M_{evac} - \left[V_c - \frac{m_{gp} + m_p}{\rho_l(\omega_g, T, P)}\right]\rho_g(T,P) \tag{4.2}$$

where M_{tot} is the total mass after exposure to ethylene, M_{evac} is the evacuated mass of the capsule prior to exposure. This mass consists of the capsule apparatus charged with LDPE. The total volume of the capsule is V_c, while the mass of the dry polymer sample is m_p , and ρ_l is the density of the polymer solution at the experimental conditions. The liquid density was calculated with the GCLF-EoS. In addition, it depended on the mass of gas in the polymer requiring an iterative scheme to be applied. The parameters used in the GCLF-EoS are reported in Table 4-3.

In the case where water is present in the capsule, M_{evac} is the total mass of the capsule with the polymer and water present. The volume of the headspace was adjusted by subtracting the volume of water added to the capsule, V_w resulting in the following expression for analysis of the ternary data:

$$m_{gp} = M_{tot} - M_{evac} - \left[V_c - V_w - \frac{m_{gp} + m_p}{\rho_l(\omega_g, T, P)} \right] \rho_g(T, P) \tag{4.3}$$

Ideally one would know the vapor composition in order to analyze a ternary system. In the absence of a method for sampling the vapor mixture, the system can be treated as pseudo-binary. V_w was measured prior to charging the capsule with ethylene. It was assumed the water was distributed as adsorbed water on the pellets, absorbed water in the pellets, and possibly some water in the bottom of the capsule. However, the solubility of ethylene in water can be assumed negligible and any change in the system is likely due to the shift in equilibrium between the LDPE-water mixture with ethylene.

Table 4-3: GCLF-EoS Parameters for LDPE-ethylene system

	v_i^* (m^3/mol)		ε_{ii} (J/mol)		k_{ij}	
	80°C	100°C	80°C	100°C	80°C	100°C
LDPE	2.84×10^{-2}	2.84×10^{-2}	962.8	973.1	0.031	0.015
Ethylene	5.41×10^{-5}	5.50×10^{-5}	589.6	596.2		

The solubility was reported as the weight fraction of the gas in the polymer:

$$\omega = \frac{m_{gp}}{m_{gp} + m_p} \tag{4.4}$$

For experiments below T_m, the weight fraction was adjusted to an amorphous polymer basis using the crystallinity of the sample.

The diffusion coefficient was calculated using the solutions of Crank [14] for spherical geometry. Data were obtained in the initial slope region and the limiting slope region. The resulting expressions for the diffusion coefficient for the respective solutions are:

$$D = \frac{\pi R^2}{36}\left(\frac{\partial\left(M_t/M_\infty\right)}{t^{1/2}}\right)^2 \tag{4.5}$$

and

$$D = -\frac{R^2}{\pi}\left(\frac{\partial \ln\left(1 - M_t/M_\infty\right)}{t}\right) \tag{4.6}$$

where the terms in the parentheses are the slope of the data.

4.3.2 Error Analysis

Because of the complexity of the system with water it is imperative to quantify the uncertainty in the measurements of the solubility and diffusivity. This was done through a propagation of error analysis.

The uncertainty in a calculated quantity ΔF can be estimated based on the uncertainty in the measurements of the quantities, x_i on which F depends as given by the following propagation of error equation [19]:

$$\Delta F^2 = \sum_i \left(\frac{\partial F}{\partial x_i} \Delta x_i \right)^2 \tag{4.7}$$

where Δx_i is the uncertainty in the measured quantity, x_i. Therefore, for the uncertainty in the calculation of the solubility from the capsule method, the following expression was used:

$$\begin{aligned} \Delta\omega^2 = &\left(\frac{\partial \omega}{\partial M_{tot}} \Delta M_{tot} \right)^2 + \left(\frac{\partial \omega}{\partial M_{evac}} \Delta M_{evac} \right)^2 + \left(\frac{\partial \omega}{\partial V_c} \Delta V_c \right)^2 + \left(\frac{\partial \omega}{\partial V_w} \Delta V_w \right)^2 \\ &+ \left(\frac{\partial \omega}{\partial m_p} \Delta m_p \right)^2 + \left(\frac{\partial \omega}{\partial \rho_l} \Delta \rho_l \right)^2 + \left(\frac{\partial \omega}{\partial \rho_g} \Delta \rho_g \right)^2 \end{aligned} \tag{4.8}$$

The uncertainty in the mass was ± 0.1mg. Using the method described by Palamara [10], the uncertainty in the capsule volume was found to be approximately 0.2 cm^3. The uncertainty in the volume of water added to the capsule was only 0.045 cm^3. However, for cases where water was present in the capsule, the volume of the capsule was assumed to have an additional 4% uncertainty because the distribution of the water was unknown. The uncertainty in the polymer solution density was taken as 1% based on reported results [20,21]. The gas density was calculated using the BWR equation of state

and it was assumed no error resulted from the calculation. However, the uncertainty in the temperature and pressure resulted in an uncertainty of approximately 1%. Combining Eq. 4.3 and Eq. 4.4 and differentiating with respect to each variable resulted in an uncertainty in the solubility of 11% or less for the binary experiments and 20% or less for experiments with water.

A similar procedure was employed for estimating the uncertainty in the diffusivity measurements.

$$\Delta D^2 = \left(\frac{\partial D}{\partial R}\Delta R\right)^2 + \left(\frac{\partial D}{\partial Slope}\Delta Slope\right)^2 \qquad (4.9)$$

In this case, the standard error in the regression of the data points was used to estimate the error in the diffusivity. The uncertainty in the estimation of the LDPE pellet radius was 0.02 cm. Differentiation of Eq. 4.9 gave an uncertainty of about 20% for diffusion coefficients measured with the capsule method.

4.4 Results

4.4.1 Dry Data

The first step in this work was to measure the diffusion coefficient and solubility of ethylene in LDPE under normal (dry) conditions. The dry data are shown in Table 4-4. Doing so provided a baseline for comparisons of the binary system in the presence of water (wet). The solubility data collected with the capsule method are shown in Figure 4-6. In all the results presented, the solubility is based on the amorphous region of polymer.

Although wet data were not collected at 120°C, the dry data at that temperature were used to verify the proper temperature trend above T_m of the LDPE sample used in this study. The trend is consistent with results obtained by Davis [12] at 150°C using the pressure decay technique.

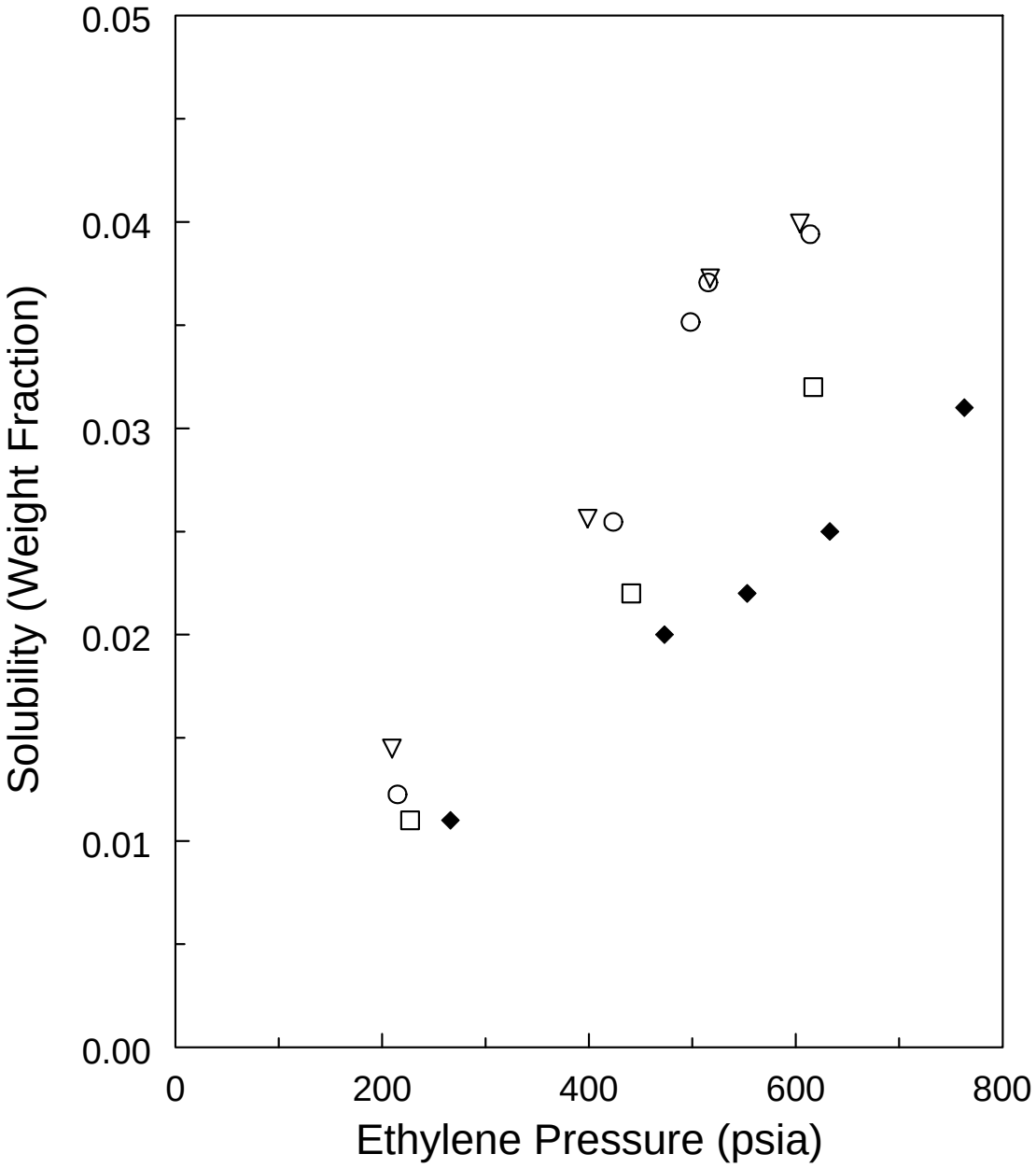

Figure 4-6: Solubility results for ethylene in LDPE at 80 (○), 100 (▽), and 120°C (□) obtained with the capsule method. Results at 150°C (◆) were obtained with the pressure decay technique [12].

The data are linear over the pressure range tested. Other researchers [22,23] have observed similar behavior. The data at 80 and 100°C show no noticeable difference. It was suspected that elastic effects may be present in LDPE. This possibility is discussed in a later section. The water is not expected to significantly influence the crystalline nature of the polymer; therefore, testing was still performed on the samples at these temperatures.

The diffusion of ethylene in dry LDPE as a function of ethylene pressure is shown in Figure 4-7. There is generally good agreement between the results of the pressure decay technique and the capsule method. The data show the expected trend with temperature. In addition there is no dependence on concentration of ethylene. This indicates a lack of free volume effects which is due to testing well above the T_g of the polymer [24]. There is considerably more scatter in the data at 80°C from both methods. Values of the diffusion coefficient at 80°C were in the range of 2.08 ~ 3.97 x 10^{-6}, while the values at 100°C were in the range of 6.51 ~ 8.73 x 10^{-6}.

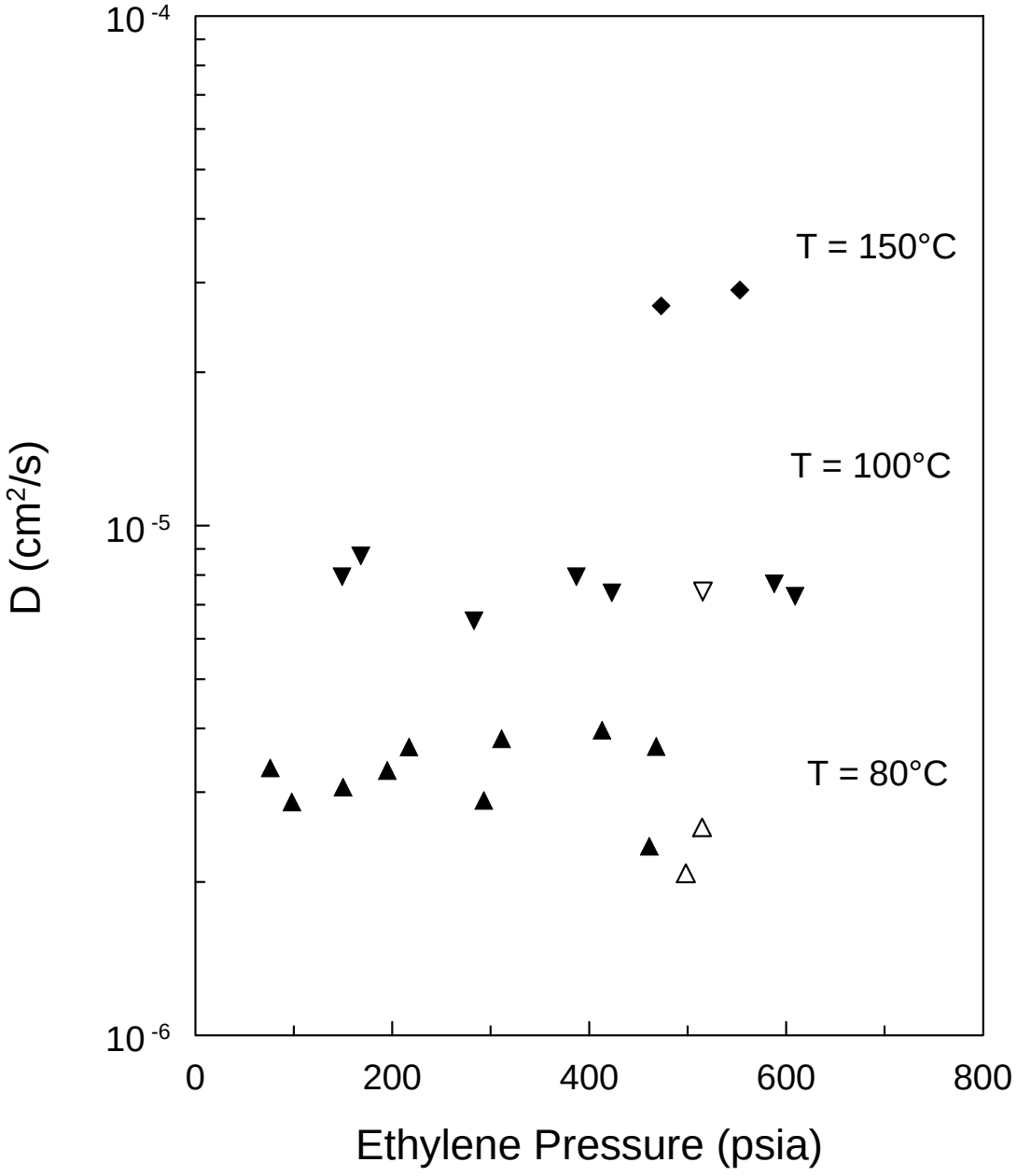

Figure 4-7: Diffusivity results for ethylene in LDPE at 80°C (△capsule, ▲ pressure decay) and 100°C (▽ capsule, ▼ pressure decay). Results at 150°C (◆) were obtained with the pressure decay technique [12].

4.4.2 Wet Data

Wet data were collected at high pressures of ethylene to minimize the error due to water diffusing out of the capsule. The product of D and P typically give a constant value. Thus as pressure is increased, the diffusion coefficient decreases. The wet data are shown in Table 4-5.

The solubility results for 80 °C are shown in Figure 4-8. There is considerable scatter in the results, especially for the wet data. Data collected in the presence of water had larger error due to the higher uncertainty in capsule volume, V_c. In the application of the GCLF-EoS to correlate the dry data the group contributions were used to predict the pure component parameters but k_{ij} was treated as an adjustable parameter to properly fit the data. A moderate value of k_{ij} was required to fit the data at 80°C. There appears to be a slight increase in solubility of ethylene in the presence of water at this temperature, although the point at 787 psia shows a decrease in solubility. In addition the dry data obtained with the capsule method above 500 psia appear to be higher than the results from the pressure decay technique and the trend of the capsule data below that pressure.

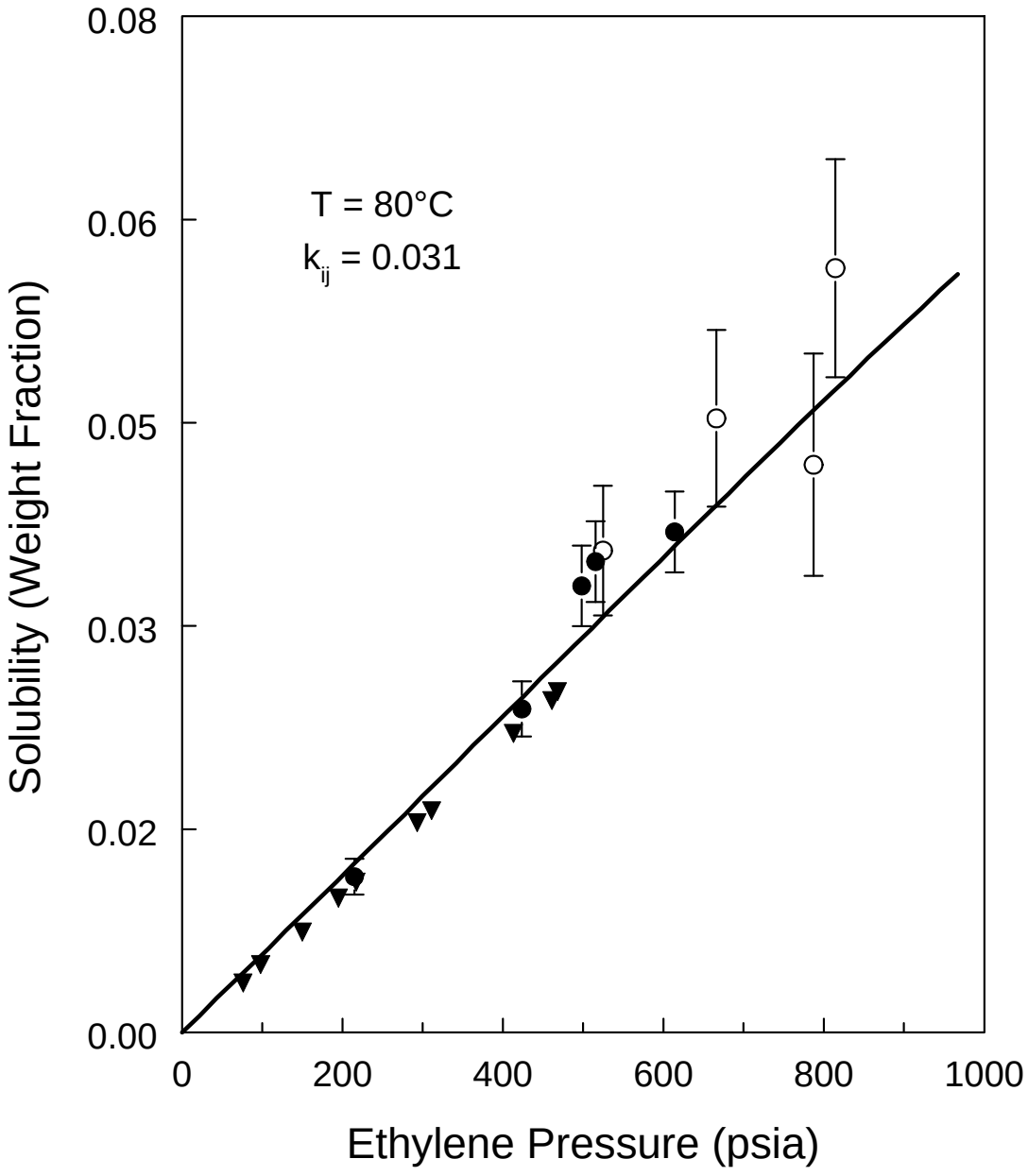

Figure 4-8: Solubility of ethylene in LDPE at 80°C. Dry data were taken with pressure decay (▼) and the capsule method (●). Data with water (○) were taken with the capsule method. The binary experimental data were used to obtain the interaction parameter, k_{ij}, used in the GCLF-EoS (–).

The data at 100°C show a similar trend to that of 80°C. The GCLF-EoS gave a good correlation of the data at 100°C with a considerably lower k_{ij}. In this case, the ethylene solubility was unaffected by the water within experimental error. Taking into account the results at both temperatures, it is concluded that water does not have a pronounced effect on the thermodynamics of the system.

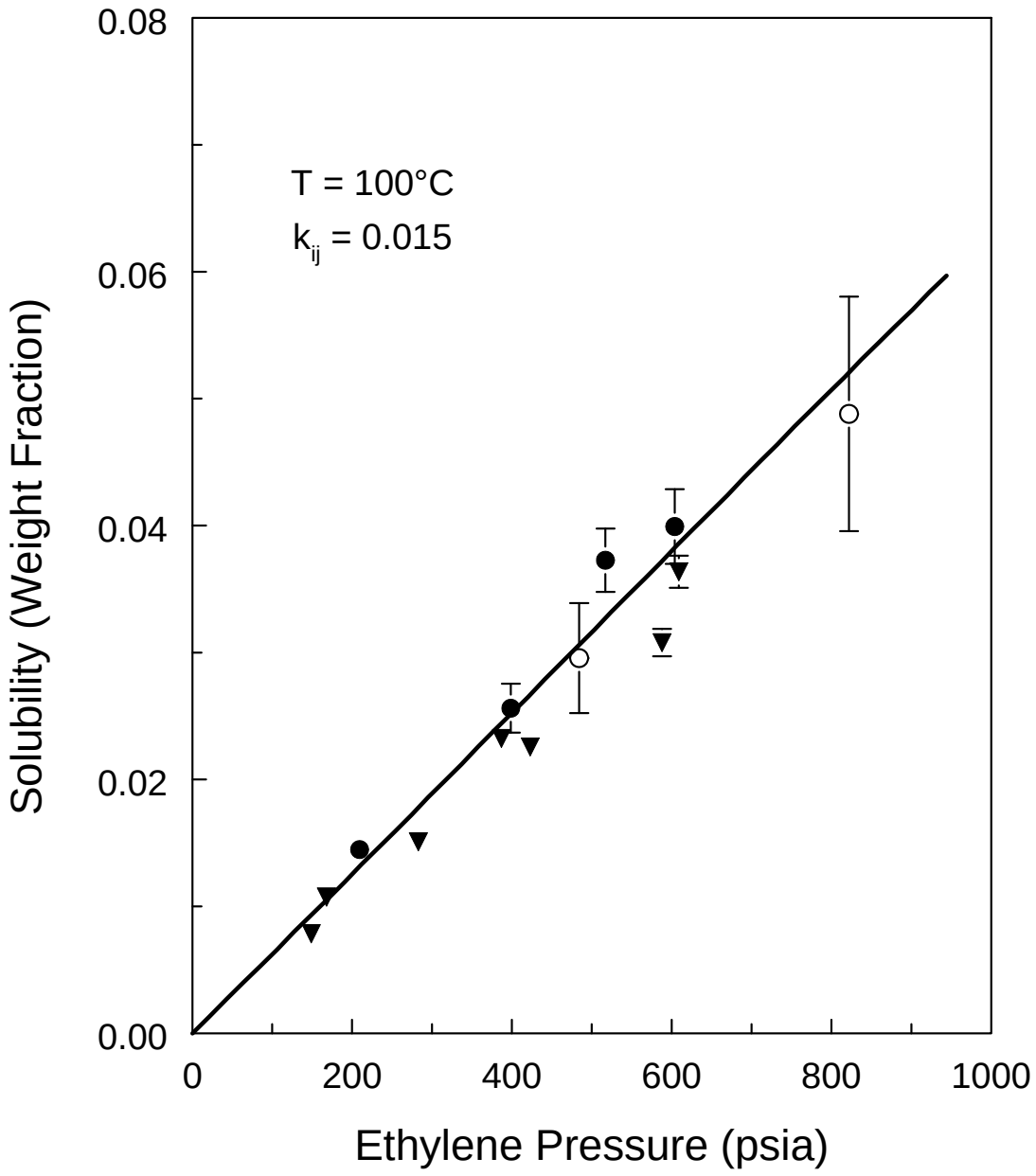

Figure 4-9: Solubility of ethylene in LDPE at 100°C. Dry data were taken with pressure decay (▼)and the capsule method (●). Data with water (○) were taken with the capsule method. The binary experimental data were used to obtain the interaction parameter, k_{ij}, used in the GCLF-EoS (–).

The diffusivity of ethylene in LDPE as a function of pressure at 80 and 100°C is shown in Figure 4-10 and Figure 4-11, respectively. The diffusion coefficient was independent of ethylene concentration. This was expected because the temperature was sufficiently high that free volume effects were expected to be absent as noted earlier. The error in these measurements was as high as 20%. The data from the pressure decay technique and the capsule method agree reasonably well. In addition the diffusion coefficients were higher at 100°C as expected. No observable influence of water on the diffusion behavior was evident at either temperature. This is in agreement with the observed lack of influence on the solubility of ethylene. The diffusion results are actually significant because it is expected that most compounds will plasticize the polymer and lead to an increase in the diffusion coefficient. Overall, it is concluded that the diffusion coefficient of ethylene is not significantly influenced by the presence of water. Results found by Galdamez et al. [25] support these findings. Using IGC they showed that water did not significantly influence the solubility or diffusivity of cyclohexane and 1-octene in LDPE.

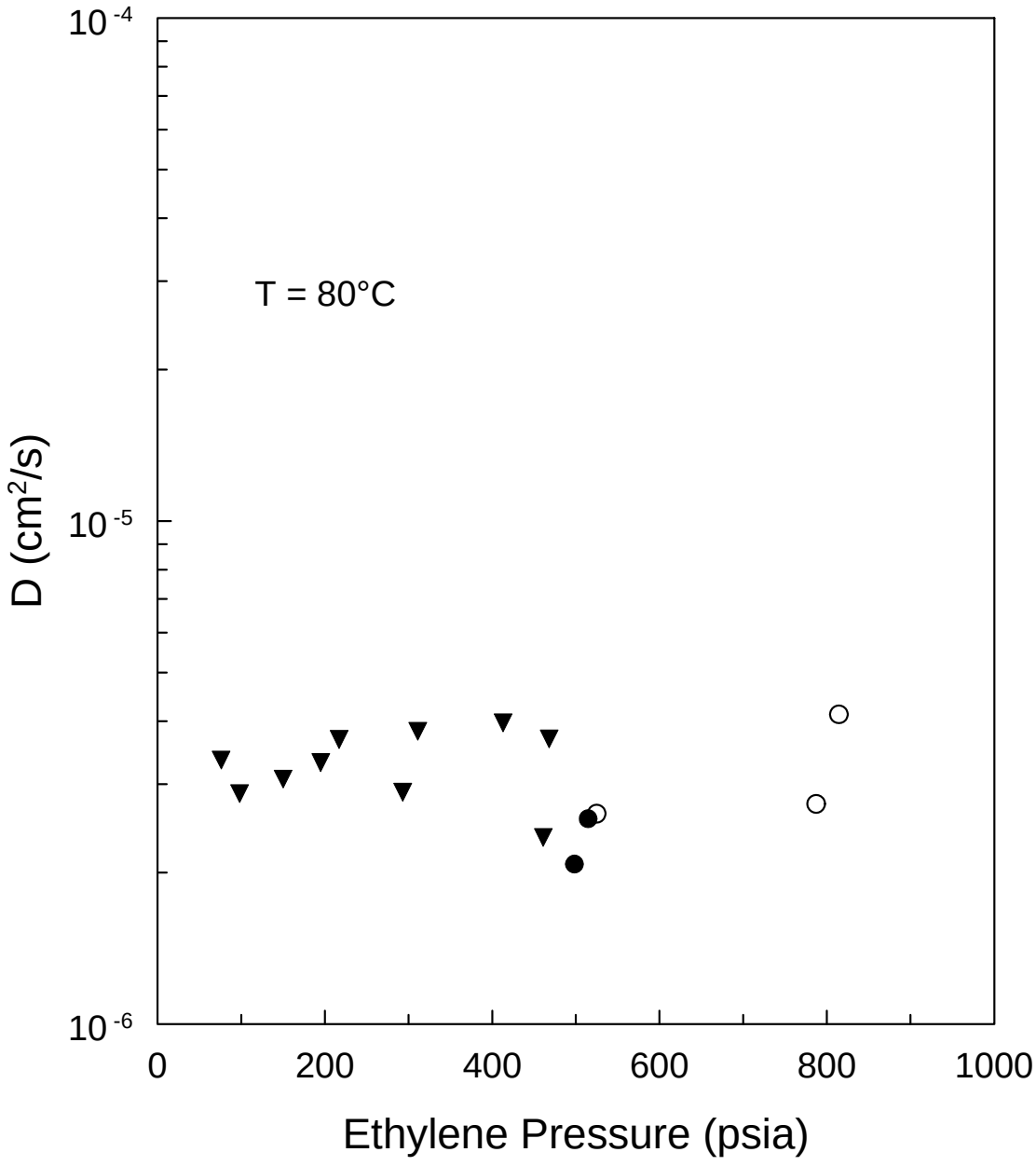

Figure 4-10: Diffusivity of ethylene in LDPE at 80°C. Dry data were taken with pressure decay (▼) and the capsule method (●). Data with water (○) were taken with the capsule method.

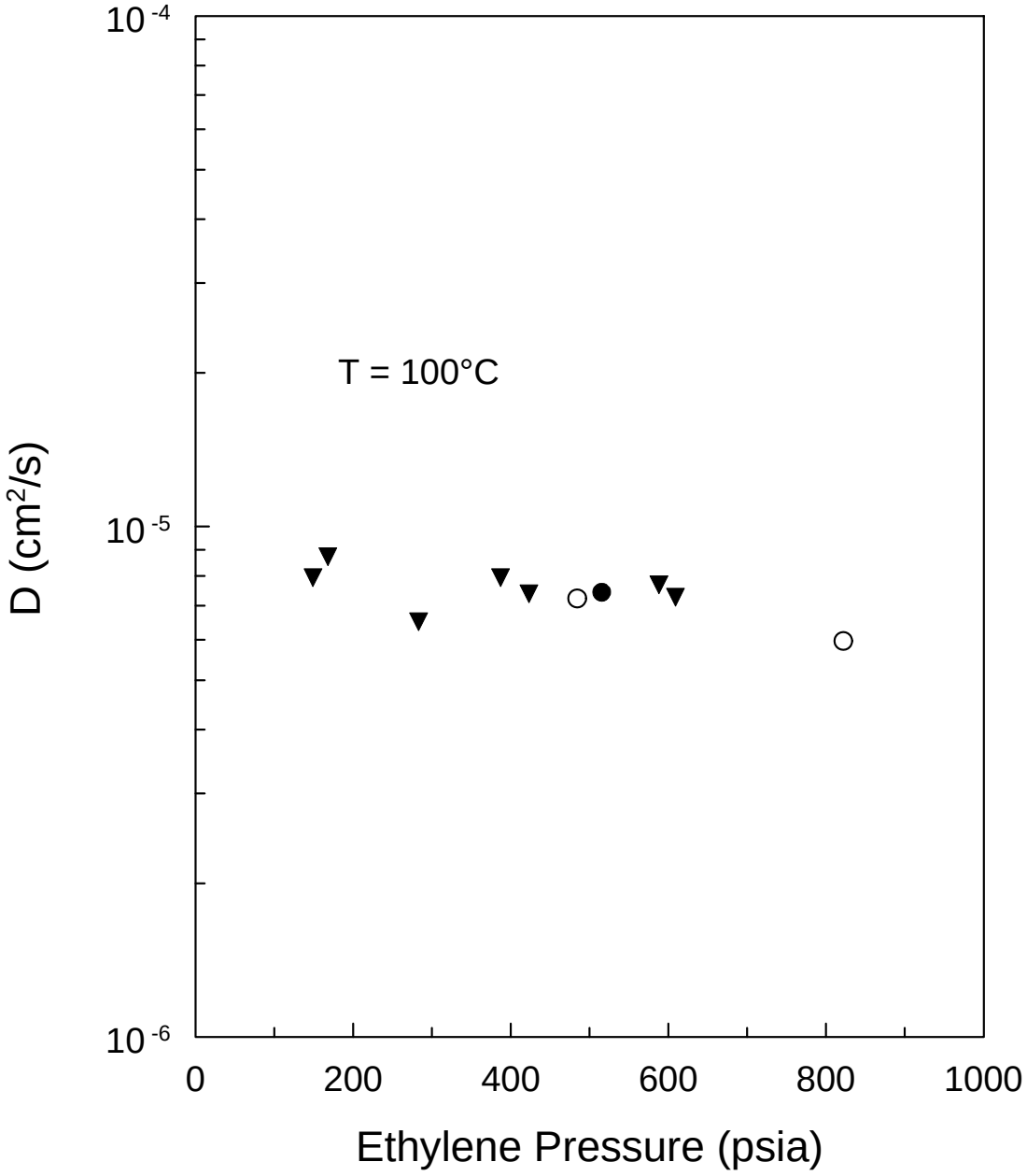

Figure 4-11: Diffusivity of ethylene in LDPE at 100°C. Dry data were taken with pressure decay (▼) and the capsule method (●). Data with water (○) were taken with the capsule method.

Table 4-4: Dry Data for LDPE-ethylene*

T(°C)	Ethylene Pressure (psia)	Solubility (weight fraction)	Diffusion Coefficient (cm^2/s)
80	76	0.004	3.4×10^{-6}
	98	0.005	2.9×10^{-6}
	150	0.008	3.1×10^{-6}
	195	0.011	3.3×10^{-6}
	215	**0.012**	**-**
	217	0.012	3.7×10^{-6}
	293	0.017	2.9×10^{-6}
	311	0.017	3.8×10^{-6}
	413	0.024	4.0×10^{-6}
	424	**0.025**	**-**
	461	0.026	2.4×10^{-6}
	468	0.027	3.7×10^{-6}
	498	**0.037**	**2.1×10^{-6}**
	515	**0.035**	**2.6×10^{-6}**
	614	**0.039**	**-**
100	149	0.008	7.9×10^{-6}
	168	0.011	8.7×10^{-6}
	209	**0.014**	**-**
	283	0.015	6.5×10^{-6}
	387	0.023	7.9×10^{-6}
	399	**0.026**	**-**
	423	0.023	7.4×10^{-6}
	517	**0.037**	**7.4×10^{-6}**
	588	0.031	7.7×10^{-6}
	604	**0.040**	**-**
	609	0.036	7.3×10^{-6}
120	**227**	**0.011**	**-**
	441	**0.022**	**-**
	617	**0.032**	**-**

* Values in bold were obtained using the capsule method

Table 4-5: Wet Data for LDPE-ethylene

T(°C)	Ethylene Pressure (psia)	Solubility (weight fraction)	Diffusion Coefficient (cm^2/s)
80	**525**	**0.038**	**2.6×10^{-6}**
	666	**0.048**	**-**
	787	**0.045**	**2.7×10^{-6}**
	814	**0.060**	**4.1×10^{-6}**
100	**484**	**0.008**	**7.2×10^{-6}**
	822	**0.011**	**6.0×10^{-6}**

4.4.3 Solubility Behavior Below T_m

As shown in Figure 4-6 unexpected solubility behavior at 80 and 100°C was observed in this work. Typically one would expect the solubility to be higher at 80°C. There are two possible explanations for the observed behavior. Each will be considered.

4.4.3.1 Elastic Effects

The DSC results indicate that the LDPE is semi-crystalline up to about 115°C and thus the amorphous phase at 80 and 100°C, should be approximately the same. The reason for the apparent identity in solubility could be elastic effects the crystalline region imposes on the amorphous region. Elastic effects are phenomena where crystalline regions of semi-crystalline polymers restrict the interactions of the amorphous region with solvent molecules. This can result in a lower observed solubility than expected for semi-crystalline polymers such as LDPE. Michaels and Hausslein [26] observed these effects in their study of the sorption of p-xylene in polyethylene. Doong and Ho [27]

proposed an elastic factor for use in activity coefficient models based on sorption data measured for aromatics in polyethylene. Castro et al. [28] carried out a similar study involving alkanes in polyethylene and polypropylene. In a publication by Lutzow et al. [29], the authors noted a difference in the amorphous polymer based solubility of toluene n-heptane in LDPE and HDPE. They concluded that the amorphous region was affected by the different crystallinities of the two samples, but did not go so far as to identify elastic effects as the reason for the behavior. Banaszak et al. [30] added an elastic contribution to the PC-SAFT equation of state in their study of ethylene and 1-hexene in linear low density polyethylene. Most recently, Serna et al. [31] incorporated an elastic term based on the work of Michaels and Hausslein into a version of the UNIFAC model and a predictive equation of state. Their work was based on IGC data on polyethylene and a wide range of solvents. The above authors all concluded that the crystalline regions impose restrictions on the amorphous regions in polyethylene. In addition, the constraint on the amorphous region decreases as T_m is approached. Therefore, the elastic effect is higher at 80°C and the true region available for sorption is lower, thus producing a lower solubility. The fitted binary interaction parameters from the GCLF-EoS illustrate the effect.

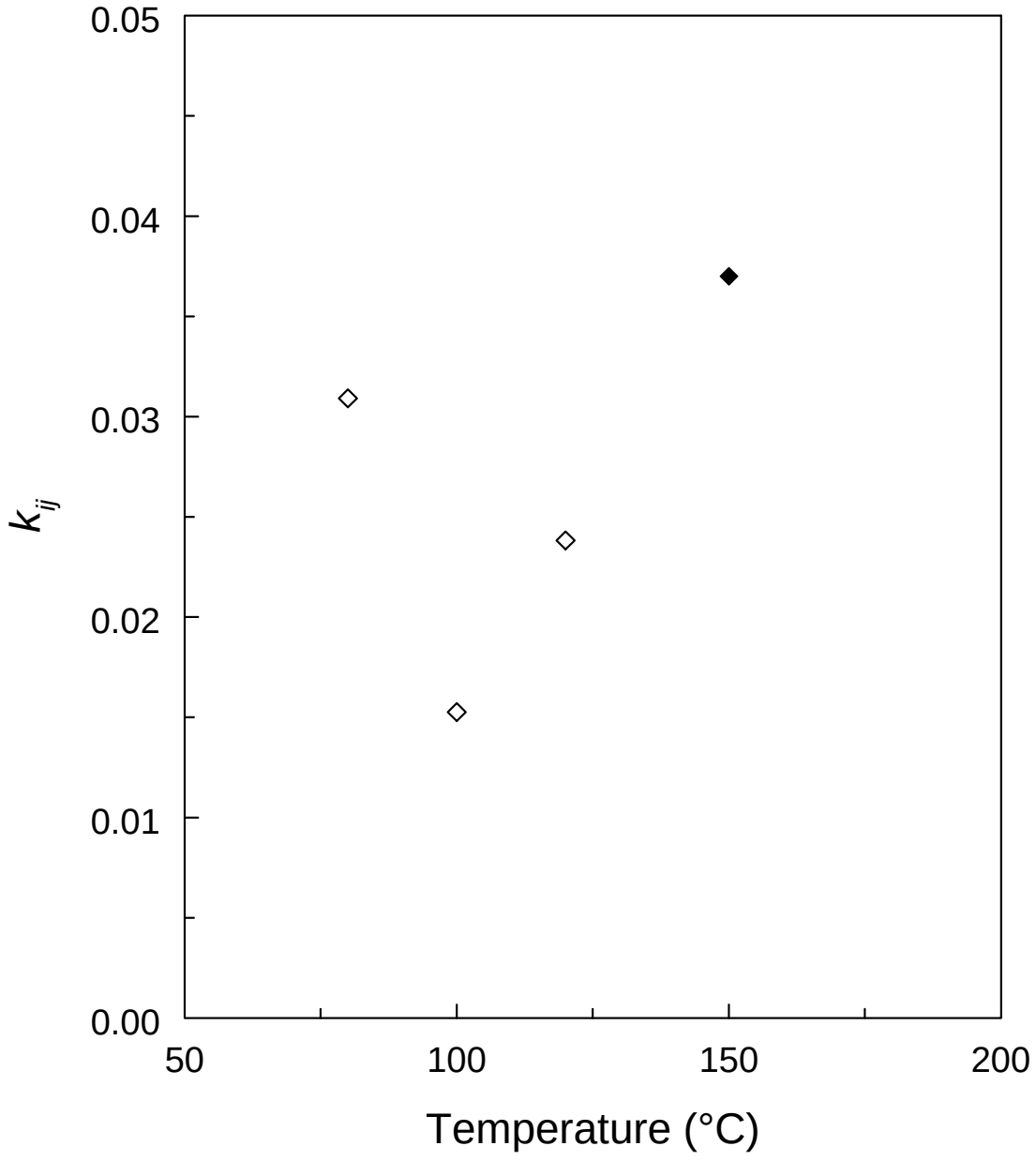

Figure 4-12: Plot of GCLF-EoS binary interaction parameters from fit of experimental data. Parameters fit to experimental data at 80, 100, and 120°C in this work (◇) are compared with a value obtained at 150°C by Davis et al. [12] (◆).

The data in Figure 4-12 show a clear trend with temperature that is not followed at 80°C. In physical terms the value of k_{ij} at that temperature is higher because the solubility is lower. Generally, a higher k_{ij} means the solvent is less soluble in the polymer at a given temperature. The reason for the apparent lower solubility may be the elastic effect imposed on the amorphous region by the crystalline region.

4.4.3.2 Partial Crystal Melting

An alternative explanation for the 80-100°C results observed in Figure 4-6 is partial melting of crystals below T_m. An increase in the amorphous region of polyethylene at 100°C would serve to counter the expected influence of temperature. This would result in a higher solubility than expected at 100°C compared to the data at 80°C. However, the data at 100°C generally follows the same trend with temperature as the data at 120 and 150°C as shown in Figure 4-6. Based on the results of the present study, the elastic effect seems more likely to be the real influence in the system. Future work could include measurement of accurate PVT data on the LDPE sample which would allow for calculation of the crystallinity as a function of temperature.

4.5 Conclusions

Data was collected on LDPE-ethylene and the influence of water on the system was investigated. The data showed good agreement among the two techniques employed in the study. The solubility at 80°C showed a possible increase due to the presence of water. However, the data at 100°C showed no influence. The diffusion coefficient measured under wet conditions did not show significant change compared to the dry values at either temperature. The solubility below T_m showed interesting behavior that may be due to elastic effects or partial melting of crystals. Although elastic effects seem more likely based on the binary interaction parameters regressed for the GCLF-EoS, data on the crystallinity as a function of temperature would be necessary to confirm this. The results of this study do not indicate that stripping rates should be significantly higher due to use of steam rather than gas as the stripping agent.

4.6 References

1. Albalak, R. J. *Polymer Devolatilization*; Marcel Dekker, Inc.: New York, **1996**.

2. Englund,S. M. Monomer Removal from Latex. *Chem. Eng. Prog.* **1981**, *77*, 55-59.

3. Araujo, P. H. H.; Sayer, C.; Poco, J. G. R.; Giudici, R. Techniques for Reducing Residual Monomer Content in Polymers: A Review. *Polym. Eng. Sci.* **2002**, *42*, 1442-1468.

4. Salazar, R.; Ilundain, P.; Alvarez, D.; Da Cunha, L.; Barandiaran, M. J.; Asua, J. M. Reduction of the Residual Monomer and Volatile Organic Compounds by Devolatilization. *Ind. Eng. Chem. Res.* **2005**, *44*, 4042-4050.

5. Mehos, G.; Quick, D. Removal of Residual Monomers from Polymer Emulsions by steam stripping. *Sep. Sci. Technol.* **1994**, *29*, 1841-1856.

6. Mantell, G. J.; Barr, J. T.; Chan, R. K. S. Stripping VCM from PVC resins. *Chem. Eng. Prog.* **1975**, *71*, 54-62.

7. Chan, R. K. S.; Patel, C. B.; Gupta, R.; Wornan, C. H.;Grandin, R. E. Batch Stripping of Vinyl Chloride. *J. Macromol. Sci., Chem.* **1982**, *A17*, 1045-1064.

8. Humkey, R. G.; Ryan, D. J. Apparatus for Stripping Residual Solvent from Polymer Pellets. U.S. Patent 3,958,585, **1976**.

9. Matthews, F. J.; Fair, J. R.; Barlow, J. W.; Paul, D. R. Solvent Removal from Ethylene-Propylene Elastomers. 1.Determination of Diffusion Mechanism. *Ind. Eng. Chem. Prod. Res. Dev.* **1986**, *25*, 58-64.

10. Palamara, J. E.; Davis, P. K.; Suriyapraphadilok, U.; Danner, R. P.; Duda, J. L.; Kitzhoffer, R. J.; Zielinski, J. M. A Static Sorption Technique for Vapor Solubility Measurements. *Ind. Eng. Chem. Res.* **2003**, *42*, 1557-1562.

11. Palamara, J. E.; Mulcahy, K. A.; Jones, A. T.; Danner, R. P.; Duda, J. L. Solubility and Diffusivity of Propylene and Ethylene in Atactic Polypropylene by the Static Sorption Technique. *Ind. Eng. Chem. Res.* **2005**, *44*, 9943-9950.

12. Davis, P. K.; Lundy, G. D.; Palamara, J. E.; Duda, J. L.; Danner, R. P. New Pressure-Decay Techniques to Study Gas Sorption and Diffusion in Polymers at Elevated Pressures. *Ind. Eng. Chem. Res*. **2004**, *43*, 1537-1542.

13. Palamara, J. E. Thermodynamics and Transport of Penetrants in Mesophase Pitch and High Polymers. Ph.D. Thesis, The Pennsylvania State University, University Park, PA, **2003**.

14. Crank, J. *Mathematics of Diffusion, 2nd ed.*; Clarendon Press: Oxford, UK, **1973**.

15. Data collected by J. E. Palamara, Center for the Study of Polymer-Solvent Systems, **2001**.

16. Data collected by P. K. Davis, Center for the Study of Polymer-Solvent Systems, **2001**.

17. Wunderlich, B.; Czornyj, G. Study of Equilibrium Melting of Polyethylene. *Macromolecules* **1977**, *10*, 906-913.

18. Thomas, W.; Zander, M. Pressure-Density-Temperature Measurements of Ethylene. *Int. J. Thermophys.* **1980**, *1*, 383-296.

19. Bevington, P. R.; Robinson, D. K. *Data Reduction and Error Analysis for the Physical Sciences, 2nd ed.*; McGraw-Hill: Boston, MA, **1992**.

20. Lee, B. -C. Prediction of Phase Equilibria in Polymer Solutions. Ph.D. Thesis, The Pennsylvania State University, University Park, PA, **1995**.

21. Danner, R. P.; Hamedi, M.; Lee, B. -C. Applications of the Group-Contribution, Lattice-Fluid Equation of State. *Fluid Phase Equilib.* **2002**, *619*, 194-197.

22. Liu, D. D.; Prausnitz, J. M. Solubilities of Gases and Volatile Liquids in Polyethylene and in Ethylene-Vinyl Acetate Copolymers in the Region 125-225°C. *Ind. Eng. Chem. Fundam.* **1976**, *15*, 330-335.

23. Cheng, Y. L.; Bonner, D. C. Solubility of Nitrogen and Ethylene in Molten, Low-Density Polyethylene to 69 Atmospheres. *J. Polym. Sci. B: Polym. Phys.* **1978**, *16*, 319-333.

24. Zielinski, J. M.; Duda, J. L. Predicting Polymer/Solvent Diffusion Coefficients Using Free Volume Theory. *AIChE J.* **1992**, *38*, 405-415.

25. Galdamez, J. R.; Jones, A. T.; Danner, R. P.; Duda, J. L. Effect of Water on Transport and Thermodynamic Behavior in Polyethylene Systems. Submitted to *Polymer* **2007**.

26. Michaels, A. S.; Hausslein, R. W. Elastic Factors Controlling Sorption and Transport Properties of Polyethylene. *J. Polym. Sci. Part C* **1965**, *10*, 61-86.

27. Doong, S. J.; Ho, W. S. W. Sorption of Organic Vapors in Polyethylene. *Ind. Eng. Chem. Res*. **1991**, *30*, 1351-1361.

28. Castro, E. F.; Gonzo, E. E.; Gottifredi, J. C. The Analysis of Sorption Data of Organic Vapors in Polymeric Membranes through Novel Theories. *J. Membr. Sci.* **1996**, *113*, 57-64.

29. Lutzow, N.; Tihminlioglua, A.; Danner, R. P.; Duda, J. L.; De Haan, A.; Warnier, G.; Zielinski, J. M. Diffusion of Toluene and n-Heptane in Polyethylenes of Different Crystallinity. *Polymer* **1999**, *40*, 2797–2803.

30. Banaszak, B. J.; Lo, D.; Widya, T.; W. H. Ray; de Pablo, J. J.; Novak, A.; Kosek, J. Ethylene and 1-Hexene Sorption in LLDPE under Typical Gas Phase Reactor Conditions: A Priori Simulation and Modeling for Prediction of Experimental Observations. *Macromolecules* **2004**, *37*, 9139-9150.

31. Serna, L.V.; Becker, J. L.; Galdamez, J. R.; Danner, R. P.; Duda, J. L. Elastic Effects on Solubility in Semicrystalline Polymers. Submitted to *J. Appl. Polym. Sci.* **2007**.

Chapter 5

Solubility Predictions for Copolymer Systems

5.1 Introduction

Copolymers are unique materials that have properties based on the constituent homopolymer segments that make up the molecule. The composition of the copolymer can be adjusted to tailor physical properties such as T_g, viscosity, and chemical resistance. Commercial interest in copolymers has increased dramatically in recent years. Compared to homopolymer-solvent systems, there is significantly less vapor-liquid equilibria (VLE) data for copolymer systems. This fact increases the need for accurate thermodynamic models capable of *a priori* predictions to assist the process engineer in design and operation tasks.

For copolymer-solvent systems there exist only a few models capable of making such predictions. In Chapter 2, two of the more popular models were described. In this chapter, they are applied to copolymer systems. In a sense, a copolymer system is similar to polymer-solvent-cosolvent systems. The additional homopolymer repeat unit can often have a marked influence on the system. As the composition of the copolymer changes so will its phase equilibrium with solvents.

Although others have studied the performance of predictive models with respect to copolymers [1-6], the author is unaware of anyone examining the predictive capabilities in terms of anomalous solubility behavior observed in certain systems. This particular capability would require significant sophistication in quantifying the intermolecular interactions that can exist in copolymer-solvent systems. In this chapter the following systems are examined with a focus on systems where the copolymer has either higher or lower solubility than either of the respective homopolymers: poly(vinyl acetate) (PVAc)-poly(ethylene) (PE) in toluene and *n*-heptane, poly(styrene) (PS)-poly(methyl methacrylate) (PMMA) in acetone and chloroform, and poly(acrylonitrile) (PAN)-poly(butadiene) (PB) in acetonitrile.

5.1.1 Predictive Thermodynamic Modeling of Copolymer Systems

5.1.1.1 UNIFAC Models

The UNIFAC models allow for calculation of the activity coefficient of a species *i* in solution with any number of other species. To implement a copolymer in these models, the copolymer is defined as a pseudo-component in a binary mixture with solvent. The groups are defined such that the weight fraction of each repeat unit gives the proper composition of the copolymer. Such a definition only permits calculation assuming the copolymer is random in nature. Affects due to blockiness cannot be characterized. Once the copolymer has been developed as a molecule with the appropriate groups, the activity

coefficient of solvents can be calculated. In this work the UNIFAC-FV [7] and UNIFAC-vdW-FV [8] models described in Chapter 2 were the ACMs tested.

5.1.1.2 GCLF-EoS

Lee and Danner treated the copolymer as a pseudo-component having a weight based distribution of repeat units which gave the appropriate proportion of species in the copolymer [4]. Table 5-1 shows an example of this approach for the 50% copolymer[1] of PE and PVAc studied in this work.

Table 5-1: 50% Copolymer of PVAc-PE (nominal M_n = 100000)

Repeat Unit	Number of Units	M_n in copolymer
PE	1782	49992
PVAc	581	50018

There is roughly a 3:1 ratio of PE to PVAc repeat units. Therefore, the repeat unit of the copolymer can be assumed to have the structure shown in Figure 5-1.

[1] The composition of copolymers described in this work is in weight percent.

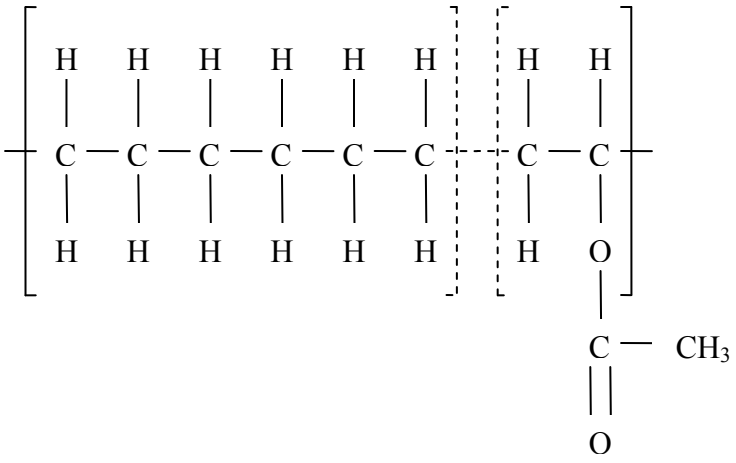

Figure 5-1: Structure of PVAc-PE copolymer. There are three PE repeat units for every PVAc repeat unit.

Palamara et al. [9] applied the Panayiotou-Vera EoS (PV-EoS) to VLE of poly(vinyl alcohol) PVOH-PVAc copolymers and homopolymers with methanol, water, and methyl acetate. In their work mixing rules for the copolymer based on the homopolymer parameters were introduced for parameterization of the equation of state.

The mixing rule introduced for v_C^* is given in Eq. 5.1:

$$v_C^* = \sum_i^n x_i \hat{v}_i^* \frac{M_C}{M_{[i]}} \tag{5.1}$$

where x_i is the mole fraction of repeat unit type *i* in the copolymer, $\hat{v}_i^*$ is the hard-core volume of repeat unit type *i*, M_C is the molecular weight of the copolymer, and $M_{[i]}$ is the molecular weight of a single repeat unit of type *i*.

The pure component interaction energy parameter for the copolymer is based on the surface area fraction weighted values for the respective homopolymers:

$$\varepsilon_C = \sum_i^n \sum_j^n Q_{C,i} Q_{C,j} \left(\varepsilon_{kk,i} \varepsilon_{kk,j}\right)^{1/2} \tag{5.2}$$

where $\varepsilon_{kk,i}$ and $\varepsilon_{kk,j}$ is the pure component interaction energy of the homopolymer of type *i* and *j*. $Q_{C,i}$ is the surface area fraction of repeat unit *i* based on the mole fraction in the copolymer:

$$Q_{C,i} = \frac{x_i \hat{q}_i}{\sum_i^n x_i \hat{q}_i} \tag{5.3}$$

The summation is carried out over all the repeat units in the copolymer.

The surface area parameter of the repeat unit, $\hat{q}_i$, is given by the following:

$$\hat{q}_i = \frac{q_i}{n_{C,i}} \tag{5.4}$$

where q_i is given by Eq. 2.34 and $n_{C,i}$ is the number of repeat units of type *i* in the copolymer.

The binary interaction parameter can be calculated using a surface area fraction weighted value of the two homopolymer-solvent values:

$$k_C = \sum_i^n Q_{C,i} k_{ij} \tag{5.5}$$

In the pure predictions made in this work the copolymer was treated as a pseudo-component following the suggestion of Lee and Danner [4]. For the case where the

binary interaction parameters were adjusted to give a better fit of the data, Eq. 5.5 was used to calculate k_C.

5.2 Results

The first examples are of systems where the solubility of the copolymer falls intermediate between the two homopolymer solubilities in the solvent. The results of the comparison for the two UNIFAC predictions for the PVAc-PE system with *n*-heptane at 70°C are shown in Figure 5-2. In all cases presented, solid lines represent homopolymer predictions while dashed lines represent copolymer predictions.

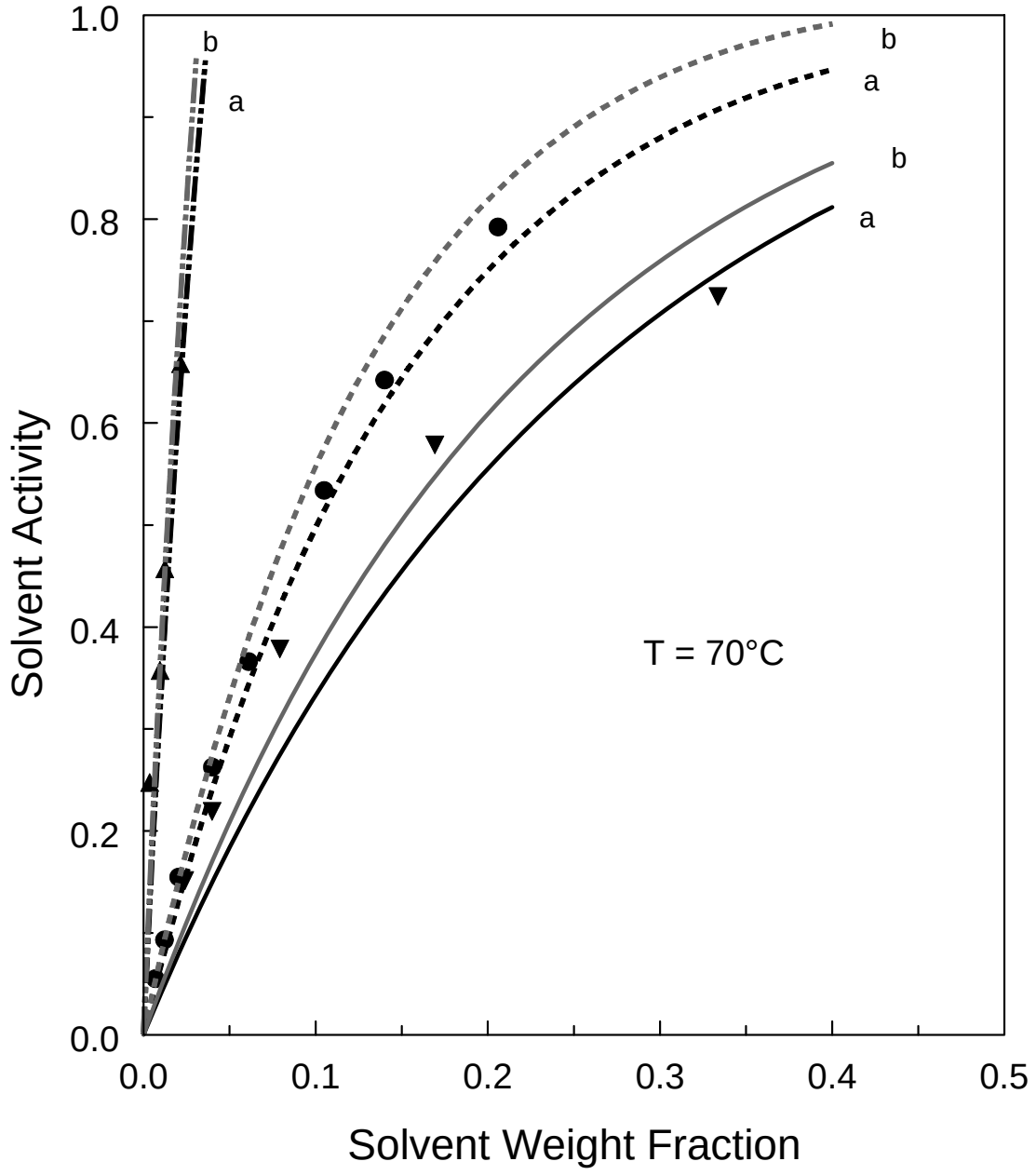

Figure 5-2: UNIFAC predictions of *n*-heptane in PVAc (— · ·), PE (———), and P(E-co 50% VAc) (– – –). *n*-Heptane experimental data for PVAc (▲) [13], PE (▼) [12], and P(E-co 50% VAc) (●) [13]. For clarity the black lines are labeled "a" (UNIFAC-FV) while the grey lines are labeled "b" (UNIFAC-vdW-FV).

Both versions of the model accurately predict the solubility of PVAc-*n*-heptane. Both versions of UNIFAC overpredict the solubility in PE slightly. Prediction of the solubility in the copolymer is equally good with respect to the experimental data.

Table 5-2 provides the pure component parameters used in the GCLF-EoS predictions for PE, PVAc, and P(E-co 50% PVAc) with *n*-heptane and toluene.

Table 5-2: GCLF-EoS pure component parameters used in the predictions for PE, PVAc, and P(E-co 50% PVAc) with *n*-heptane and toluene.

	v_i^* (cm^3/g)	ε_{ii} (J/mol)
P(E-co 50% VAc)	0.924	1032.5
PE	1.079	958.0
PVAc	0.769	1133.4
n-heptane	1.289	830.9
toluene	1.063	994.2

Table 5-3 lists values of k_{ij} used in those predictions. The values in parentheses were obtained by adjusting k_{ij} to properly fit the experimental data. In the case of the copolymer the adjusted value was calculated using Eq. 5.5.

Table 5-3: Binary interaction parameters for PE-PVAc system.

Polymer	Solvent			
	n-heptane		toluene	
PE	0	(0.0019)	0	(0.0273)
PVAc	0.0096	(0.0424)	0.0096	(0.0256)
P(E-co 50% VAc)	0.0055	(0.0187)	0.0055	(0.0266)

Figure 5-3 shows the GCLF-EoS prediction for the PVAc-PE system with *n*-heptane. The model does a good job predicting the solubility of *n*-heptane in PE. In all the results presented, the weight fractions are on an amorphous polymer basis, i.e., the PE and copolymer experimental data were corrected for crystallinity. The GCLF-EoS overpredicts the solubility of PVAc in *n*-heptane. Improved prediction of the system was attained by adjusting the binary interaction parameter. Using a value of 0.0256 gave good agreement with the experimental data. Adjusting the binary interaction parameter gave only slight improvement over the pure prediction of the solubility of *n*-heptane in PE. The pure prediction for the 50% copolymer solubility is quite good in this case. The prediction of the solubility in the copolymer is worse when using the calculated value of k_{ij} from the two fitted k_{ij} values. Although the UNIFAC models give better prediction for the homopolymers, GCLF-EoS more accurately predicts the solubility of *n*-heptane in the copolymer.

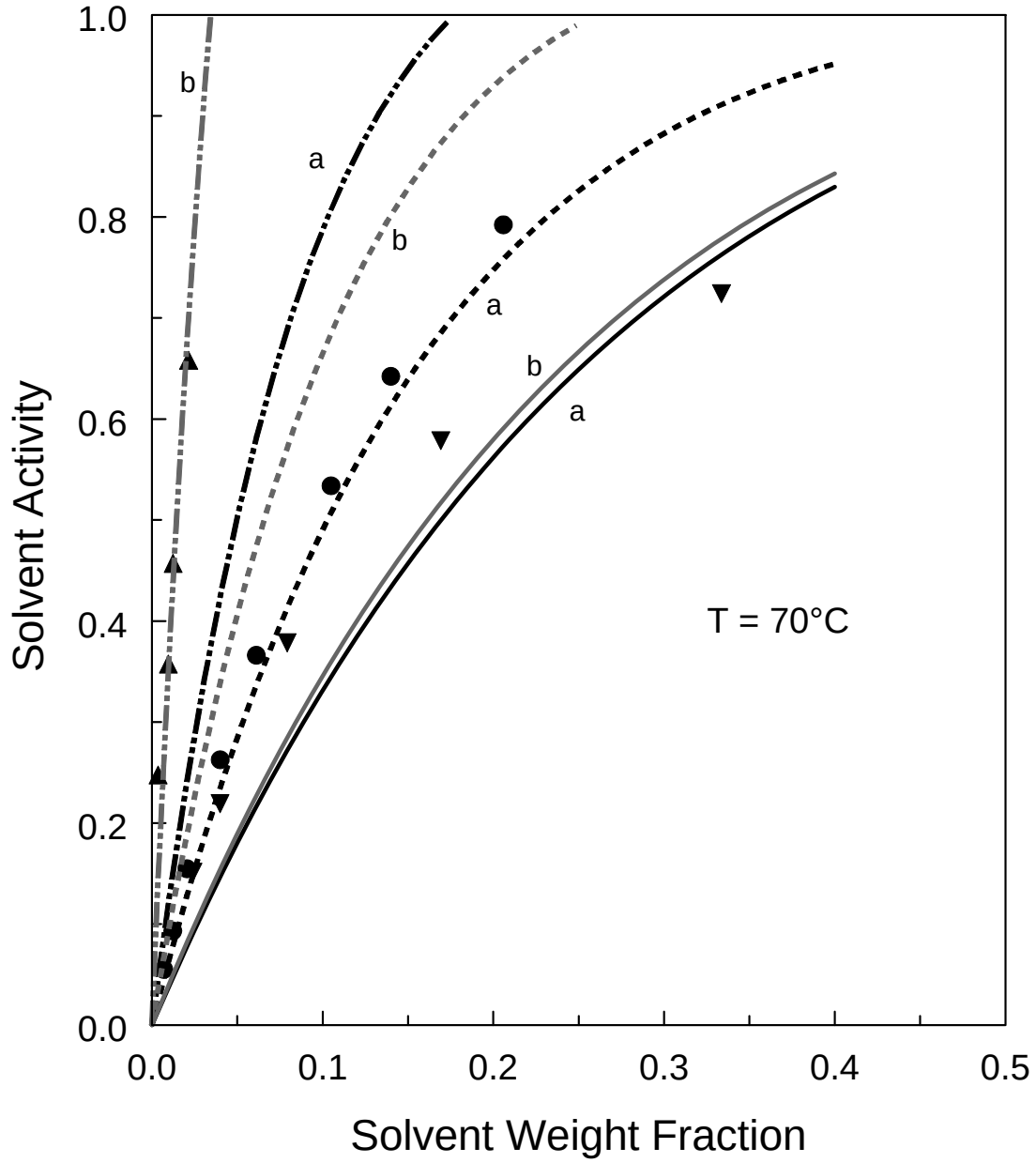

Figure 5-3: GCLF-EoS predictions of *n*-heptane in PVAc (— · ·), PE (———), and P(E-co 50% VAc) (– – –). *n*-Heptane experimental data for PVAc (▲) [13], PE (▼) [12], and P(E-co 50% VAc) (●) [13]. For clarity the black lines are labeled "a" (pure prediction) while the grey lines are labeled "b" (adjusted k_{ij} values). In the case of the copolymer the k_{ij} using the adjusted values was calculated from Eq. 5.5.

The second system examined was PS, PMMA, and a 50% copolymer in chloroform at 50°C. The results of the comparison with the UNIFAC models are shown Figure 5-4. In this case, chloroform is most soluble in PMMA and least soluble in PS. Its solubility in P(S-co-50% MMA) lies between the two homopolymers. UNIFAC-vdW-FV does quite well for the system PS-chloroform while UNIFAC-FV overpredicts the solubility. The UNIFAC models give almost identical predictions for chloroform in PMMA. The prediction is good up to moderate concentrations but overpredicts the solubility in the region of high solvent concentration. Similar results are observed for the copolymer. At low to moderate concentrations UNIFAC-vdW-FV shows quantitative accuracy in predicting the copolymer data.

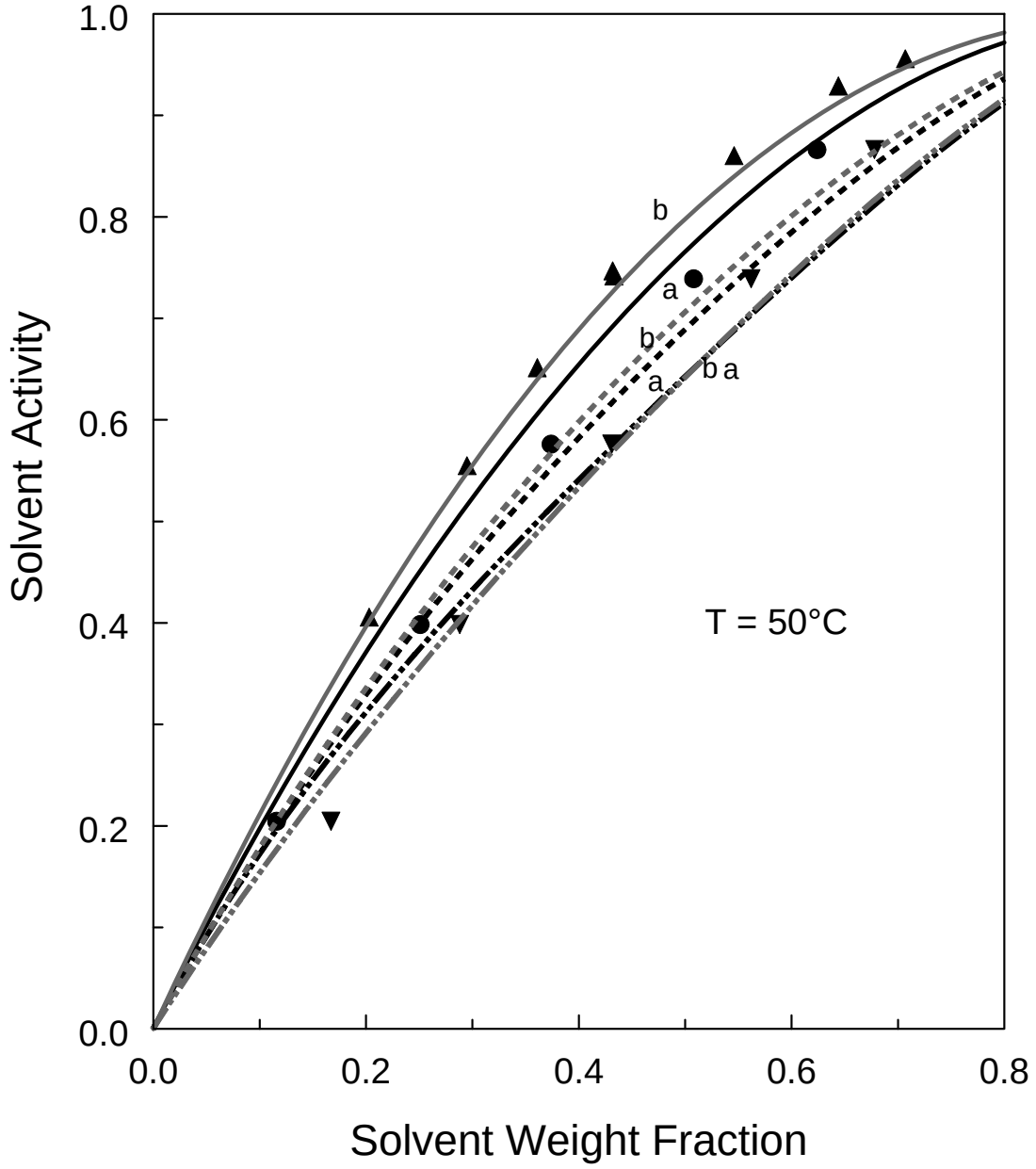

Figure 5-4: UNIFAC predictions of chloroform in PS (——), PMMA (— · ·), and P(S-co 50% MMA) (– – –). Experimental data of chloroform in PS (▲) [10], PMMA (▼) [11], and P(S-co 50% MMA) (●) [11] at 50°C. The black lines are UNIFAC-FV ("a") while the grey lines are UNIFAC-vdW-FV ("b").

The prediction results of GCLF-EoS for the PS-PMMA system in chloroform are shown in Figure 5-5. The pure component parameters and binary interaction parameters used for the predictions are listed in Tables 5-4 and 5-5 , respectively.

Table 5-4: GCLF-EoS pure component parameters used in the predictions for PS, PMMA, and P(S-co 50% PMMA) with chloroform and acetone.

	v_i^* (cm^3/g)	ε_{ii} (J/mol)
P(S-co-50% PMMA)	0.832	1093.1
PS	0.866	1141.4
PMMA	0.796	1051.1
chloroform	0.625	994.8
acetone	1.194	974.5

Table 5-5: Binary interaction parameters for PS-PMMA system.

	Solvent			
Polymer	chloroform		acetone	
PS	0.0110	(0.0101)	0.0047	(-0.0006)
PMMA	0.0204	(0.0230)	0.0109	(0.0089)
P(S-co 50% MMA)	0.0046	(0.0163)	0.0205	(-.0109)

For this system, GCLF-EoS does poorly in predicting the solubility of chloroform in the homopolymers. In Figure 5-5, the upper curve is the solubility curve for PMMA-chloroform. GCLF-EoS predicts that chloroform is least soluble in PMMA, although the data indicate that chloroform is most soluble in that homopolymer compared to PS and P(S-co 50% MMA). GCLF-EoS does a good job predicting the solubility of PS-chloroform with little improvement resulting from adjustment of the binary interaction parameter to fit the experimental data. Interestingly, the model predicts that chloroform should show higher solubility in the copolymer compared to the two homopolymers. In this case, use of the calculated k_{ij} for the copolymer gave significant improvement and properly represented the behavior observed experimentally.

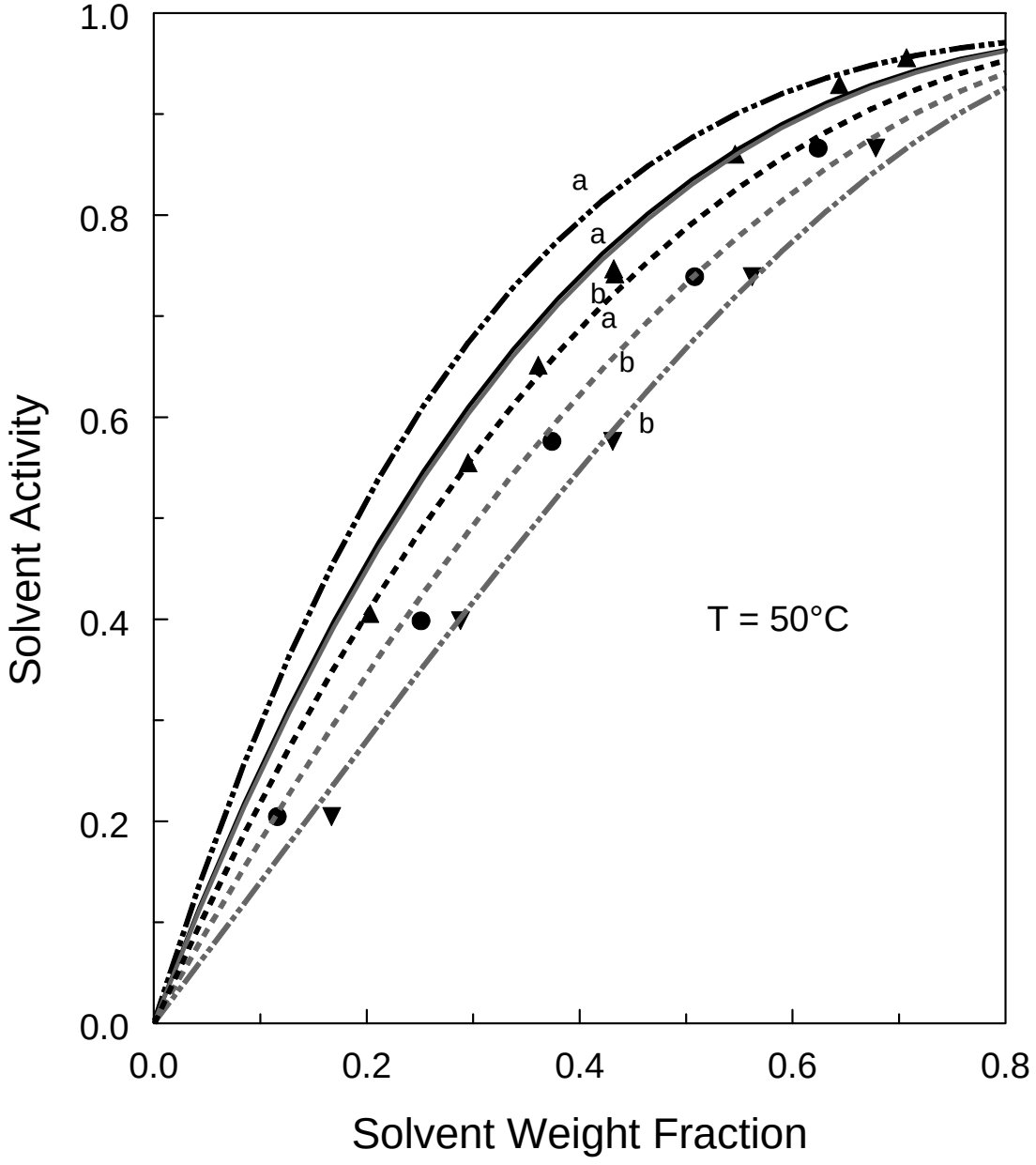

Figure 5-5: GCLF-EoS predictions of chloroform in PS (——), PMMA (— · ·), and P(S-co 50% MMA) (– – –). Experimental of chloroform in PS (▲) [10], PMMA (▼) [11], and P(S-co 50% MMA) (●) [11] at 50°C. The black lines are pure prediction ("a") while the grey lines were obtained by using adjusted k_{ij} values ("b").

In certain systems, unique solubility has been observed in copolymers compared to the solubility in the respective homopolymers. This can occur when the intermolecular forces in the copolymer are significantly affected by the presence of solvent. This type of behavior was recently observed by Zielinski [13] for toluene in a copolymer of PVAc and PE. The results are shown in Figure 5-6.

UNIFAC-FV and UNIFAC-vdW-FV give overpredictions of the solubility of toluene in the homopolymers as well as the copolymer. The predictions of PVAc-toluene show the largest deviation from the experimental results. UNIFAC-FV gives nearly equal overprediction for PE-toluene while UNIFAC-vdW-FV shows the same trend to a lesser degree. The most interesting result is that both models predict that toluene has higher solubility in the copolymer compared to either PVAc or PE. This trend was observed experimentally. The physical reason may be due to steric effects. In the case of PVAc-toluene, the interactions between the acetate group and toluene are suppressed due to steric hindrance of the neighboring repeat units. In the PVAc-PE copolymer, the distance between acetate groups is larger and this exclusion is lessened. The result is a higher solubility in the copolymer. In the case of *n*-heptane, as shown in Figures 5-2 and 5-3 the chain structure prevents the solvent from taking advantage of the reduced steric hindrance in the copolymer and the result is an average solubility in the copolymer.

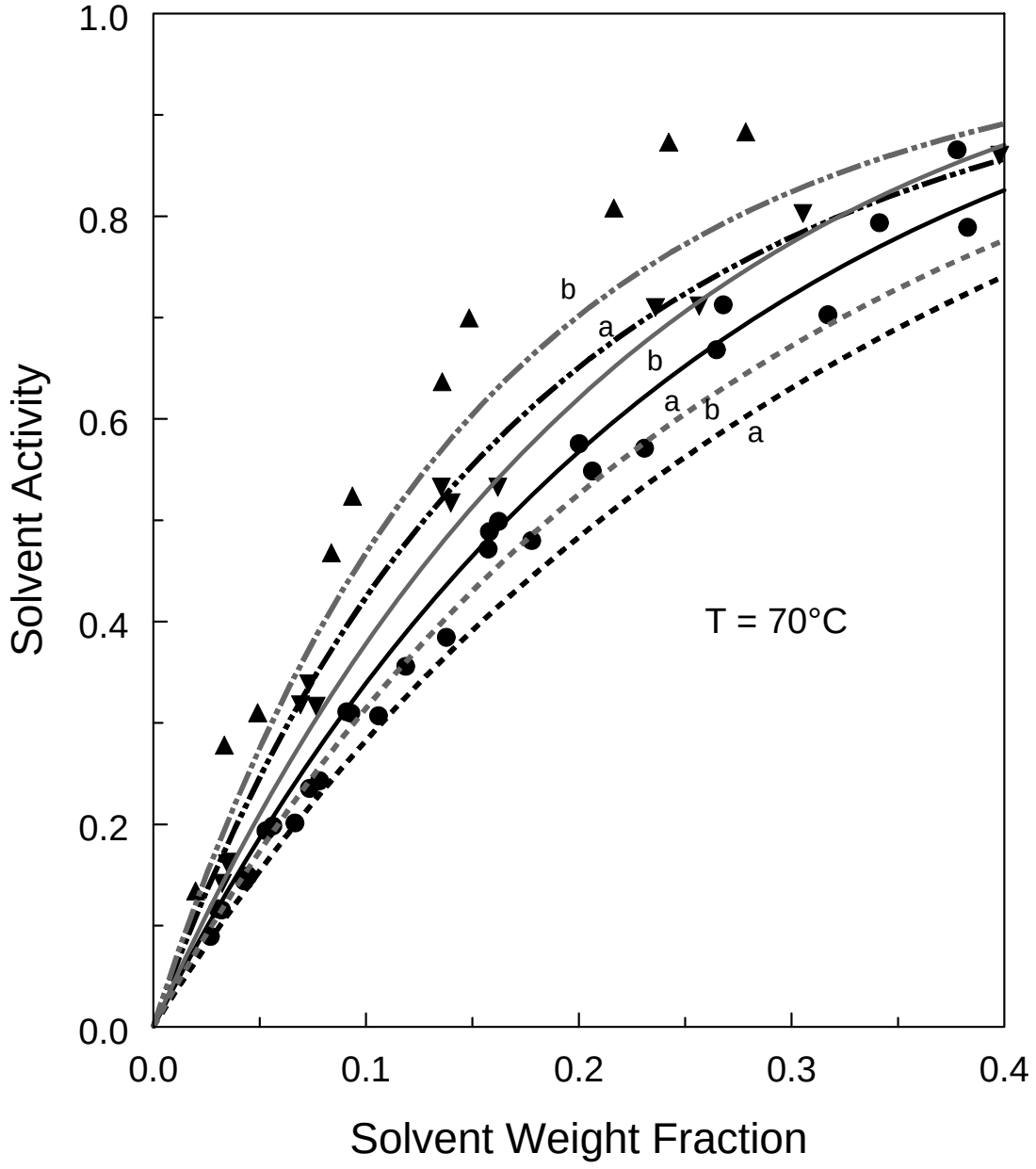

Figure 5-6: UNIFAC predictions of toluene in PVAc (— · ·), PE (———), and P(E-co 50% VAc) (– – –) at 70°C. Toluene experimental data for PVAc (▲) [13], PE (▼) [12], and P(E-co 50% VAc) (●) [13]. The black lines are UNIFAC-FV ("a") while the grey lines are UNIFAC-vdW-FV ("b").

UNIFAC-vdW-FV does quite well predicting the solubility of toluene in the P(E-co 50% VAc) copolymer giving quantitative agreement with the data within experimental error up to about 10 wt% of solvent. UNIFAC-FV overpredicts the solubility in the copolymer but still captures the higher solubility behavior of the copolymer-toluene system.

The results of the GCLF-EoS prediction for this system are shown in Figure 5-7. The pure component parameters and binary interaction parameters used for the predictions are listed in Table 5-2 and 5-3, respectively. The pure prediction of the copolymer-toluene solubility is nearly the same as that of the UNIFAC models. However, in this case the GCLF-EoS predicts that the solubility of the copolymer is an average of the two homopolymers, contrary to the experimental data. The apparent result shows agreement between GCLF-EoS and the copolymer-toluene experimental data. However, this is more a cancellation of errors effect than a true prediction of the trend. Upon adjusting the k_{ij}, good agreement was found for the homopolymer-toluene systems. When a k_{ij} for P(E-co 50% VAc) was calculated based on the two homopolymer adjusted values, the model predicted the solubility fell between the two homopolymers. Consequently, the prediction for the copolymer was worse using the weighted average of the adjusted values. To get an improved result the k_{ij} was fit to the experimental data for toluene with the copolymer. The resulting k_{ij} was found to be 0.0095.

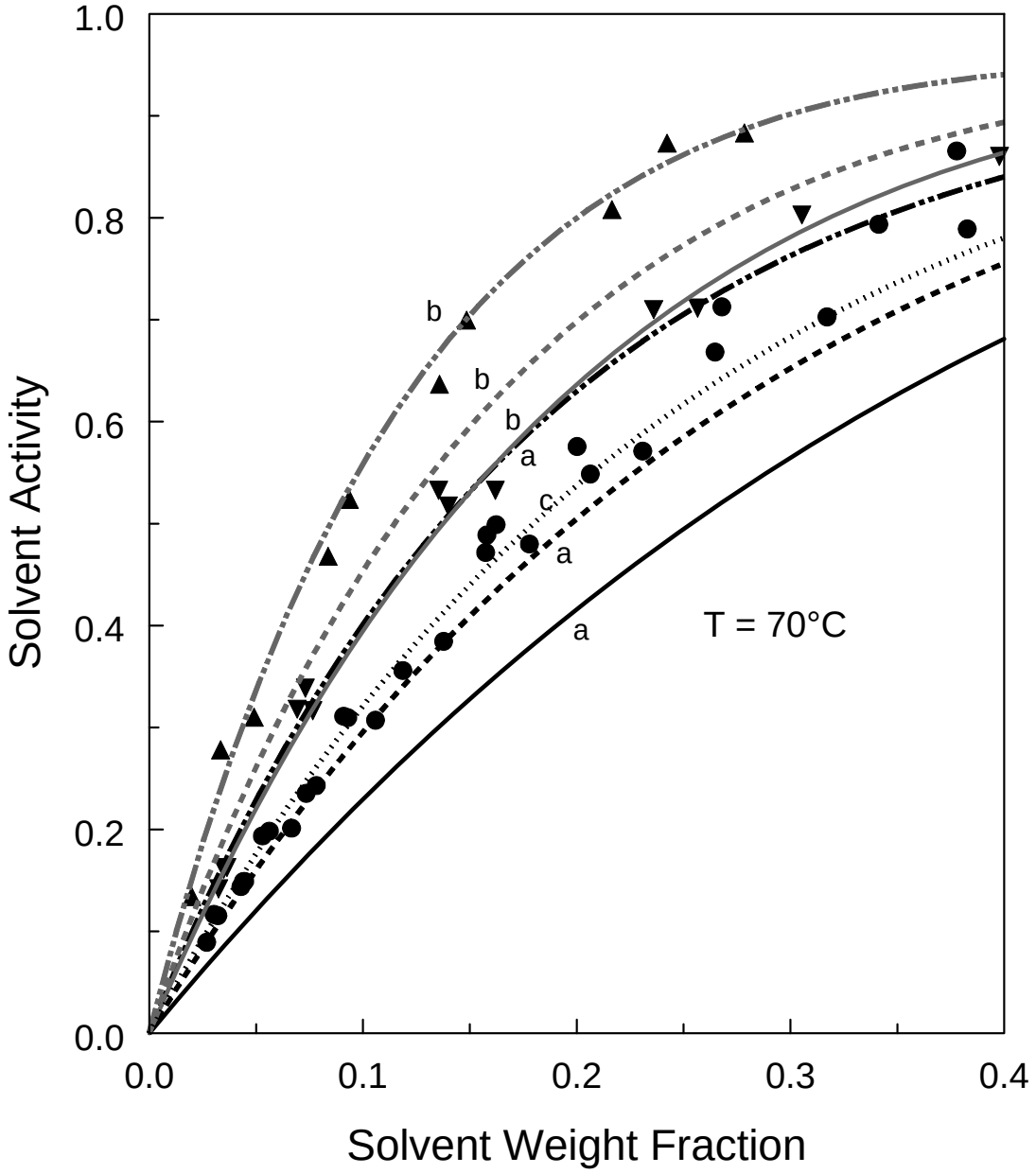

Figure 5-7: GCLF-EoS predictions of toluene in PVAc (— · ·), PE (———), and P(E-co 50% VAc) (– – –) at 70°C. Toluene experimental data for PVAc (▲) [13], PE (▼) [12], and P(E-co 50% VAc) (●) [13]. The black lines are pure prediction ("a") while the grey lines were obtained by using adjusted k_{ij} values ("b"). The dashed black line (▪▪▪▪▪▪▪▪▪) was obtained by fitting k_{ij} to a value of 0.0095 using the copolymer data ("c").

Figure 5-8 shows the results for acetone in PS, PMMA, and P(S-co 50% MMA) at 50°C. Both UNIFAC models capture the distinct trend with concentration at high activities of acetone. UNIFAC-FV does quite well predicting the solubility of PS-acetone up to moderate concentrations of solvent. In addition, both models predict the copolymer solubility to be slightly higher than both homopolymers up to about 20 wt% of acetone. The experimental data indicate that acetone is less soluble in the copolymer compared to the homopolymers. Neither model captures this trend.

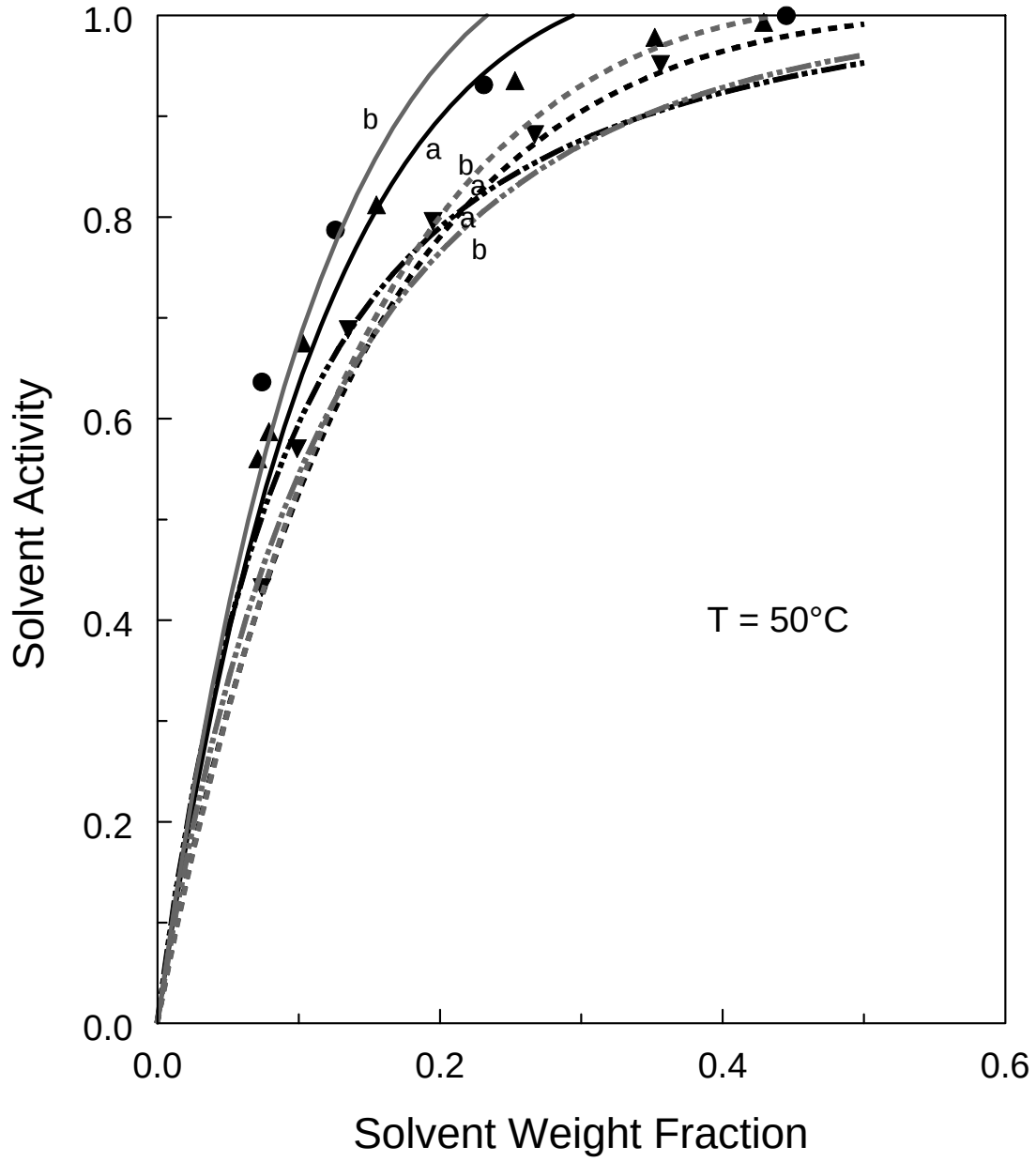

Figure 5-8: UNIFAC predictions of acetone in PS (———), PMMA (— · ·), and P(S-co 50% MMA) (– – –) at 50°C. Experimental data for PS (▲) [10] , PMMA (▼) [11], and P(S-co 50% MMA) (●) [11] with acetone. The black lines are UNIFAC-FV ("a") while the grey lines are UNIFAC-vdW-FV ("b").

The GCLF-EoS predictions for this system are shown in Figure 5-9. The pure component parameters and binary interaction parameters used for the predictions are listed in Tables 5-4 and 5-5, respectively. There is slight underprediction for acetone in PS and PMMA. It is unclear why the PS-acetone pure prediction is the only case that exhibits significant curvature. As Table 5-5 indicates a rather large k_{ij} adjustment was required to fit the experimental data for that system. Yet little improvement is actually observed. The curvature in the data as the solvent activity approaches unity may be due to association which the GCLF-EoS does not account for.

The GCLF-EoS predicts that acetone is slightly more soluble in P(S-co 50% MMA) compared to PS and PMMA up to about 15 wt% of the solvent. Using an adjusted k_{ij} for the homopolymers gave slight improvement although the trend of the data is not really captured. The calculated k_{ij} based on the adjusted k_{ij} values did not improve the prediction. Only after adjusting the k_{ij} using the experimental data for the copolymer was good representation of the data obtained. A value of 0.0114 for the binary interaction parameter was required.

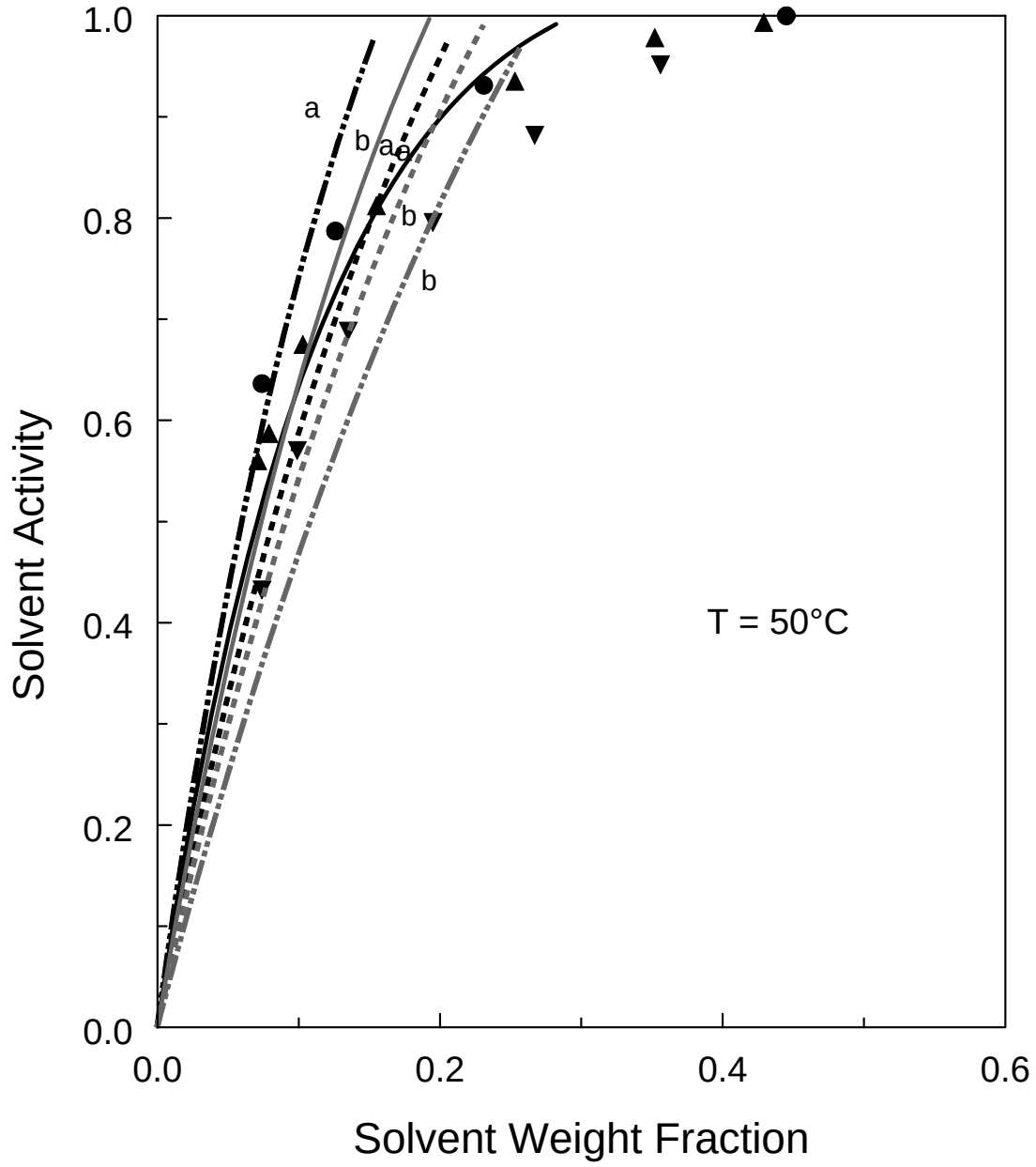

Figure 5-9: GCLF-EoS predictions of acetone in PS (———), PMMA (— · ·), and P(S-co 50% MMA) (– – –) at 50°C. Experimental data for PS (▲) [10], PMMA (▼) [11], and P(S-co 50% MMA) (●) [11] with acetone. The black lines are pure predictions ("a") while the grey lines were obtained by adjusting k_{ij} ("b").

Gupta and Prausnitz observed [14] and commented [15] on the increased affinity of acetonitrile for P(B-co 51% AN) compared to PB and PAN. The GCLF-EoS lacks the appropriate nitrile groups to develop the parameters used for prediction of this system. However, the UNIFAC models contain the groups and the comparison of those models to the experimental data is presented in Figure 5-10. UNIFAC-FV predicts both solubilities in the homopolymers quite well. UNIFAC-vdW-FV does well for PB-acetonitrile but there is significant overprediction for PAN-acetonitrile. Both models predict about the same solubility of acetonitrile in the copolymer. The proper trend of the copolymer having higher solubility than the respective homopolymers is accurately predicted.

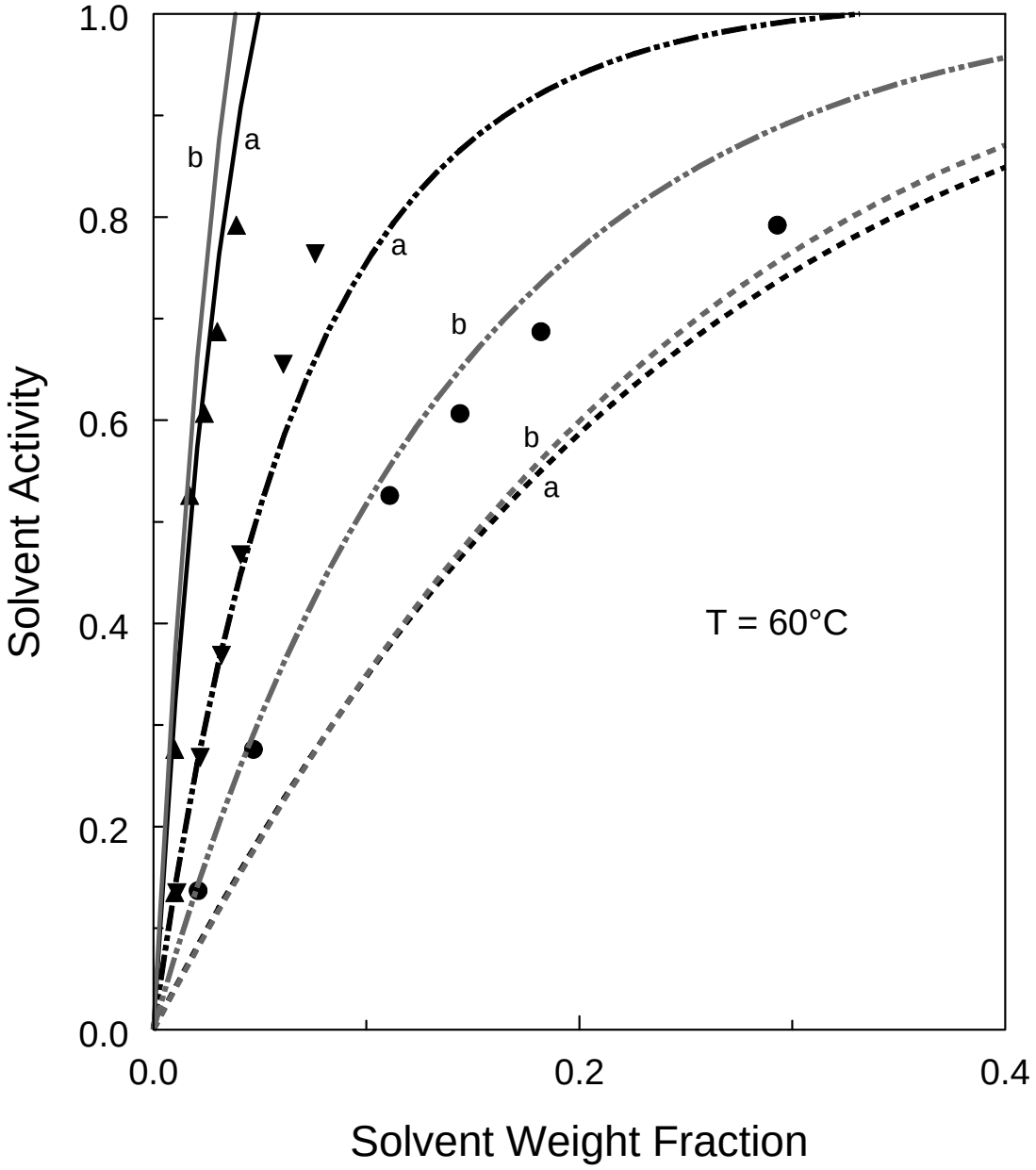

Figure 5-10: UNIFAC predictions of acetonitrile in PB (———), PAN(— - -), and P(B-co 51% AN) (– – –) at 60°C. Experimental data for PB (▲), PAN (▼), and P(B-co 51% AN) (●) taken from Gupta and Prausnitz [14]. The black lines are UNIFAC-FV ("a") while the grey lines are UNIFAC-vdW-FV ("b").

During the course of this work it was suspected that the free volume term (which depends on knowledge of the copolymer density) in the UNIFAC-FV and UNIFAC-vdW-FV predictions might be solely responsible for capturing the unique behavior observed in two of the cases where the copolymer-solvent solubility was not a weighted average of the homopolymer-solvent solubilities. In order to test the theory predictions were made with the original UNIFAC model without a free volume term. The results are shown in Figure 5-11. In both cases where UNIFAC-FV and UNIFAC-vdW-FV accurately predicted the trend of higher solvent solubility in the copolymer, the original UNIFAC also predicted such behavior. This indicates that the UNIFAC combinatorial and residual terms alone are sufficient for predicting the solubility of solvents in copolymers when it does not simply fall intermediate between the two homopolymers.

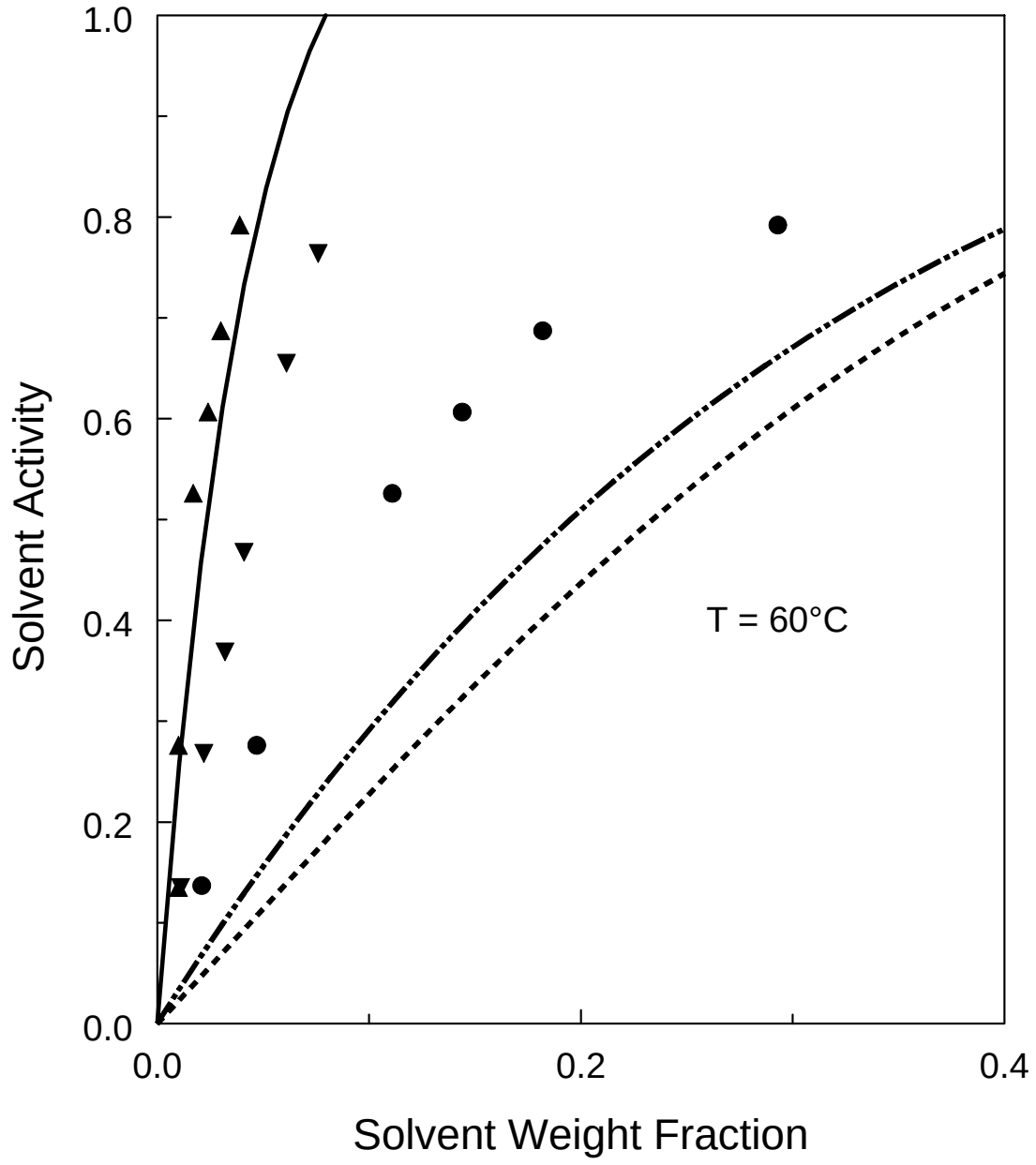

Figure 5-11: Predictions made with UNIFAC (no free volume term) of acetonitrile in PB (———), PAN(— · ·), and P(B-co 51% AN) (– – –) at 60°C. Experimental data for PB (▲), PAN (▼), and P(B-co 51% AN) (●) taken from Gupta and Prausnitz [14].

5.3 Conclusions

The UNIFAC-FV and UNIFAC-vdW-FV models show a better capability than GCLF-EoS for predicting anomalous behavior in copolymer systems. This is likely due to differences in the calculation methods of the energetic parameters in UNIFAC models compared with the equation of state. The GCLF-EoS did predict higher solubility in the case of chloroform with a PS-PMMA copolymer although such a trend was not observed experimentally. This indicates that the mixing rules do not dictate that the solubility always be predicted to fall between the two homopolymers when treating the copolymer as a pseudo-component. However, it seems that using the mixing rule of Palamara et al. [9] combined with the adjusted binary interaction parameters does guarantee that the solubility in the copolymer will be a weighted average of the two homopolymer solubilities.

5.4 Future Work

There is an obvious need for more sophisticated methods for characterizing the unique interactions which can be present in copolymer systems. The most direct approach would be to develop parameters for common copolymer repeat units. However, this tends toward a further empirical nature and less general group contribution scheme. Overall, more VLE data is needed for copolymer systems so that further comparisons like that of this chapter can be carried out and the specific intermolecular interactions can be better understood.

5.5 References

1. Iwai, Y.; Ishidao, T.; Miyamoto, S.; Ikeda, H.; Arai, Y. Solubilities of Nonane Vapor in Styrene-Butadiene Copolymers at 100 and 130°C. *Fluid Phase Equilib.* **1991**, *68*, 197-205.

2. Bogdanic, G.; Fredenslund, A. Prediction of Vapor-Liquid Equilibria for Mixtures with Copolymers. *Ind. Eng. Chem. Res.* **1995**, *34*, 324-331.

3. Pappa, G. D.; Voutsas, E. C.; Tassios, D. P. Prediction of Activity Coefficients in Polymer and Copolymer Solutions Using Simple Activity Coefficient Models. *Ind. Eng. Chem. Res.* **1999**, *38*, 4975-4984.

4. Lee, B. -C.; Danner, R. P. Application of the Group-Contribution Lattice-Fluid Equation of State to Random Copolymer-Solvent Systems. *Fluid Phase Equilib.* **1996**, *117*, 33-39.

5. Hamedi, M.; Lutzow, N.; Betz, H. S.; Duda, J. L.; Danner, R. P. Thermodynamic Behavior of Ethylene-Styrene Interpolymers. *Ind. Eng. Chem. Res.* **2001**, *40*, 3002-3008.

6. Danner, R. P.; Hamedi, M.; Lee, B. -C. Applications of the Group-Contribution Lattice-Fluid Equation of State. *Fluid Phase Equilib.*, **2002**, *194-197*, 619-639.

7. Oishi, T.; Prausnitz, J. M. Estimation of Solvent Activities in Polymer Solutions Using a Group-Contribution Method. *Ind. Eng. Chem. Process Des. Dev.*, **1978**, *17*, 333-339.

8. Kannan, D. C.; Duda, J. L.; Danner, R. P. A Free-Volume Term Based on the van der Waals Partition Function for the UNIFAC Model. *Fluid Phase Equilib.*, **2205**, *228-229*, 321-328.

9. Palamara, J. E.; Zielinski, J. M.; Hamedi, M.; Duda, J. L.; Danner, R. P. Vapor-Liquid Equilibria of Water, Methanol, and Methyl Acetate in Poly(vinyl acetate) and Partially and Fully Hydrolyzed Poly(vinyl alcohol). *Macromolecules* **2004**, *37*, 6189-6196.

10. Bawn, C. E.; Wajid, M. A. High Polymer Solutions Part 7 - Vapour Pressure of Polystyrene Solutions in Acetone, Chloroform, and Propyl Acetate. *Trans. Faraday Soc.*, **1956**, *52*, 1658-1664.

11. Tanbonliong, J. O.; Prausnitz, J. M. Vapor-Liquid Equilibria for Some Binary and Ternary Polymer Solutions. *Polymer*, **1997**, *38*, 5775-5783.

12. Lutzow, N.; Tihminlioglua, A.; Danner, R. P.; Duda, J. L.; De Haan, A.; Warnier, G.; Zielinski, J. M. Diffusion of Toluene and *n*-Heptane in Polyethylenes of Different Crystallinity. *Polymer* **1999**, *40*, 2797–2803

13. Zielinski, J. M. Air Products and Chemicals. Private Communication **2007**.

14. Gupta, R. B.; Prausnitz, J. M. Vapor-Liquid Equilibria of Copolymer + Solvent and Homopolymer + Solvent Binaries: New Experimental Data and Their Correlation. *J. Chem. Eng. Data* **1995**,*40*, 784-791.

15. Gupta, R. B.; Prausnitz, J. M. Vapor-Liquid Equilibria for Copolymer/Solvent Systems: Effect of "Intramolecular Repulsion" *Fluid Phase Equilib.* **1996**, *117*, 77-83.

Appendix A

Development of Multicomponent UNIFAC-vdW-FV Program

A.1 Introduction

Fast, simple calculations of polymer-solvent phase equilibria are important to process engineers. They can be useful in drying processes, reactions, and engineering of foams and films. Many times the engineer only needs a qualitative understanding of the system. This is where group contribution predictions can fill an important need.

In this work, a standalone software package was developed for making phase equilibria calculations with the UNIFAC-vdW-FV model. As described in Chapter 2, Kannan et al. [1] have shown this model to give improved predictions for aqueous and most non-aqueous systems compared to other free volume ACMs. The software was built as an MS-DOS application which creates exportable text files of the prediction results. A sizeable polymer and solvent library is built into the package. The program also provides the option of adding new molecules to the existing library. For improved prediction results, the user can enter experimental polymer and/or solvent densities instead of using calculated values.

A.2 Description of Program

The program was coded in the Fortran 90 programming language. The workspace contains 1 main program and 12 subroutines. After coding the routines, extensive testing was conducted to insure the accuracy of the results. Values calculated with the program were checked against hand calculations.

Next, the program was packaged as a distributable version with the executable file and input files which contain the solvent and polymer group parameters. Figure A-1 shows the folder that contains these files.

The package is distributed with two molecule libraries (solvent and polymer). The current library contains 111 solvents and 24 polymers. The library of polymers and solvents are listed in Tables A-2 and A-3, respectively.

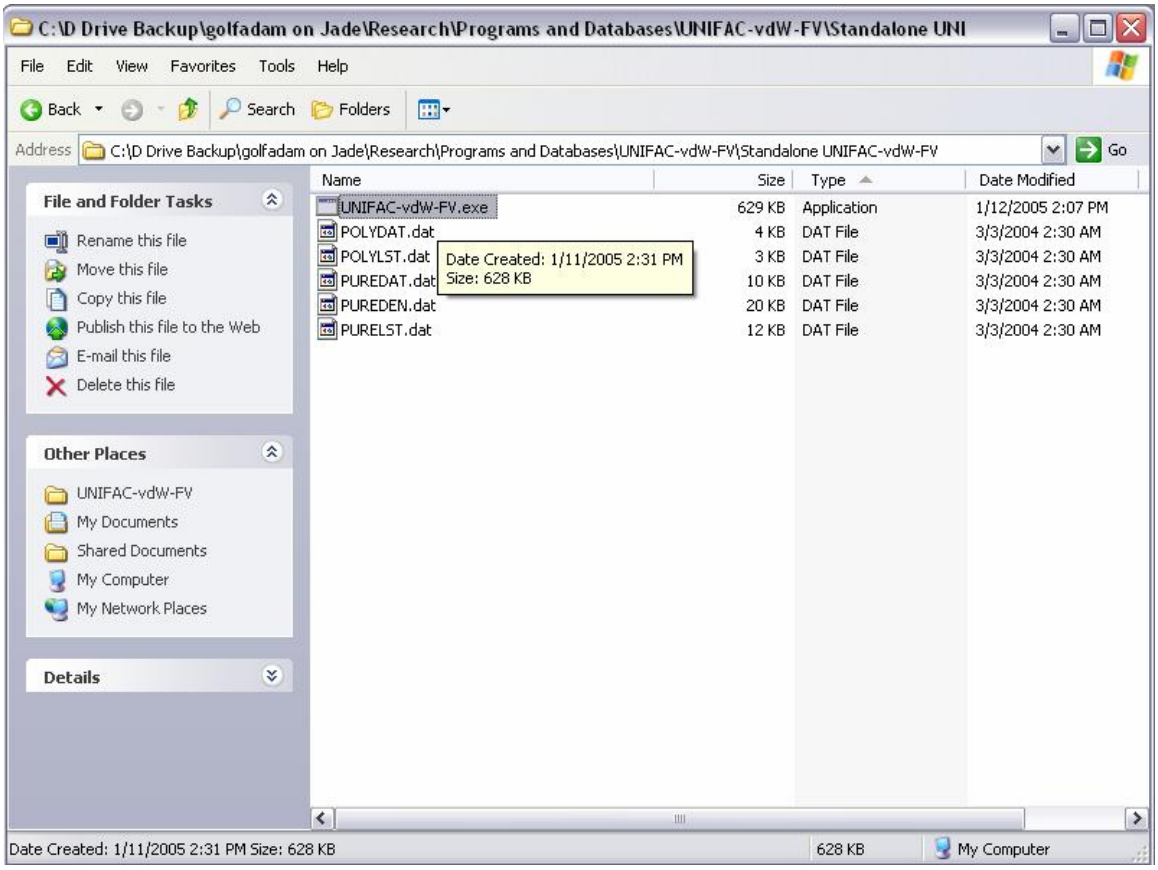

Figure A-1: The program folder contents containing the executable program "UNIFAC-vdW-FV.exe".

A.3 Operation of the Program

The first thing the user does upon receiving the package is copy the folder to their hard disk. This is necessary because when the program runs, the output file is modified and the program must write to the source directory. To run a prediction, the icon called “UNIFAC-vdW-FV.exe” is double-clicked. An MS-DOS window opens which serves as the input environment. The introduction screen features a brief overview of the program, followed by a question asking whether the user would like to add a new molecule to the

data files. If the user does not wish to enter a new molecule, they enter the main subroutine for running a prediction. The first thing that must be provided is the system temperature in Celsius. The user then is asked to specify the number of components in the system. The current software version allows for binary (polymer-solvent) and ternary (polymer-solvent-solvent) predictions.

A.4 Performing a Binary Prediction

The required inputs in the order they are encountered are described in this section.

A.4.1 Polymer Molecular Weight or Number of Repeat Units

The user has a choice of specifying the number average molecular weight or the number of repeat units. If the number of repeat units is specified, the program automatically calculates the polymer molecular weight.

A.4.2 Solvent ID#

The Solvent ID# for each solvent is listed in Table A-3. After entering the ID#, the program responds with the corresponding name of the solvent so the user can verify the correct ID# was entered.

A.4.3 Polymer ID#

The polymer IDs are found in Table A-2. After entering the ID#, the program responds with the corresponding name of the polymer so the user can verify the correct ID# was entered.

A.4.4 Solvent Density

The density of the solvent is used in determining the free volume contribution to the activity coefficient. For existing solvents in the Solvent ID List, the user is given an option of entering a known density at the system temperature.

If the user chooses not to enter a density, the program calculates it using the Rackett equation:

$$Y = \frac{A}{B^{\left[1+\left(1-\frac{T}{C}\right)^{D}\right]}} \tag{1.1}$$

where Y is the liquid molar density, A, B, C, and D are coefficients available in tables in the Physical and Thermodynamic Properties of Pure Chemicals: Data Compilation (DIPPR) [2], and T is the system temperature in Kelvin. The liquid molar density is multiplied by the solvent molecular weight to obtain the correct units.

A.4.5 Polymer Density

The density of the polymer is also used in determining the free volume contribution to the activity coefficient. For existing polymers in the Polymer ID List, the user is given an option of entering a known density at the system temperature. If the user chooses not to enter a density, the program calculates the specific volume (inverse density) using the Tait equation:

$$V = A_0 + A_1(T - T_0) + A_2(T - T_0)^2 \qquad (1.2)$$

where V is the specific volume, A_0, A_1, and A_2 are coefficients available in the "Handbook of Polymer Solution Thermodynamics" by Danner and High [3], T is the system temperature in Kelvin, and T_0 is the reference temperature (273.15 K) .

A.4.6 Solvent Vapor Pressure

The solvent vapor pressure is used to determine the partial pressure of the solvent in the vapor. For the binary case, it is assumed the polymer only exists in the liquid phase, and therefore, the partial pressure of the solvent is equal to the total pressure (assuming ideal gas behavior).

For existing solvents in the Solvent ID List, the user is given an option of entering a known vapor pressure at the system temperature.

If the user chooses not to enter a vapor pressure, the program calculates it using the DIPPR vapor pressure equation [2], which has the following form:

$$Y = \exp\left(A + \frac{B}{T} + C\ln(T) + DT^{E} \right) \tag{1.3}$$

where Y is the vapor pressure, A, B, C, D, and E are coefficients, and T is the system temperature in Kelvin.

A.4.7 Weight Fraction Range

The user is given the option of specifying a range of weight fractions for either the polymer or the solvent. The user first specifies the lower (starting) value of the weight fraction. If the starting value is set to zero, the first calculation will be the infinite dilution activity coefficient. The upper (final) value of the weight fraction is then specified. The user can then specify the number of data points they wish to predict. The minimum is 1 data point. The maximum is unlimited.

A.5 Performing a Ternary Prediction

The required inputs for the ternary case are mainly the same as that of the binary case. The main difference is in the input of the weight fraction range for the prediction.

A.5.1 Weight Fraction Range

Because two weight fractions must be defined to full specify the composition of the liquid, the user is allowed to hold one of the three weight fractions constant. The user

then specifies a range for one of the two remaining weight fractions. An example of this is shown in Figure A-2.

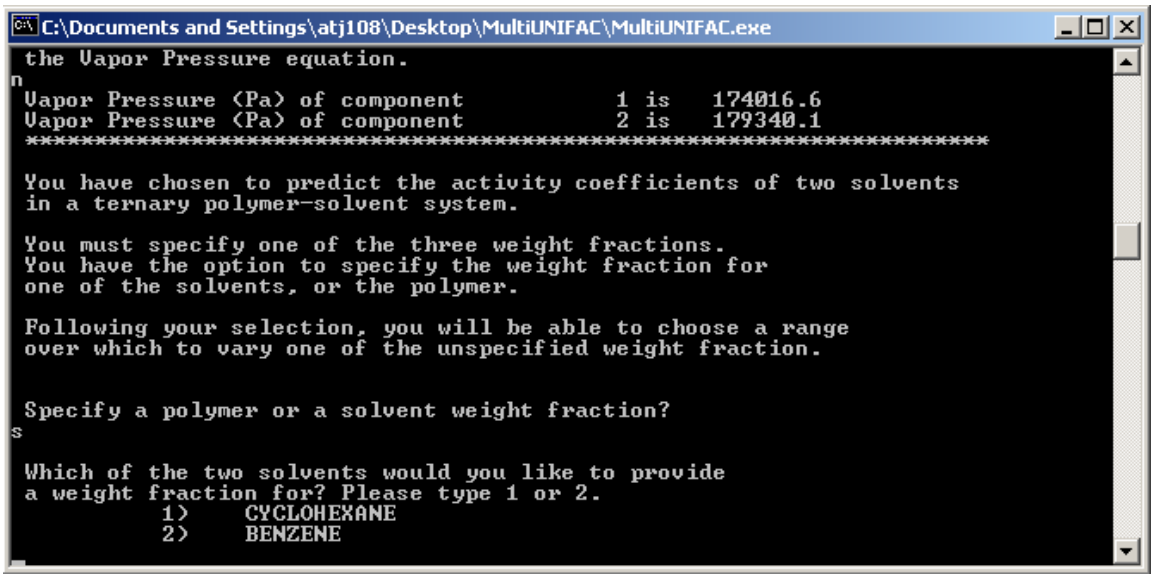

Figure A-2: Example of the solvent weight fraction specification for a ternary case.

Upon choosing a solvent, they then enter the weight fraction. To simplify the process, the program then automatically asks the range over which to vary the other solvent weight fraction. If the user chooses to hold the polymer weight fraction constant, the program asks the weight fraction of the polymer. The program then automatically asks the range over which to vary Solvent 1 weight fraction. Again, if the starting weight fraction for the second solvent is set to zero, the first calculation will be the infinite dilution activity coefficient of that solvent with the mixture of the two other solvents at finite concentration.

A.6 Obtaining the Prediction Results

For both the binary and ternary predictions, once the number of data points is specified the program runs and when it has completed, the user is prompted to enter a filename for the output file. If an error is encountered in execution of the prediction, a message will display in the MS-DOS window instead. If the program runs without error, an output file will be placed in the folder called "UNIFAC-vdW-FV". The file can easily be imported to Microsoft Excel or any other spreadsheet program.

An example of the output file for a binary case is provided in Table A-1. In the table “SolventWF” refers to solvent weight fraction and “WFAC” refers to weight fraction activity coefficient.

Table A-1: Sample output for a binary prediction

SolventWF	WFAC	Activity	Total_Pressure(kPa)	Total_Pressure(psia)
0.1	4.738	0.474	82.45	11.958
0.144	4.179	0.604	105.046	15.236
0.189	3.716	0.702	122.129	17.713
0.233	3.327	0.776	135.095	19.594
0.278	2.999	0.833	144.958	21.024
0.322	2.719	0.876	152.466	22.113
0.367	2.479	0.909	158.173	22.941
0.411	2.271	0.934	162.499	23.569
0.456	2.091	0.953	165.761	24.042
0.5	1.933	0.967	168.203	24.396

A.7 Addition of Molecules to Library

The UNIFAC-vdW-FV program allows for the addition of molecules to the solvent and polymer library. The only required information to add a new molecule is the group information.

A.7.1 Adding a Solvent

Upon specifying that the user would like to add a solvent, the program immediately displays the ID# that the new solvent will be assigned. The user is then asked to enter a name for the new solvent. This name is arbitrary because the program only requires the user to enter the ID# when running the program. The solvent name can be up to 29 characters in length. Spaces should be omitted or represented with an underscore. The user then is asked to enter the chemical formula of the solvent.

A brief description of the Rackett equation is provided after the user enters the chemical formula. The user is then asked whether they would like to provide the Rackett constants for the new solvent. As mentioned previously, it is recommended that the user enter these constants if they are available. The Rackett constants for many solvents are available in tables in the Physical and Thermodynamic Properties of Pure Chemicals: Data Compilation (DIPPR) [2]. If the user does not provide Rackett constants, then they must provide the solvent density (kg/m^3) at the system temperature when a prediction is run involving the new solvent.

A description of the Vapor Pressure equation is then provided, followed by a question asking whether the user wishes to enter the Vapor Pressure constants. Again the user is encouraged to enter these constants if they are available. The constants are also available in tables in the Physical and Thermodynamic Properties of Pure Chemicals: Data Compilation (DIPPR) [2]. If the user does not provide Vapor Pressure constants, then they must provide the solvent vapor pressure (Pa) at the system temperature when a prediction is run involving the new solvent.

The next step in adding a new solvent involves specifying the subgroup information. The user must decide the proper way to represent the molecule in terms of the available groups. Once this is decided, the user provides the program with the total number of distinct subgroup types in the new solvent. Following the user's response, the program asks for the subgroup number of the first group. The group definitions have been provided by Danner and High [3]. Following the entry of a subgroup number, the program asks for the number of groups of that particular type in a single solvent molecule, $\nu_k^{(i)}$. This process is repeated for each distinct subgroup that occurs in the new solvent.

Once all of the subgroup information is entered, the program displays the molecular weight of the new solvent that was added. This value is calculated based on the molecular weight of the groups in the molecule, and can be used as a check to verify the new solvent was entered correctly.

A.7.2 Adding a polymer

Upon specifying that the user would like to add a polymer, the program immediately displays the ID# that the new polymer will be assigned. The user is then asked to enter a name for the new polymer. This name is arbitrary because the program only requires the user to enter the ID# when running the program. The polymer name can be up to 35 characters in length. Spaces should be omitted or represented with an underscore. The user then is asked to enter the abbreviation of the polymer.

A brief description of the Tait equation is provided after the user enters the polymer abbreviation. The user is then asked whether they would like to provide the Tait constants for the new polymer. As mentioned previously, it is recommended that the user enter these constants if they are available. The Tait constants for many polymers are available by Danner and High [3]

The user is only required to enter the first three Tait constants (A_0,A_1,A_2) because UNIFAC-vdW-FV does not account for pressure effects and should only be used at low to moderate pressures. If the user does not provide Tait constants, then they must provide the polymer density (kg/m^3) at the system temperature when a prediction is run involving the new polymer.

The next step in adding a new polymer involves specifying the subgroup information. For this step, the user should consider a single repeat unit of the polymer. The user must decide the proper way to represent the repeat unit in terms of the available groups. Once this is decided, the user provides the program with the total number of distinct subgroup types in the repeat unit. Following the user's response, the program asks for the subgroup number of the first group. Following the entry of a subgroup number, the program asks for the number of groups of that particular type in a single repeat unit, $\nu_k^{(i)}$. This process is repeated for each distinct subgroup that occurs in the repeat unit.

Table A-2: Polymer List

ID#	Abbreviation	Polymer Name
1	BR	BUTADIENE RUBBER
2	HDPE	HIGH DENSITY POLYETHYLENE
3	I-PB	ISOTACTIC POLYBUTYLENE
4	I-PP	ISOTACTIC POLYPROPYLENE
5	LDPE	LOW DENSITY POLYETHYLENE
6	PA-6	POLYAMIDE-6
7	PAR	POLYARYLATE
8	PBMA	POLY(n-BUTYL METHACRYLATE)
9	PC	POLYCARBONATE
10	PDMS	POLY(DIMETHYLSILOXANE)
11	PEG	POLY(ETHYLENE GLYCOL)
12	PETP	POLY(ETHYLENE TEREPHTHALATE)
13	PHENOXY	PHENOXY
14	PIB	POLYISOBUTYLENE
15	PMMA	POLY(METHYL METHACRYLATE)
16	PMP	POLY(4-METHYL-1-PENTENE)
17	POM	POLY(OXYMETHYLENE)
18	POMS	POLY(ORTHOMETHYLSTYRENE)
19	PS	POLYSTYRENE
20	PT	POLY(TETRAHYDROFURAN)
21	PTFE	POLY(TETRAFLOUROETHYLENE)
22	PVAL	POLY(VINYL ALCOHOL)
23	PVAC	POLY(VINYL ACETATE)
24	PVC	POLY(VINYL CHLORIDE)

Table A-3: Solvent List

ID#	Solvent Name	Molecular Formula
1	ETHANE	C2H6
2	PROPANE	C3H8
3	ISOBUTANE	C4H10
4	n-PENTANE	C5H12
5	n-HEXANE	C6H14
6	2-METHYLPENTANE	C6H14
7	2,3-DIMETHYLBUTANE	C6H14
8	n-HEPTANE	C7H16
9	n-OCTANE	C8H18
10	n-DECANE	C10H22
11	CYCLOPENTANE	C5H10
12	METHYLCYCLOPENTANE	C6H12
13	CYCLOHEXANE	C6H12
14	METHYLCYCLOHEXANE	C7H14
15	2-METHYL-2-BUTENE	C5H10
16	1-HEPTENE	C7H14
17	1,3-BUTADIENE	C4H6
18	ISOPRENE	C5H8
19	BENZENE	C6H6
20	TOLUENE	C7H8
21	ETHYLBENZENE	C8H10
22	m-XYLENE	C8H10
23	p-XYLENE	C8H10
24	STYRENE	C8H8
25	ACETALDEHYDE	C2H4O

51	METHYL FORMATE	C2H4O2
52	n-BUTYL FORMATE	C5H10O2
53	METHYL ACETATE	C3H6O2
54	ETHYL ACETATE	C4H8O2
55	n-PROPYL ACETATE	C5H10O2
56	n-BUTYL ACETATE	C6H12O2
57	VINYL ACETATE	C4H6O2
58	DIETHYL ETHER	C4H10O
59	DIISOPROPYL ETHER	C6H14O
60	METHYL tert-BUTYL ETHER	C5H12O
61	ETHYL PROPYL ETHER	C5H12O
62	1,4-DIOXANE	C4H8O2
63	CARBON TETRACHLORIDE	CCL4
64	ETHYL CHLORIDE	C2H5CL
65	DICHLOROMETHANE	CH2CL2
66	CHLOROFORM	CHCL3
67	1,2-DICHLOROETHANE	C2H4CL2
68	TRICHLOROETHYLENE	C2HCL3
69	TETRACHLOROETHYLENE	C2CL4
70	MONOCHLOROBENZENE	C6H5CL
71	n-BUTYL CHLORIDE	C4H9CL
72	BROMOBENZENE	C6H5BR
73	METHYL IODIDE	CH3I
74	ETHYL IODIDE	C2H5I
75	TRIETHYLAMINE	C6H15N

76	DIETHYLAMINE	C4H11N
77	n-BUTYLAMINE	C4H11N
78	ISOPENTANE	C5H12
79	N,N-DIETHYLANILINE	C10H15N
80	NITROMETHANE	CH3NO2
81	NITROETHANE	C2H5NO2
82	ACETONITRILE	C2H3N
83	DMSO	DMSO
84	PYRIDINE	C5H5N
85	PHENETOLE	C8H10O
86	HEXAFLUOROBENZENE	C6F6
87	N,N-DIMETHYLFORMAMIDE	C3H7NO
88	epsilon-CAPROLACTAM	C6H11NO
89	NITROBENZENE	C6H5NO2
90	FURFURAL	C5H4O2
91	WATER	H2O
92	CARBON DISULFIDE	CS2
93	n-NONANE	C9H20
94	1-OCTANOL	C8H18O
95	DI-n-PROPYL ETHER	C6H14O
96	TETRAHYDROFURAN	C4H8O
97	1,2,3,4-TETRAHYDRANAPHTHALENE	C10H12
98	1,1,2-TRICHLOROETHANE	C2H3CL3
99	1,2,4-TRIMETHYLBENZENE	C9H12
100	n-UNDECANE	C11H24

101	ANISOLE	C7H8O
102	tert-BUTYL ACETATE	C6H12O2
103	2,4-DIMETHYLPENTANE	C7H16
104	n-DODECANE	C12H26
105	ETHYL FORMATE	C3H6O2
106	1-HEPTANOL	C7H16O
107	2,2,4-TRIMETHYLPENTANE	C8H18
108	2-METHYLHEXANE	C7H16
109	n-BUTANE	C4H10
110	DIISOBUTYL KETONE	C9H18O
111	ISOBUTYLAMINE	C4H11N

A.8 References

1. Kannan, D. C.; Duda, J. L.; Danner, R. P. A Free-Volume Term Based on the van der Waals Partition Function for the UNIFAC Model. *Fluid Phase Equilib.*, **2005**, *228-229*, 321-328.

2. Daubert, T. E.; Danner, R. P. *Physical and Thermodynamic Properties of Pure Compounds*: *Data Compilation*; Taylor and Francis: New York, **1994**.

3. Danner, R. P.; High, M. S. *Handbook of Polymer-Solution Thermodynamics*; Design Institute for Physical Property Data, American Institute of Chemical Engineers: New York, **1993**.

VITA

Adam T. Jones

Education

Ph.D., Chemical Engineering, The Pennsylvania State University

B.S., Chemical Engineering, Iowa State University, 2002

Work Experience

2002-Present Research Assistant, Center for the Study of Polymeric Systems

2001-2002 Research Assistant, Department of Chemical Engineering, Iowa State University

Publications

Jones, A. T.; Derawi, S.; Danner, R. P.; Duda, J. L. A Simplified Approach to Vapor–Liquid Equilibria Calculations with the Group-Contribution Lattice-Fluid Equation of State. *Fluid Phase Equilib.* **2007**, *In Press*.

Palamara, J. E.; Mulcahy, K. A.; Jones, A. T.; Danner, R. P.; Duda, J. L. Solubility and Diffusivity of Propylene and Ethylene in Atactic Polypropylene by the Static Sorption Technique. *Ind. Eng. Chem. Res.* **2005**, *44*, 9943-9950.

Awards

George A. and Ruth S. Robb Graduate Fellowship in Chemical Engineering, Penn State, 2007

Arthur and Elizabeth Rose Memorial Graduate Fellowship in Chemical Engineering, Penn State, 2006

Walter R. and Aura Lee Supina Graduate Fellowship in Chemical Engineering, Penn State, 2002

Organizations

Associate Member, AIChE

Member, USATT